Theoretical Studies in Palladium and Platinum Molecular Chemistry

Alain Dedieu

Laboratoire de Chimie Quantique, UMR 7551 CNRS/ULP, Université Louis Pasteur, 4 rue Blaise Pascal, 67000 Strasbourg, France

Received April 19, 1999

Contents

Alain Dedieu was born in 1947 and graduated from the Ecole Nationale Supérieure de Chimie de Strasbourg in 1969. He completed his Ph.D. degree from the Université Louis Pasteur, Strasbourg, in 1975. After one year of postdoctoral studies with Professor Roald Hoffmann at Cornell University, he came back to the Université Louis Pasteur, where he is now Directeur de Recherche at the Centre National de la Recherche Scientifique. His main research interests are in theoretical transition metal chemistry, with an emphasis on the reactivity aspects.

I. Introduction

The chemistry of palladium and platinum is one of the most extensive and versatile fields of chemistry. This results from the fact that these two metals can very easily form adducts with many organic and inorganic molecules. These adducts are in turn very reactive, thus opening the field of catalysis, either homogeneous or heterogeneous. Many books and reviews have been devoted to these palladium and platinum compounds, see for instance refs 1−12; other reviews will be mentioned in due course. Being written by experimentalists, they are mostly dealing with the experimental aspects, although they sometimes quote some theoretical studies but without a critical assessment of their performance.

Yet both palladium and platinum complexes have been the subject of numerous theoretical studies, as early as in the 1980s. The reasons for this feature are manifold. First, Pd and Pt complexes in the oxidation state +2 (which dominates their chemistry) are usually four-coordinate square-planar complexes. With ligands such as phosphine or amine that can be modeled by PH_3 or NH_3, the systems are rather small and were relatively easy to compute in the early stages of theoretical transition-metal chemistry. Moreover, these complexes generally have a dominant ground-state configuration. They can be, therefore, treated adequately at the correlated level by single-reference methods, although some specific interactions such as metal to CO bonding or agostic bonds may require relatively high-level-type calculations. Relativistic effects are expected to be more important for Pt than for Pd, but the use of relativistic pseudopotentials can overcome this difficulty for the spin-free effects. Another feature that can explain why such systems were tackled quite early is that many reactions undergone by these complexes are prototype reactions of organometallic chemistry: consider, for instance, the oxidative addition of H_2 on $Pd(PH_3)_2$ or $Pt(PH_3)_2$, the CO and the C_2H_4 insertion

10.1021/cr980407a CCC: $35.00
Published on Web 02/09/2000

into the metal−CH_3 bond, the nucleophilic addition on an ethylene coordinated to either Pd or Pt, or on a Pd−allyl moiety, etc.

The interested reader will find some account of these early studies in reviews, especially in two review articles which were published in a special issue of *Chemical Reviews* about 10 years ago on "Quantum Theory of Matter".[13,14] Since then, methodologies at hand have been greatly improved, combining sophistication and speed of calculations. In the meantime, the computer resources have been greatly improved also. All these factors have allowed for treatment of systems and reactions which are close to the experimental ones and which were not previously amenable to theoretical investigations.

Our aim is, therefore, to review the quantum chemical studies on Pd and Pt *molecular systems* that have been carried out since 1990. We will not address studies dealing with surface chemistry or solid-state chemistry. We will also restrict ourselves to quantum mechanics calculations and exclude from the scope of this article molecular mechanics calculations and molecular dynamics calculations, although we are aware of the increasing importance of these techniques in the modeling of organometallic chemistry. We are also well aware that some of the material covered here will be addressed in other review articles of this issue. We want, however to give a comprehensive overview of the palladium and platinum chemistry and show the continuity between studies dealing with very small systems (most often involving bare metal atoms or ions and for which experiments have been carried out in the gas phase) and studies involving large metal complexes with a whole variety of ligands (and for which the relevant experiments have been carried out in solution). Thus, the remainder of the paper will be organized as follows: Recent studies that pertain to the structure of mononuclear systems will be analyzed in section II and those of polynuclear systems in section III. We will then, in section IV, discuss the reactivity of Pd and Pt complexes following the usual classification that relies on reaction types, i.e., oxidative addition and reductive elimination, migratory insertion, deinsertion and β-hydride elimination, nucleophilic attack on coordinated ligands, substitution reactions, oxidation reactions. We will end by briefly quoting studies that have been devoted to catalytic cycles.

However, before going into a detailed survey, it is worth mentioning a salient difference in the electronic structure of the Pd and Pt atoms, since it may lead to different structures and distinct reactivities for systems containing either Pd or Pt. The electronic ground state of Pd corresponds to a closed-shell d^{10} configuration, the open-shell d^9s^1 configuration lying 0.95 eV (i.e., 21.9 kcal mol^{-1}) above. In contrast, for Pt the d^9s^1 state is the ground state, the d^{10} configuration being 0.48 eV (11.1 kcal mol^{-1}) higher.[15] A correct and balanced description of the relative energies of these two states is therefore essential, especially to account for reactivity differences with systems in which the field created by the ligand is relatively moderate, i.e., with systems having a low oxidation state and/or a low coordination number.

II. Mononuclear Compounds

A. Metal Hydrides

The hydrido complexes of Pd and Pt form a class of compounds of particular interest in chemistry, not only because of their intrinsic structure and bonding properties, but also because of their relevance to metal-catalyzed or metal-mediated reactions.[16,17] Among the ones which have been the most accurately treated are the diatomic Pd−H and Pt−H systems. In this case gas-phase data exist against which theoretical calculations can be tested. Also there have been numerous studies of the interaction of the naked metal with H_2, since it bears an obvious relationship to the oxidative reaction of H_2 in transition-metal chemistry and homogeneous catalysis and to H_2 chemisorption in metal surface chemistry and heterogeneous catalysis.

1. Pd–H and Pt–H

Pd−H. Since the first pioneering studies of Balasubramanian et al.[18] and of Langhoff et al.[19] on PdH, subsequent calculations have been carried out, either to compare the bonding in Pd−H to the bonding in other second-row transition metal hydrides, fluorides, or chlorides[20] or to test the accuracy of the theoretical model. In addition to the treatment of electron correlation, special attention has been paid to the inclusion of the relativistic effects. Thus, in the course of a comprehensive study on the low-lying states of the second-row transition-metal hydrides, the Pd−H system has been again considered by Balasubramanian[21] but with a larger basis set than in ref 18 and with a small core pseudopotential[22] instead of a large one. Moreover, the more accurate CASSCF/SOCI method was used instead of the CASSCF/FOCI one. For an account of the methods used by Balasubramanian in his investigations, we refer the reader to ref 23. A much better agreement with the experimental values,[24−26] especially the most recent one of 56 ± 6 kcal mol^{-1} deduced from the ion beam experiments,[26] was found for the dissociation energy values D_e (55.4 kcal mol^{-1}) and for ω_e of the $^2\Sigma^+$ ground state. The computed equilibrium bond length R_e, which was already in good agreement with experiment in the previous study, did not change appreciably. One should also mention that these CASSCF/SOCI results are in better agreement with experiment (for D_e and ω_e) than the previous MCPF results of Langhoff et al.[19] One should note, however, that the basis used in the latest study of Balasubramanian did not yield a correct separation of the ^3D and ^1S atomic states of Pd, since it favored the ^3D state over ^1S. Thus, the D_e value had to be corrected by the $^3D-^1S$ separation of 0.72 eV found in the large core pseudopotential calculations.[21]

As far as the relativistic effects are concerned, a very thorough investigation by Sjøvoll et al.[27] has confirmed that the inclusion of relativistic effects (at least the spin-free ones) is crucial for a proper description of the low-lying states of the Pd−H molecule: the nonrelativistic calculations yield excited states that are too high in energy, by as much as 0.23 eV for the $^2\Delta$ state (which is the first excited

state). A bond contraction has also been observed, especially in the excited states. It amounts to only 0.02 Å in the $^2\Sigma^+$ ground state. Similar results had been found by Jenderek and Marian.[28] Marian and Fleig have also recently determined the rovibronic spectra of PdH and PdD.[29] Their calculations take into account the effects of spin−orbit, spin−rotational, and orbit-rotational coupling between the three lowest electronic states $^2\Sigma^+$, $^2\Delta$, and $^2\Pi$. They stress, in particular, the need of a precise correlation treatment prior to the inclusion of the spin−orbit, spin-rotational, and orbit−rotational couplings.

This conclusion has also been reached by Sjøvoll et al.[27] Their calculations are also important in that they allow one to assess the performance of various methodologies for including spin−orbit interaction effects. The two-component calculations (based on the second-order Douglas−Kroll spin−orbit operator) are in reasonable agreement with the four-component calculations (based on the Dirac−Coulomb operator) but only once a careful choice of the orbital basis for the CI calculations has been done. The spin−orbit interaction is found to be significant, especially for the excited $^2\Pi$ and $^2\Delta$ states which mix substantially. On the other hand, the spin−orbit coupling is relatively small for the $^2\Sigma^+$ ground state, as already noticed by Balasubramanian.[21] Thus, when dealing with the ground-state properties of larger systems, one can probably neglect spin−orbit coupling. One essentially needs to account for the mass velocity and Darwin terms, either through first-order perturbation theory if one uses an all-electron basis set for Pd, or via the use of an effective core potential.

Pt−H. Somewhat different conclusions have emerged from the theoretical studies carried out on Pt−H. The first studies were aimed at improving earlier calculations[30−35] and at analyzing how to include the relativistic effects. Gropen et al.[36] have compared the use of relativistic effective core potentials (RECP) and of first-order perturbation theory to account for the spin-free effects (using a rather flexible basis set and treating electron correlation at the multireference CI level). For Pt alone, their RECP calculations give a better agreement with experiment for the $^3F-^3D$ and $^1S-^3D$ state separation than in the previous calculations. In contrast, first-order perturbation theory fails in reproducing the experimental ordering: the computed ordering is $^3D < ^3F < ^1S$ instead of $^3D < ^1S < ^3F$ experimentally. On the other hand, for Pt−H, first-order perturbation theory is in agreement with experiment,[37] since it yields the $^2\Delta$ state being below the $^2\Sigma$ state, whereas the inverse is found in the RECP calculations. One should note, however, that the Pt−H, bond length computed in the RECP calculations is in better agreement with experiment.[38]

In fact, inclusion of the spin-dependent effects is quite important for Pt−H and cannot be neglected if one wants to get a reasonable agreement with experiment. In the CASSCF/FOCI + RCI study of Balasubramanian, the spin−orbit interaction has been introduced via the addition of spin−orbit matrix elements to the CI matrix.[34] The ground state is found to be the $\Omega = 5/2$ state followed by the lowest $\Omega = 1/2(1)$ and $\Omega = 3/2(1)$ excited states and finally the $\Omega = 3/2(2)$ and $\Omega = 1/2(2)$ states.[34] The relative importance of the spin-free and spin-dependent relativistic effects has been assessed by Dyall.[39] His study, which neglects the correlation effects to concentrate only on the relativistic effects, shows clearly that the inclusion of the spin−orbit interaction is crucial to the understanding of the level structure of the molecule, much more than for Pd−H. The division of states into two groups (the $\Omega = 5/2$ ground state, the lowest $\Omega = 1/2(1)$ and $3/2(1)$ and the $\Omega = 3/2(2)$ and $1/2(2)$ excited states) has its origin in the spin−orbit splitting. By comparing the results of spin-free no-pair variational calculations with those of first-order perturbation theory, the spin-free effects beyond first order are obtained and are found to be quite important.

Visscher et al.[40] have gone one step further by performing fully, i.e., four-component, relativistic configuration interaction calculations on the lowest states of Pt−H. As in Dyall's study,[39] the relativistic Dirac−Hartree−Fock equations have been solved but this has been followed by relativistic configuration interaction calculations. The inclusion of electron correlation does not profoundly affect the excitation energies of the spin−orbit mixed states. On the other hand, it has a significant impact (especially the dynamic correlation in the d shell) on the values obtained for spectroscopic properties. The equilibrium bond length is shortened by about 0.04 Å, and the corresponding harmonic frequencies are higher by several hundreds of cm^{-1}.

These calculations can be considered as benchmark calculations against which the accuracy of less expensive approaches can be tested. Such tests are important to delineate methodologies which could be reliably used to account for relativistic effects in larger systems of chemical interest. Marian and co-workers[41,42] have implemented a two-step procedure in which a spin-independent no-pair Hamiltonian is first used in CASSCF and MRCI calculations and spin−orbit interaction effects are taken into account subsequently through variational perturbation theory. They obtained a good agreement with the four-component results. Very recently, Sjøvoll et al.[43] have assessed the validity of this approach by comparing the effect of treating the spin−orbit coupling on the same footing as electron correlation through a spin−orbit CI procedure, to the effect of introducing it in a separate and final step (in the same way as Marian and co-workers). The coupling between electron correlation and spin−orbit coupling is found to be very weak, both approaches giving agreement with experiment and with the four-component relativistic calculations of Visscher et al. Their results also point to an almost atomic character of the spin−orbit coupling in Pt−H. In fact, the main source of error, which had been largely overlooked previously, lies in the difficulty of obtaining an orbital basis of good quality for all the investigated states.

Schwarz and co-workers have resorted to a parametrized one-electron spin−orbit Hamiltonian and calibrated on Pt−H the parameter—which takes the form of an effective nuclear charge Z_{eff}—for its use

in molecular calculations.[44] The calculations were carried out in conjunction with a CASSCF wave function, using the small core relativistic pseudopotential of Stevens et al.[45] The results appear to be quite promising since the correct state ordering and clustering is obtained. The bond lengths are somewhat overestimated and the frequencies underestimated due to the neglect of dynamic electron correlation. As we shall see later, the same method has been applied to [PtO], $[PtO]^+$, and $[PtCH_2]^+$. Hess et al. have devised an effective one-electron spin−orbit Hamiltonian using well-defined approximations, by averaging the two-electron contribution to the spin−orbit matrix elements over the valence shell.[46] Calculations on Pt−H have been carried out using a modification to work with an effective core potential valence wave function.[47] The agreement with the all-electron results turns out to be excellent. Calculations have also been carried out with a one-electron pseudopotential having an averaged d^9 open shell in the core, the ultimate aim being to treat systems containing a large number of Pt atoms.[48] The results obtained with this pseudopotential compare well with the average of the three low-lying states $^2\Delta$, $^2\Sigma^+$, and $^2\Pi$.

To end this section one should mention that in contrast to PtH, little work has been performed on the $[PtH]^+$ cation in order to solve the existing controversy between earlier calculations of Wang and Pitzer[32] which favor a $^3\Delta$ ground state and those of Balasubramanian[49] which give a ground state with 0^+ symmetry dominated by the nonrelativistic $^1\Sigma^+$ configuration. It has been found that the spin−orbit coupling effects are much greater in $[PtH]^+$ than in $[PdH]^+$ and have to be taken into account for $[PtH]^+$. For instance, the lowering of the $^1\Sigma_o^+$ state with respect to the $^1\Sigma^+$ λ−s state is 184 cm^{-1} in $[PdH]^+$ and 1655 cm^{-1} in $[PtH]^+$. As in the neutral system, the effects are even larger for the excited states: the $^3\Delta_3-^3\Delta$ splitting amounts to 1390 cm^{-1} in $[PdH]^+$ and to 4359 cm^{-1} in $[PtH]^+$. The net result is a decrease of the $0^+(^1\Sigma_o^+)-3(^3\Delta_3)$ separation. The more recent Dirac−Hartree−Fock calculations of Dyall et al.[39] support the earlier results of Balasubramanian,[49] although they yield an increased separation between the 3 and 0^+ states on inclusion of the spin−orbit effects.

2. Pd–H_2 and Pt–H_2

The studies on Pd−H and Pt−H bear an obvious relationship to those that have been carried on Pd−H_2 and Pt−H_2. A detailed assessment of the factors that govern the interaction between the naked metal atoms and H_2 is of primary importance if one wants to have a deep understanding of the oxidative addition reactions that are undergone by palladium and platinum clusters or complexes.

In fact, many theoretical studies had been devoted to this topic prior to 1990,[50−57] some of them including an estimate of the relativistic spin−orbit effects.[49,57,58] All the studies agreed on the following results: For palladium one finds a molecular dihydrogen complex made of H_2 weakly interacting with the metal (with a Pd−H bond length varying between 1.67 and 2.05 Å, and the H−Pd−H bond angle varying between 20°and 30°). A second minimum corresponding to the product of the oxidative addition is also found but somewhat higher in energy (5.8 kcal mol^{-1})[57] and with a very small barrier for the reductive elimination back to the dihydrogen complex. In contrast, there is no dihydrogen complex with platinum, the reaction leading directly to the very stable oxidative reaction product. Low and Goddard showed that this different behavior can be traced back to the different ground state of the two metals.[55] Platinum with its d^9s^1 ground state is ideally suited for making two Pt−H *covalent* bonds in the PtH_2 bent molecule. On the other hand, palladium with its d^{10} ground state can easily form a van der Waals or more likely a Lewis acid/Lewis base complex between the empty 5s orbital and the σ_g orbital of H_2. To go to the second minimum one has to promote the electronic configuration from d^{10} to d^9s^1. Note also that in contrast to the ^1S (d^{10}) state, the ^3D (d^9s^1) state of platinum does insert spontaneously into H_2. By inclusion of the spin−orbit coupling, these two states mix, thus allowing the change of configuration in Pt and the formation of the bent complex.[49,58]

More recently, Gropen at al.,[59] using CASSCF/MRSDCI calculations with their own carefully optimized small core pseudopotential and a rather large basis set, have found for the side-on approach of H_2 toward Pt only one minimum corresponding to the oxidative addition product on the $^1A_1$ potential energy curve. Similar results have been also obtained by Diez at the DFT level.[60] In this study, which is aimed at testing several exchange-correlation functionals, a relativistic effective core potential was used in conjunction with a double-ζ basis set (polarized for the hydrogen atoms). It is not clear, however, from the references quoted in the paper whether a small-core or large-core pseudopotential was used. This makes the comparison with the previous studies somewhat difficult. All the gradient-corrected or hybrid functionals give similar results and as far as geometries are concerned in good agreement with the ab initio results. The agreement is less satisfactory for the reaction energy which is somewhat too high (compared to the ab initio results), although the hybrid functional results agree with the CASSSCF/MRSDCI results of Gropen et al.[59] (52.6 and 56.7 kcal mol^{-1} with the B3LYP and B3PW91 functionals vs 50 kcal mol^{-1} in Gropen's calculations). One should stress that DFT does not find any minimum corresponding to a linear $^3A_1$ H−Pd−H structure, in contrast to the ab initio calculations. A tentative explanation may be that all the functionals used in this paper yield a $^3D-^1S$ splitting which is too small, thus exemplifying the known propensity of DFT to favor the d^n states over the $d^{n-1}s$ ones.[61,62] This, in turn, is detrimental to the formation of covalent bonds.

To our knowledge there have not been any fully relativistic configuration interaction calculations carried out either on Pd−H_2 or Pt−H_2 similar to the one performed by Visscher et al.[40] for Pt−H. Dyall has extended his methodological study of relativistic

effects at the HF level from the Pt−H system to the PtH_2 system.[39] As in the previous studies, only one minimum is found at the relativistic level, corresponding to the oxidative addition product. The binding energy increases by as much as 4.3 kcal mol^{-1} on inclusion of the spin−orbit effects. Interestingly too, the bond angle increases when going beyond first-order perturbation theory and to a greater extent when spin−orbit effects are included. This points, in particular to the fact that relativistic effects, including the spin−orbit ones, are quite important in order to describe H_2 dissociation on Pt properly.

Since spin−orbit effects were computed to be much larger for $[PtH]^+$ [49] than for for $[PdH]^+$,[57] they have been included (via the relativistic configuration interaction method) for $[PtH_2]^+$ only in the CASSCF/MRSDCI study that Balasubramanian has performed on $[PtH_2]^+$ and $[PdH_2]^+$.[63] The results of this study are quite interesting: At the spin-free level, the $^2A_1$ ground-state potential energy curve of $[PtH_2]^+$ has two minima, the lower one with a bent geometry (as in PtH_2, the H−Pt−H bond angle and Pt−H distance amounting to 81° and 1.53 Å, respectively) and another one corresponding to a $[Pt^+-H_2]$ molecular dihydrogen complex (with H−Pt−H = 30° and Pt−H = 1.73 Å), but 11.1 kcal mol^{-1} above. When spin−orbit effects are included a significant mixing of the $^2A_2$ state, which is nearly degenerate with the $^2A_1$ state at low H−Pt−H angles, lowers the dihydrogen complex which becomes the new ground state (with H−Pt−H = 22° and Pt−H = 2.10 Å). The bent structure (with H−Pt−H = 76° and Pt−H = 1.54 Å) is now slightly higher by 1.4 kcal mol^{-1}. Thus, the effects of spin−orbit coupling are particularly crucial in this system, bringing a differential effect of 0.54 eV, i.e., 12.5 kcal mol^{-1}. For $[PdH_2]^+$, only the dihydrogen complex is found on the $^2A_1$ ground-state potential energy curve. The dissociation energy of $[PtH_2]^+$ to Pt^+ (^2D) + H_2, 28 kcal mol^{-1} was not computed in the absence of spin−orbit effects, but Balasubramanian argues that due to the weakly bound nature of the minimum, the spin−orbit stabilization should be quite similar on both sides. This rather large value (compared to the value of 9.3 kcal mol^{-1} computed for $[PdH_2]^+$) is due the relativistic mass velocity effects (the spin free ones) which stabilize the (n+1)s orbital and make it more prone to accept electron density from H_2.

At this stage, some reference to experimental results is appropriate. There has been one report of the isolation of the Pd−H_2 system at low temperature in rare-gas matrices and its characterization by vibrational spectroscopy.[64] According to this study, the η^1-H_2 and the η^2-H_2 structures are close in energy and the presence of one or another is quite dependent on the nature of the rare gas (either Kr or Xe). Unfortunately the most recent calculations that include spin−orbit effects did not address this question and considered only a side-on C_{2v} geometry. Among the investigations that were carried out prior to 1990, the SCF calculations of Nakatsuji and Hada[52] favored the side-on geometry. On the one hand, Jarque et al.[53] did find (when electron correlation is taken into account through configuration interaction calculations) a minimum on the potential energy curve for the end-on approach, this minimum being comparable in energy to the side-on one. Clearly some additional high-level calculations are needed on this topic. For the PdH_2^+ system where experiment could not definitively ascertain whether it corresponds to a bent $^2A_1$ molecular adduct or to a linear $^2\Sigma$ state,[65] the results of the CASSCF/MRSDCI calculations of Balasubramanian and Das that were reported in this joint experimental/theoretical study gave more evidence in favor of the molecular adduct.[65] Finally, one should mention here that unlike the bare platinum atom, there is a known example of a *complex* of Pt(II) which binds H_2 as a dihydrogen ligand, viz. the $[PtH(P^tBu_3)_2]^+$ cation.[66] The adduct has been characterized by NMR and its structure deduced from an MP2 geometry optimization on the $[Pt(H_2)H(PH_3)_2]^+$ model system. The computed binding energy of H_2 to $[PtH(PH_3)_2]^+$ is rather large, 16 kcal mol^{-1}.[66]

B. Bare Metal–Ligand Complexes

1. Metal Halogen Complexes

Siegbahn[20,67] has considered the PdF_n and $PdCl_n$ (n = 1, 2) systems in the framework of a comparative study of the bond strengths of the second-row transition-metal hydrides, fluorides, and chlorides. The geometries were optimized at the SCF level (with the Hay−Wadt[68] small-core pseudopotential), the bonding and energetics being analyzed from an all-electron MCPF wave function (with mass−velocity and Darwin relativistic effects accounted for through first-order perturbation theory). Looking first at the mono-ligated systems, one finds that the binding energies vary in the order Pd−H (51.1 kcal mol^{-1}) < Pd−Cl (62.4 kcal mol^{-1}) < Pd−F (71.1 kcal mol^{-1}), the ground-state being in all three cases $^2\Sigma^+$. As expected, the bonding is dominatingly covalent for the metal hydride whereas there is a large contribution of ionic bonding for the halides, as demonstrated by the Mulliken electron populations. Furthermore, there does not seem to be an actual participation of the 3d orbitals to the bonding: On deleting the halogen 3d functions, the lowering of the binding energies is about the same for the fluoride and the chloride, ∼12−14 kcal mol^{-1}. This lowering is traced essentially to an inferior description of the affinity of the halogen atoms in the absence of such functions, which therefore act as polarization functions. Siegbahn also emphasized the repulsive nature of the interaction between the lone pairs of the halides and the 4d electrons of palladium. Thus, the question arises of what would be the effect of a second ligand: would the proper hybridization of the metal created by the first ligand be of some help for the binding of the second ligand or would the competition for the available metal covalency reduce the binding energy of the second ligand? The comparative study of the PdH_2, PdF_2, and $PdCl_2$ systems[67] gives interesting answers: the second hydrogen in PdH_2 is bound by 10.8 kcal mol^{-1} more than the first hydrogen, whereas the second fluorine in PdF_2 and the second chlorine in $PdCl_2$ are bound by 9.2 and 20.4 kcal mol^{-1} less

Table 1. Ground State, Equilibrium Bond Angle, and Binding Energy (in kcal mol^{-1}) of the Second Ligand for the PdXY (X = H, F, Cl; Y = F, Cl) and Pd(CH$_3$)Cl Sytems

system	state	bond angle	ΔE_2(H)	ΔE_2(F)	ΔE_2(Cl)	ΔE_2(CH$_3$)
PdH_2[a]	$^1A_1$	68.0	61.9			
PdF_2[a]	$^3\Pi_g$	180.0		62.0		
PdCl[a]	$^1A_1$	98.4			42.0	
PdHF[b]	$^1A'$	90.7	48.6	69.6		
PdHCl[b]	$^1A'$	85.6	52.9		62.8	
$Pd(CH_3)Cl$[b]	$^1A'$	94.5			64.8	42.1

[a] Reference 67. [b] Reference 69.

than the first fluorine and chlorine, respectively (the corresponding binding energy of the *second* ligand now varying in the order Pd−Cl (42.0 kcal mol^{-1}) < Pd−H (61.9 kcal mol^{-1}) ≈ Pd−F(62.0 kcal mol^{-1}). The greater binding energy for the second hydride is due to the fact that whereas Pd in its d^{10} ground state is not well prepared for binding the first hydrogen and has to be promoted to the d^9s^1 state, this d^9s^1 state is just the appropriate one for the *covalent* bonding of the second hydrogen. On the other hand, the $^2\Sigma^+$ ground state in Pd−F and Pd−Cl is not well prepared for the *ionic* bonding of a second halide, and there is therefore a promotion energy to reach a state with a singly occupied π orbital which has to be paid by the second halide. The bond strength of the second halide is therefore weaker than the first one. In fact, it turns out that $PdCl_2$ prefers the bent *covalent* $^1A_1$ structure (as in PdH_2) over the linear ionic structure (which is computed to be 1.7 kcal mol^{-1} above). PdF_2, on the other hand, adopts the linear $^3\Pi_g$ ionic structure. Note here than in contrast to PdH_2, the inclusion of relativistic effects is not necessary to account for the bent structure. Finally, although the chemical effect of the 3d functions on the halides is again not very important, the decrease of the binding energy upon deletion of the 3d functions is much smaller than for the monohalides (3.5 kcal mol^{-1} only for $PdCl_2$) This indicates that the *relative* effects of including these functions is not negligible and that at least one 3d function should be included in calculations on larger systems.

In the mixed PdHX systems (X = F, Cl),[69] the covalent bonding dominates, since for both systems the computed equilibrium structure is bent (the H−M−X angle amounting to 90.7° and 85.6°, respectively, i.e., close to the optimal 90° for covalent sd-hybridized bonds). The Pd−Cl bond is 20.8 kcal mol^{-1} weaker in PdHCl than the one in $PdCl_2$, whereas the Pd−H bond is only 9 kcal mol^{-1} weaker than the one in PdH_2. This again can be rationalized in terms of the various contributions of covalency and ionicity to the bonding. Table 1 summarizes some of the results of these studies on MH_2, MX_2, and MHX, together with some results obtained for MCH_3Cl. As expected, the Pd−Cl bond strengths are quite similar whereas the Pd−CH_3 bond is weaker than the Pd−H bond by 10.7 kcal mol^{-1}. This is due to the increased electron−electron repulsion of the metal d electrons with the CH_3 electrons. The GVB + CI calculations of Reynolds and Carter give a value of 12.3 kcal mol^{-1} for the energy difference between Pt−H and Pt−CH_3.[70]

Interestingly, the enhanced covalent bonding on going from metal fluoride to metal chloride has been also observed in $[PtF_6]^z$ and $[PtCl_6]^z$ ($z = 0, 1-, 2-$) by Macgregor in his DFT study of the redox potentials of third-row hexahalide complexes.[71] This effect may explain why on oxidation of $PtCl_6^-$, the chloride array would be oxidized rather than the metal center. Thus, on removal of one electron, the hypothetical $PtCl_6$ may have not been observed because of its instability with respect to Pt−Cl bond cleavage and formation of Cl_2. The energy of the process $PtCl_6 \rightarrow PtCl_4 + Cl_2$ is indeed computed to be exothermic by 1.2 kcal mol^{-1}, in contrast to the process $PtF_6 \rightarrow PtF_4 + F_2$ which is endothermic by 77.5 kcal mol^{-1}.[71] Note that since the geometry of the PtX_4 system was not optimized (but maintained at the geometry found for PtX_6), one expects the chloride reaction to be more exothermic and the fluoride reaction to be less endothermic. The value of 77.5 kcal mol^{-1} is quite large however, thus optimizing the PtX_4 geometry should not alter the conclusions.

In the above DFT study the Pt−Cl and the Pt−F bond lengths were optimized at the LDA level (with quasirelativistic corrections). The computed value for $[PtCl_6]^{2-}$, 2.38 Å, is found to be somewhat greater than the experimental average value, 2.34 ± 0.04 Å. In an attempt to test how gradient-corrected exchange correlation functionals perform for Werner-type transition-metal complexes, Deeth et al. have performed LDA and BP86 (with Becke's 88 exchange functional[72]) calculations on $[PtCl_6]^{2-}$ and $[PdCl_6]^{2-}$ (with a larger basis set, including d and f functions on the halides).[73] Although the optimized bond lengths are in better agreement with experiment at the LDA level, 2.36 Å instead of 2.42 Å at the BP86 level, the computed heterolytic bond dissociation energies show the reverse trend: 409 kcal mol^{-1} at the LDA level and 392 kcal mol^{-1} at the BP86 level, to be compared with average thermochemical data of 372 kcal mol^{-1}. A similar behavior is also found for $[PdCl_6]^{2-}$ (and for square-planar $[PdCl_4]^{2-}$, $[Pd(CN)_4]^{2-}$, $[Pd(H_2O)_4]^{2+}$ systems as well[74]). The agreement with experiment is better in this case; the corresponding values are LDA 428 kcal mol^{-1}, BP86 412 kcal mol^{-1}, experiment 416 kcal mol^{-1}. Note that the overestimation of the Pd−Cl bond length is not due to the crystal environment in experiments, since a calculation on $\{K_8[PdCl_6]\}^{6+}$ cluster yields values similar to the vacuo ones.[73] The difference between the LDA and BP86 heterolytic bond strengths is ascribed to a poorer description of the balance between covalent and ionic bonding at the LDA level: LDA seems to overestimate the covalent binding. The BP functional on the other hand give more ionic bonding than the LDA one. Thus, this study clearly shows how crucial a correct description of the balance between covalent and ionic bonding found by Siegbahn in the smaller system is. In line with all these results, the comparison between experimental deformation density maps and calculated ones for $K_2[PtCl_6]$ and $K_2[PdCl_6]$ (at either the HF or the SDCI level) shows an aspherical distribution of the d electrons caused by covalent bonding through the e_g orbitals.[75]

2. Metal σ-Donor Ligand Complexes

A few studies have been performed on the metal−phosphine bond. They give a quite detailed picture of the bonding and of the level of calculation needed to correctly account for this bond, traditionally viewed as being of dative type. In their study Pacchioni and Bagus[76] have considered the bare metal−ligand Pd−PX_3 system (X = H, F, CH_3, OCH_3) and the bis-ligand system *trans*-L−Pd−PX_3 with L = CO or NH_3. The investigation was limited in most instances to the HF level (with the small-core RECP of Hay and Wadt,[68] its associated basis set, and a relatively flexible basis set for the ligands). The SCF wave functions were analyzed by means of the constrained orbital variation (CSOV) technique, which allows one to separate σ and π effects. This shows that the d functions on phosphorus play a significant role in the bonding but essentially as polarization functions to favor the formation of hybridized π orbitals on P−X and not as genuine acceptor orbitals. All phosphine ligands considered in the study were found to act simultaneously as a σ donor and π acceptor, the alkylphosphine having an appreciable π acidity. Other components of the bonding include Pd polarization (via 4d hybridization with 5s and 5p orbitals) and electron−electron repulsion between Pd and PX_3. According to this analysis the polarization of the ligand by Pd is negligible. The σ donation varies only slightly as a function of X, in contrast to the π back-donation. That the σ-donor ability does not vary too much is at variance with the usual assumption, based essentially on the pK_a values of the phosphonium ions or on the measurement of the stretching frequencies of CO in $(CO)_nMPX_3$ as a function of X. But Pacchioni and Bagus showed that the proton affinities are not a good measure of the σ-bonding ability and that the ν_{CO} shifts can be correlated to the π acidity only. This study has been extended by Fantucci et al.[77] who have included correlation effects (at either the MP2 or BP86-DFT level) and assessed the importance of relativistic effects in the DFT calculations on $Pt(PX_3)_2$ (X = H, F). It has been argued on the basis of these calculations that there is a strong interplay of polarization, correlation, and relativistic effects. Thus, the previous analysis of Pacchioni and Bagus is somewhat oversimplified. Pt sd rehybridization through relativistic effects seems to be quite essential for a reliable prediction and according to Fantucci et al.[77] is largely underestimated by the RECP approach.

The most extended methodological study carried out to date on such dative bonds is the one of Yates and co-workers.[78] They considered several ECPs and basis sets and various post-Hartree−Fock methods (up to the QCISD(T) and CCSD(T) level) and compared them to DFT methods with either a local density functional (S-VWN) or a nonlocal one (B-LYP). If a reasonable bond length can be obtained at a moderate level of calculation (e.g., at the MP2 or at a nonlocal DFT level with a valence double-ζ basis set including polarization functions on phosphorus), reliable energetics are much more difficult to achieve. The energy of the model reaction Pd−PH_3 + CO → Pd−CO + PH_3 was computed. To obtain a reliable value, a rather large and well-balanced basis set between the metal and the ligand is apparently required, together with a high level of calculation, either QCISD(T) or CCSD(T). The DFT calculations seem to greatly overestimate the reaction energy. Thus, recourse to some additivity scheme has been proposed if such high-level calculations cannot be performed when dealing with larger systems. One should stress, however, that the quest for reliability was hampered by the fact that no experimental value is available. Moreover, to assess differential effects it would have been desirable to get bond dissociation energies for Pd−PH_3 and Pd−CO.

At this stage it might be worth emphasizing that the $Pd(PX_3)_n$ systems which have been thoroughly analyzed by quantum chemical methods contain relatively small phosphine ligands. Going to larger phosphine ligands can be done through the use of integrated MO + MM methods. We will not discuss this topic since it is the subject of a review in the present issue. Let us simply mention the calculations on $Pt(PR_3)_2$ (with R = Me, ^{t}Bu, and Ph).[79] It would be interesting to see how such methods can perform on the $M(P^tBu_2H)_3$ system (M = Pd, Pt). SCF calculations have been performed on the Pt system[80] for which a crystal structure exists. They account, in particular, for the fact that the P−H atom lies in the coordination plane, as a result of steric hindrance and not because of Pt···H agostic-type interactions.

The bonding of Pd to NH_3 is similar to the one to PH_3 (although in this case the π back-donation is unlikely). This bonding has been discussed by Blomberg et al. in the context of the N−H bond oxidative addition to second-row transition-metal atoms (since the primary event in this reaction is the formation of a molecular precursor of NH_3 with the metal).[81] The geometry optimization was performed at the SCF level only, whereas the energetics were obtained at the MCPF level. Thus, the computed Pd−N bond length may be too long by about 0.10−0.15 Å. The energetics were computed at the MCPF level and at the CCSD(T) level with a large basis. It is noteworthy that the CCSD(T) level of theory increased the binding by 1 kcal mol^{-1} only, up to 17.6 kcal mol^{-1}. Blomberg's view of the Pd−NH_3 bonding uses valence-bond-type arguments and is similar to the one put forth for metal monocarbonyls. The bonding is described as resulting from a balance between the electron−electron repulsion between the ligand and the metal on one hand, and an electron−nuclear attraction between the lone-pair electrons and a partially unshielded core on the other hand. This unshielding is obtained through the mixture of the low-spin coupled d^9s^1 state into the d^{10} state. Of the two hybrids that form, one points toward the lone pair and the other is perpendicular to the metal−ligand bond, Figure 1. By placing two electrons in the latter the repulsion is decreased. This picture also holds for the Pd−H_2O system which has been studied by the same authors,[82] although the binding energy is smaller, 5.4 kcal mol^{-1}, due to the presence of two tight lone pairs instead of a diffuse one for NH_3. It can be easily reconciled with MO theory language: one would speak of a four-electron repulsive interac-

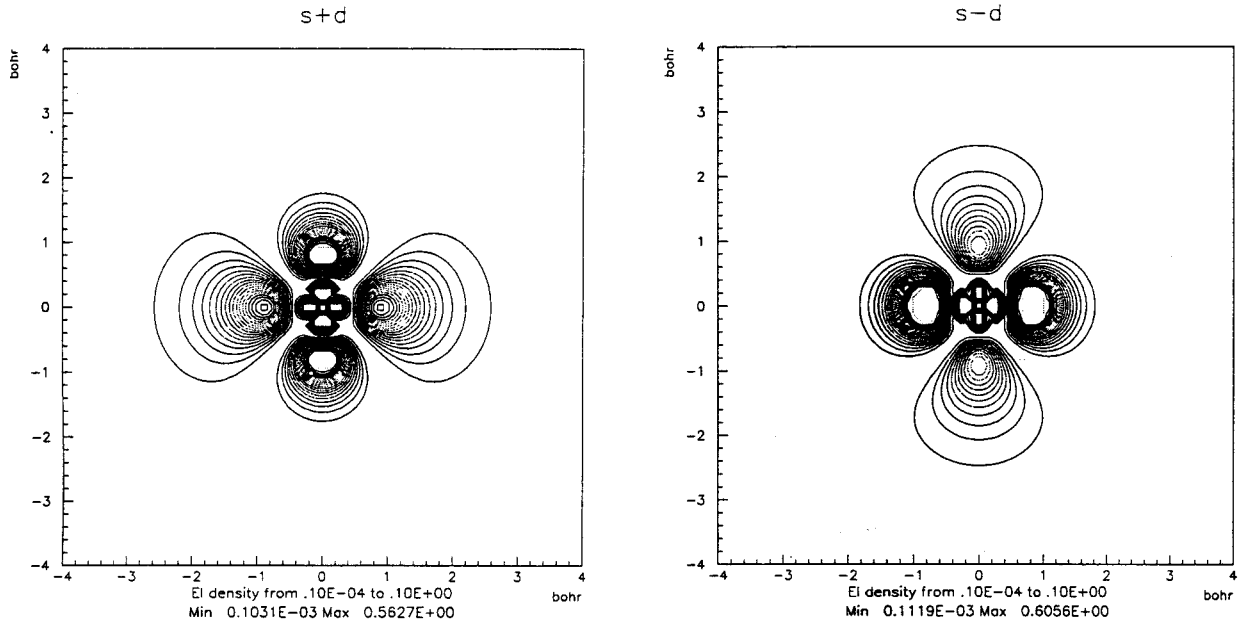

Figure 1. The s + d and s − d hybrids. (Reprinted with permission from Blomberg et al. *New J. Chem.* **1991**, *15*, 727.)

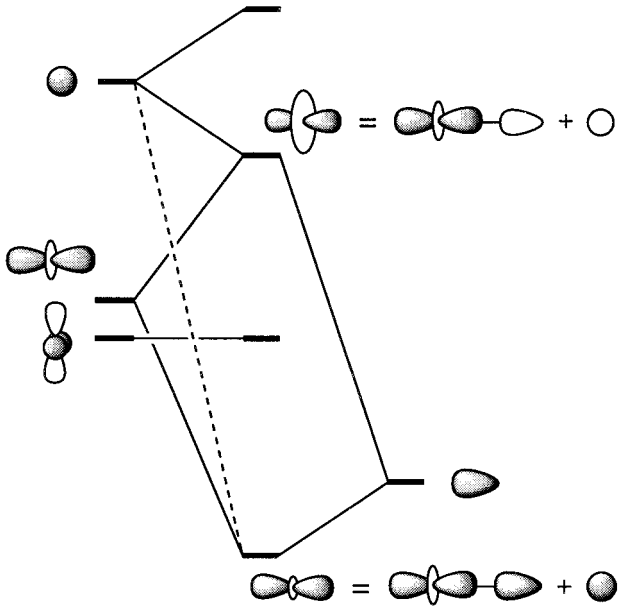

Figure 2. Schematic molecular orbital interaction diagram for a metal to ligand interaction.

tion between the doubly occupied d_{z^2} orbital and the σ lone pair, decreased by the mixing with the empty 5s orbital, Figure 2. The resulting hybridized orbitals shown in Figure 2 are nothing other than the two hybrids mentioned above. Note, however, that this MO picture considers only the repulsion between the 5σ(CO) and the d_{z^2} orbitals, in contrast with Blomberg's picture where the whole electron−electron repulsion is more correctly taken into account.

3. Metal Carbonyl and Nitrosyl Complexes

Following the active research that had concentrated on the description of the bonding in Pd−CO prior to 1990 (see ref 83 for a short review), a few more studies have appeared since. Smith and Carter performed a comparative study of MCO and MNO (M = Pd and Pt) at the GVB + CI level.[84] For Pd−CO, the closed shell $^1\Sigma^+$ ground state is bound by 27.2 kcal mol^{-1}, in reasonable agreement with the value of 33 kcal mol^{-1} obtained previously by Siegbahn and which could be considered as a reference.[85] It is not clear, however, whether the value of 27.2 kcal mol^{-1} refers to a calculation with a large-core pseudopotential or with a small-core pseudopotential for which an additional lowering of 6.4 kcal mol^{-1} was mentioned in the Calculational Details section. The next two excited states $^3\Sigma^+$ and the open-shell $^1\Sigma^+$ state are much higher in energy and unbound with respect to the ^{1}S Pd ground state.

Bauschlicher and co-workers have looked at the cationic systems $[Pd(CO)]^+$ and $[Pd(CO)_2]^+$ in the framework of an ab initio study on the first- and second-row transition-metal mono- and dicarbonyl positive ions.[86] Although the bonding in these systems can be described along the lines used for their neutral analogues (i.e., with the sd-hybridization mechanism to reduce the electron−electron repulsion), the π back-donation effects are very small due to the positive charge and thus the bonding is dominated by the electrostatics. The calculations have been carried out at the MCPF level using a small-core pseudopotential[68] and a rather large polarized basis set (on the ligands as well as on the metal). They can, therefore, be considered as quite reliable and used as a benchmark (vide infra). For $[PdCO]^+$ the optimized Pd−C bond length is 2.29 Å, i.e., larger than in the neutral system as a consequence of the reduced Pd → CO back-donation. The dissociation energy found for $[PdCO]^+$, 31.5 kcal mol^{-1}, is of the same order of magnitude as the one computed by Siegbahn and co-workers for PdCO.[85] For the dicarbonyl system $[Pd(CO)_2]^+$, the computed dissociation energy of the second carbonyl amounts to 27.6 kcal mol^{-1}, i.e., slightly less than the dissociation of CO in $[PdCO]^+$.

PtCO was also considered in the work of Smith and Carter:[84] it has the same closed-shell $^1\Sigma^+$ ground state as PdCO and the same first two excited states,

Table 2. Summary of the Main Results Obtained for the First Bond Dissociation Energies (in kcal mol^{-1}) of Pd(CO)$_n$ and Pt(CO)$_n$

system	PdCO	$Pd(CO)_2$	$Pd(CO)_4$	PtCO	$Pt(CO)_2$	$Pt(CO)_4$	ref
MCPF	33[a]						85
GVB + CI	27.2[b]			18.5[b]			84
CASSCF + CI				49.9[b] (38.0[c])			88
MP2			14.5[b]			18.8[b]	96
CCSD(T)			7.5[d,e]			10.9[d,f]	96
LDA-DFT	71.0[g]						83
			25.9[h]			20.4[h]	91
NL-DFT	49.8[g]						83
	48.4[i]			65.0[i]			90
			12.3[j]			15.7[j]	91
			13.1[k]			13.4[k]	95
experiment				77 ± 12			89

[a] The relativistic effects are estimated via first-order perturbation theory. [b] Using a relativistic pseudopotential. [c] Including spin−orbit correction. [d] ΔH_0 value. [e] The ΔE value is 7.8 kcal mol^{-1}. [f] The ΔE value is 12.1 kcal mol^{-1}. [g] Using a relativistic model potential. [h] No relativistic effects included. [i] Relativistic effects obtained via a two-component transformation. [j] Relativistic effects accounted for via the quasirelativistic method. [k] Using a relativistic pseudopotential.

although $^3\Sigma^+$ is comparatively much lower (at 7.4 kcal mol^{-1} instead of 20.7 kcal mol^{-1} in PdCO) due to the preference of Pt for the ^{3}D ground state. In the $^1\Sigma^+$ state, Pt is promoted from the ^{3}D to the ^{1}S state in order to avoid the electron−electron repulsion between the 5σ of CO and the 6s orbital. Thus, the computed dissociation energy of PtCO to the ground state of Pt is much lower (18.5 kcal mol^{-1} only) than the Pd−CO dissociation energy. Although this value is much lower than the previous theoretical estimates, it was claimed to be more reliable since it arose from the most highly correlated wave function used to date. However, CASSCF calculations[87] followed by MRSDCI calculations,[88] which were performed later by Roszak and Balasubramanian, led to a value of 42.9 kcal mol^{-1} (with respect to ground state of Pt), which upon inclusion of the unlinked quadruple clusters contribution through the Davison correction rose to 49.9 kcal mol^{-1}.The inclusion of the spin−orbit coupling effects, which are particularly important for the excited states of PtCO (the ones which correlate with Pt ^{3}D), lowers the dissociation energy to about 38 kcal mol^{-1}. But this value is still higher than the one of Smith and Carter. Moreover, a recent experimental estimate is much higher, 77 ± 12 kcal mol^{-1}.[89]

Some DFT studies have also been performed on PdCO and PtCO. The study of Papai et al.[83] on Pd(CO) and $Pd(CO)_2$, although being primarily aimed at a comparison with Rh(CO) and $Rh(CO)_2$, allows assessment of the performance of DFT calculations, carried out with either a local or a nonlocal (i.e., gradient corrected) exchange correlation potential. The nonlocal (NL) exchange correlation potential seems to give reasonable Pd−C bond lengths, 1.92 Å, when compared to the value obtained by Smith and Carter, 1.96 Å,[84] or to the value of Blomberg et al.,[85] 1.91 Å. For the dicarbonyl system, the linear structure predicted by experiment is only found at the nonlocal level.

No definite conclusion can be drawn for the bond dissociation energies. The NL computed bond dissociation energy for PdCO, 49.8 kcal mol^{-1},[83] is much higher than Blomberg's value. The binding energy of the second CO, 39.9 kcal mol^{-1}, is reduced compared to the bond dissociation energy in PdCO. This has been ascribed to a weaker π back-donation. The calculations of Papai et al.[83] carried out for the ions $[Pd(CO)]^+$ and $[Pd(CO)_2]^+$ yield values that are also much higher than the values obtained by Bauschlicher[86] at the post-Hartree−Fock level. On the other hand, Rösch and co-workers have obtained through gradient-corrected relativistic DFT calculations a value for PdCO of 48.4 kcal mol^{-1}.[90] More importantly, their value for the Pt−CO bond dissociation energy (to Pt ^{3}D), 65.0 kcal mol^{-1}, is at the lower range of the experimental estimate. It is still higher than the spin-free value (49.9 kcal mol^{-1}) of Roszak and Balasubramanian, however. Clearly more work is needed on both the experimental and theoretical sides to assess definitively the correct value of the bond dissociation energies in PdCO and PtCO. The propensity of the NL-DFT level to yield values of the Pd−CO bond dissociation energy that are larger than the post-Hartree−Fock ones might explain the results of Yates et al.[78] (vide supra), that the reaction energy for the $Pd-PH_3 + CO \rightarrow Pd-CO + PH_3$ process is too large in their NL-DFT calculations (by about 7 kcal mol^{-1} when compared to CCSD(T) calculations).

Li, Schreckenbach, and Ziegler have carried out an extensive NL-DFT study of the first bond dissociation energy in $Pd(CO)_4$ and $Pt(CO)_4$ (and in $Ni(CO)_4$ as well).[91] Relativistic effects were included, either through first-order perturbation theory[92,93] or through the quasirelativistic method.[94] They increase the bond dissociation energy by as much as 12 kcal mol^{-1} in the platinum case. For palladium, the effect is less crucial, the increase being only 1.4 kcal mol^{-1}. The calculations of Jonas and Thiel,[95] that use the same DFT functional but a quasirelativistic pseudopotential together with a rather large basis set (of valence triple-ζ quality and supplemented by two polarization functions on the carbon and oxygen atoms), yield about the same results, Table 2. Concomitantly, Frenking et al.[96] performed a similar study at the MP2 and CCSD(T) levels with a relativistic small-core pseudopotential[68] and a rather flexible basis set. As shown in Table 2, the MP2 level overestimates the bond dissociation energy. Taking the CCSD(T) value as a reference, one sees that, as for the mono- and dicarbonyls (vide supra), the NL-DFT value is

also slightly overestimated (by about 5 kcal mol^{-1}). The vibrational spectra of $[Pd(CO)_4]$ and $[Pt(CO)_4]$ have been calculated also by Jonas and Thiel.[95] The comparison with experimental data—when available—shows deviations on the order of 20−30 cm^{-1} only (except in one unexpected case), thus underlying the overall satisfactory performance of the DFT-BP86 calculations. Similar calculations have also been performed recently by the same authors on the yet unknown $[Pt(CO)_6]^{4+}$ system in the context of a general study on octahedral transition-metal hexacarbonyls.[97]

4. Metal Oxide and Methylidene Complexes

Metal oxide and metal carbene complexes have been investigated quite extensively by a few groups. One of the characteristics of the metal oxide molecule is the presence of several states of similar energies arising from different occupations of the highest lying molecular orbitals of σ and π symmetry. Thus, one finds two triplets $^3\Pi(\pi^{*3}\sigma^{*1})$ and $^3\Sigma^-(\pi^{*2}\sigma^{*2})$ and three singlets $^1\Sigma^+(\pi^{*2}\sigma^{*2})$, $^1\Delta(\pi^{*2}\sigma^{*2})$, and $^1\Sigma^+(\pi^{*4})$. For [PtO], the most recent experimental data agree on the $^3\Sigma^-$ ground state,[98,99] but for [PdO], the ground state is not known. Calculations by Schwerdtfeger et al.,[100] either at the MP2 level or at the CISD level, predicted the $^3\Pi$ level, at variance with earlier calculations by Bauschlicher et al.[101] that led to the conclusion that the $^3\Sigma$ and $^3\Pi$ states are very close in energy.

The palladium oxide and palladium dioxide molecules have been analyzed by Siegbahn along the same lines as the palladium chloride molecule, again in the framework of a study of the entire second-row transition metals.[102,103] The computational procedure was the same as that in the dichloride study, except for [PdO] for which a CASSCF calculation followed by a multireference ACPF calculation was necessary to describe near degeneracy effects. For this system the $^3\Sigma^-$ ground state is almost degenerate with the $^3\Pi$ state, the energy difference between the two states being only 0.3 kcal mol^{-1}. The $^3\Sigma^-$ ground state corresponds to covalent bonding between a neutral Pd atom in a $[d_\sigma^2 d_\delta^4 d\pi^3 4s^1]$ state and oxygen in a $(p_\sigma^1 p_\pi^3)$ configuration, leading to the $[1\sigma^2 2\sigma^2 1\delta^4 1\pi^4 2\pi^2]$ configuration. Thus, despite its quite large length, 1.85 Å, the Pd−O bond can be considered as a double bond. Note that in addition to the repulsion between the lone pair and the 4d electrons, the promotion energy from the d^{10} ground state of Pd to the d^9s^1 state contributes to a relatively weak binding energy of 47.7 kcal mol^{-1}. This computed value is too small, however, compared to the experimental value of 67.3 kcal mol^{-1}.[104] Increasing the active space in the multireference ACPF calculations led to an improved value of 55.2 kcal mol^{-1}. The remaining difference, 12 kcal mol^{-1}, points to the difficulty of treating second-row metal oxides. For the dioxide system, a linear geometry with a $^3\Pi_g$ ground state is found, corresponding to two double bonds.[103] The Pd−O bond in $[PdO_2]$ is indeed shorter than that in [PdO], 1.75 Å instead of 1.85 Å. The binding energy for the second oxygen is slightly smaller, 41.5 kcal mol^{-1}. The study on the metal oxides also includes a comparison with the metal superoxides and peroxides.[103] Both palladium peroxide and palladium superoxide molecules are hardly bound, by 3.4 and 4.4 kcal mol^{-1}, respectively. This is due to strong repulsive interaction between the occupied π_u orbitals of O_2 and the 4d electrons which almost cancels the covalent interactions with the π_g orbitals.

Subsequent investigations on [PdO] have been performed at the DFT level. In their study Rösch and co-workers have used either a local or a nonlocal form of the exchange correlation potential and have included spin-free relativistic effects.[90] Their data allow one to compare the nonrelativistic and the relativistic results. At the nonlocal level and with the relativistic effects included, the binding energy amounts to 62 kcal mol^{-1}, in better agreement with experiment than Siegbahn's value (the computed bond lengths are similar). The $^3\Sigma^-$ state is the ground state, the $^3\Pi$ state lying 6.5 kcal mol^{-1} above. The nonrelativistic local and nonlocal calculations of Broclawick et al. yield a $^3\Pi$ ground state, but the $^3\Sigma^-$ state is quite close in energy, less than 1 kcal mol^{-1} above.[105] However, according to Broclawick, the state reversal cannot be linked entirely to the relativistic effects since no reversal in the $^3D-^1S$ ordering was observed on inclusion of the relativistic effects in the work of Rösch and co-workers.

Both DFT studies do agree with the importance of the covalent component in the bonding picture, as shown by the CASSCF/ACPF calculations of Siegbahn, although the ionicity seems to be greater at the DFT level. According to the Mulliken population analysis, the charge on oxygen ranges from −0.35 to −0.46 in the DFT calculations and is −0.14 in the CASSCF/ACPF calculations. One should keep in mind, however, the limitations of the Mulliken population analysis.

Rösch and co-workers have also considered the [PtO] molecule.[90] As for [PdO], a $^3\Sigma^-$ ground state is obtained, in agreement with the most recent experimental data. This result is, however, at odds with the one obtained by Baerends and co-workers,[106] who on inclusion of the spin−orbit interaction found the $\pi_{1/2}^2\sigma_{1/2}^2$ state corresponding to the $^1\Sigma$ ground state. Rösch finds the bonding in [PtO] much more covalent than in [PdO], especially when the relativistic effects are included. The computed binding energy, 104.7 kcal mol^{-1}, is also much greater than in [PdO].

Covalency is also an essential part of the bonding mechanism in $PdCH_2$ and $PtCH_2$. However, since in the C_{2v} moiety the π degeneracy is broken, the formation of two covalent bonds leads to a $^1\Sigma^+$ ground state. The binding energy of $PdCH_2$ computed by Siegbahn, 50 kcal mol^{-1},[102] is quite similar to the one computed for PdO. This is probably too low, since a CCSD(T) benchmark calculation carried out with a larger and more flexible basis set (especially for the polarization functions) yielded a value of 58 kcal mol^{-1}, of which 6.2 kcal mol^{-1} has been traced to the configuration space improvement. In addition, a value of 58.2 kcal mol^{-1} can be inferred from the difference between the PCI-80 energies obtained later for the two processes $CH_4 \rightarrow CH_2 + H_2$ and $Pd + CH_4 \rightarrow PdCH_2 + H_2$.[107] One can compare these values to the CCSD(T) values obtained by Frenking for the

dissociation energies of CH_2 in $[Pd(CO)_3(CH_2)]$ and $[Pt(CO)_3(CH_2)]$, which amount to 35.6 and 51.4 kcal mol^{-1}, respectively.[108] The $PtCH_2$ system is much more strongly bound since a binding energy of 99.1 kcal mol^{-1} has been computed at the PCI-80 level (with zero-point corrections and inclusion of the spin−orbit effects).[109]

More theoretical work has been devoted to the cationic $[PdCH_2]^+$ and $[PtCH_2]^+$ systems, especially to $[PtCH_2]^+$, since this system has been identified as being the primary product of the gas-phase reaction of Pt^+ with CH_4. Bauschlicher et al. have considered $[PdCH_2]^+$ within the whole series of second-row transition-metal methylidene ions.[110] The bonding in $[PdCH_2]^+$ is as in $PdCH_2$: two covalent bonds are formed in the $^2A_1$ ground state, the σ bond involving an s + d hybrid. That the s contribution to the bonding is important is best seen from the linear relationship between the binding energies and the promotion + exchange energy loss (for an enlightening account of this concept, we refer the reader to refs 111 and 112). The unpaired electron lies in the s − d hybrid in order to maximize the electrostatic bonding and to reduce the metal−ligand repulsion. The MCPF computed binding energy is 67.5 kcal mol^{-1} (which according to Bauschlicher may be slightly too low, due to the propensity of the MCPF theory to underestimate double-bond energies). Bauschlicher's best estimate after applying a correction is 70 ± 3 kcal mol^{-1}. Note that the electrostatic energy computed from a model where the metal cation is replaced by a point charge is 64 kcal mol^{-1}. Siegbahn et al. have also calculated this binding energy in their assessment of the performance of the PCI-80 method:[113] they found a value of 72.0 kcal mol^{-1} in very good agreement with a more recent experimental estimate of 70.1 ± 3.9 kcal mol^{-1}. Interestingly, a gradient-corrected DFT calculation with a large basis set yields a value of 73.5 kcal mol^{-1}.[114]

Larger values have been obtained for the third-row analogue $[PtCH_2]^+$. Goddard's calculations gave, at the CASSCF/MRSDCI level, a dissociation energy of 113.3 kcal mol^{-1} for the $^2A_1$ ground state.[111] A correction, based on the comparison between theoretical and experimental values for $[LaCH_2]^+$, $[TaCH_2]^+$, $[WCH_2]^+$, $[OsCH_2]^+$, and $[AuCH_2]^+$ was applied, leading to the value of 123 ± 5 kcal mol^{-1}. Note that the more recent experimental value, 115 ± 4 kcal mol^{-1},[115] is closer to the uncorrected value. Whatever the exact value is, it is much greater than that for Pd^+. This is due to a much higher promotion + exchange energy loss cost in Pd^+ (89.9 kcal mol^{-1}) compared to Pt^+ (33 kcal mol^{-1}) and, in particular, to a much greater promotion energy for Pd^+, 73.6 kcal mol^{-1} vs 18.0 kcal mol^{-1} for Pt^+ (averaged over all J values). In fact, both "intrinsic" bond energies (according to the definition of Goddard, $D^{\text{intrinsic}} = D_0{}^{\text{actual}} + \Delta E^{\text{promotion}} + \Delta E^{\text{exchange}}$) would be similar.

That the bond energy is much higher for Pt^+ than for Pd^+ is a key feature of the $M^+ + CH_4 \rightarrow [MCH_2]^+ + H_2$ reaction, which can only proceed exothermically if the bond dissociation of $[MCH_2]^+$ exceeds 111 kcal mol^{-1}. Schwarz has also analyzed the various factors that account for this difference in a comparative DFT study.[62] Three functionals have been employed ranging from the local density approximation (LDA) to the LDA augmented by Becke's gradient correction to the exchange functional[72] and to the LDA + Becke and Perdew[116] corrections for the exchange correlation functional. Spin-free relativistic effects were accounted for using the quasirelativistic scheme of Ziegler, Baerends, et al.[94] All these DFT functionals yielded a value for the promotion energy of Pd^+ and Pt^+ which is too high (respectively, by 5.3 and 14.5 kcal mol^{-1} at the relativistic level). Yet the computed bond dissociation energies were too high, 92.2 and 130.8 kcal mol^{-1}, thus suggesting the propensity of these DFT methods to overestimate the "intrinsic" contribution to the dissociation energies. The comparison between the nonrelativistic calculations and the relativistic ones clearly showed the role of the spin-free relativistic effects: by stabilizing the metal s orbital and destabilizing the metal d orbitals much more for Pt than for Pd, they decrease the promotion energy.

Since the relativistic effects are especially important for $[PtCH_2]^+$ and since only the spin-free ones were taken into account in the above study, Dyall, Schwarz, and co-workers have thoroughly investigated both the spin-free and the spin-dependent relativistic effects by carrying out four-component Dirac−Fock calculations in conjunction with a MP2 treatment of electron correlation.[117] The study has been carried out along the same lines as the one on Pt−H. In particular, the spin-free and spin-dependent effects have been separated. In addition, MP2 and spin-unrestricted coupled cluster calculations (at the UCCSD(T) level) were performed with a relativistic small-core pseudopotential (either the one of Hay and Wadt[68] or the one of Christiansen et al.[118]). The spin-free effects obtained here are analogous to those of the quasirelativistic DFT study. The spin−orbit interaction strengthens the covalent double bond by increasing the 5d content of the σ bond (since the $5d_{3/2}$ orbital is lowered in energy through the splitting of the d shell) and by reducing the promotion cost of the $5d_{5/2}$ to the 6s orbital. There is about 50% quenching of the spin−orbit interaction in $[PdCH_2]^+$: the spin−orbit interaction stabilizes Pt^+ by 9.6 kcal mol^{-1} but reduces the bond dissociation energy to $Pt^+ + CH_2$ by only 5.6 kcal mol^{-1}. Interestingly, the MP2 and the CCSD(T) bond dissociation energies are almost identical, 110.2 vs 109.6 kcal mol^{-1}, respectively, with the Hay−Wadt pseudopotential and 105.4 vs 105.9 kcal mol^{-1} with the Christiansen pseudopotential. When corrected by the spin−orbit stabilization of 5.6 kcal mol^{-1}, the latter yields a value of 100.3 kcal mol^{-1} that compares well with the MP2/Dirac−Fock value of 100.8 kcal mol^{-1}. However, it is still 15 kcal mol^{-1} lower than the experimental value.[115] It is also of interest to note that in this case (as has been noted for $[NiCH_2]^+$) the B3LYP spin−orbit corrected value fits of 110.0 kcal mol^{-1} better with experiment. In fact, the overestimation of the energies of the covalent bonds by DFT compensate for other deficiencies (such as basis set deficiencies).

5. Other Bare Metal–Ligand Interactions

The interaction of other ligands with bare palladium or platinum has been the subject of some investigations. Salahub and co-workers have performed a DFT study (with local and nonlocal exchange correlation functionals) of $PdCO_2$.[119] Although no complex of this type has been isolated, it is known that CO_2 can interact with palladium surfaces. CO_2 is also known to actively take part in reactions mediated or catalyzed by palladium complexes. After the calculations of Salahub, an η^2-CO_2 complex of $Pd(PMePh_2)_2$ has been characterized spectroscopically.[120] Indeed, the calculations ended with the η^2-coordination mode as the most stable one, 8.4 kcal mol^{-1} lower than the η^1-C coordination mode (NL level value). The computed asymmetric stretch, 2018 cm^{-1}, was found to be very different from the experimental one for CO_2 on a H_2O/Pd(110) surface, viz. 1631 cm^{-1}. Salahub and co-workers noticed a large sensitivity on the surface type. The IR bands of the coordinated CO_2 in $[Pd(PMePh_2)_2(CO_2)]$ are observed at 1658 and 1634 cm^{-1}.[120] However, one might expect a greater charge transfer in the bisphosphine complex than in the bare $PdCO_2$ system, since the d_π orbital which donates electrons into the π^* orbital of CO_2 is strongly destabilized by the two phosphine ligands.[121] Yet the structure of the $[Pd(PH_3)_2(\eta^2\text{-}CO_2)]$ system that has been computed recently at the NL-DFT level has the carbon dioxide more distant from the palladium atom than in $PdCO_2$.[122] This may reflect a greater electron−electron repulsion from the $Pd(PH_3)_2$ unit compared to Pd alone. The two C−O bond lengths are shorter in $[Pd(PH_3)_2(CO_2)]$ than in $PdCO_2$, implying less π back-donation. One should stress, however, that the computational characteristics are different in these two calculations, in particular the calculations of $[Pd(PH_3)_2(CO_2)]$ did not incorporate nonlocal exchange and correlation corrections in the geometry optimization procedure. It would be interesting to have a comparison between calculations carried out with the same methodological procedure. The reduction product $[Pd(PH_3)_2(CO_2)]^-$ has been also investigated.[122] Its structure corresponds to an η^1-CO_2 coordination mode consistent with a singly occupied orbital made of the Pd $5p_z$ orbital and of the π^*CO_2 orbital (which is highly localized on the in-plane p orbital of the central carbon atom). In the context of the structure of the bare $PdCO_2$ complex, it is worth mentioning that the geometry of the isoelectronic Pd(allene) complex that has been optimized by Blomberg et al. (at the HF level) also displays an η^2-coordination mode.[107]

MCSCF calculations have been carried out on the $[PtCN]^-$ and $[PtNC]^-$ systems[123] to model the properties of CN^- adsorbed on a platinum electrode, using the large-core relativistic pseudopotential of Hay and Wadt[124] and a polarized ANO basis set for CN. They yield $[PtCN]^-$ being more stable than $[PtNC]^-$ by 25.4 kcal mol^{-1}. The difference in the corresponding vibrational frequencies (2244.5 cm^{-1} in $[PtCN]^-$ and 2197.8 cm^{-1} in $[PtNC]^-$) has been taken as an argument to support the experimental proposal of the existence of two distinct adsorption processes, one via C and the other via N. Similar results were obtained from subsequent calculations carried out at the DFT level (using the B3PW91 hybrid exchange correlation functional).[125] It is noteworthy that for the pseudo-tetrahedral $[Pt(CO)_3(CN)]^-$ and $[Pt(CO)_3(NC)]^-$ systems, a comparable bond dissociation energy difference of 18.4 kcal mol^{-1} has been computed at the CCSD(T)//MP2 level by Frenking and co-workers. For the corresponding Pd systems, the energy difference is somewhat smaller, 12 kcal mol^{-1}.[108]

Many-body calculations of the core hole spectrum and of the valence photoemission of $[PdN_2]$ system have been performed.[126,127] The results have been compared to [NiCO], $[NiN_2]$, and [PdCO]. Hall and co-workers have carried out a DFT-B3LYP study of the various isomers of $[PdC_x]^+$ ($x = 3-24$), in connection with experimental ion mobility studies.[128] For $x < 10$, linear clusters are preferred over ring-containing structures. The monocyclic rings become more stable beginning at $x = 11$ and are close in energy to each other. Thus, the calculations predict for the ion mobility studies a shift in the nature of the dominant isomer at $x = 10$. For larger cluster with $x = 20$ and 24 the $2 + 2$ adducts are less stable than the cyclic rings (because of added ring strain). However, all these isomers are less stable than the graphitic sheets.

Siegbahn has analyzed and computed for the entire second-row of transition metals the metal−carbon bond strength for ligands that are representative of various hybridization on carbon, of different steric and electronic requirements.[129,130] The Pd−C bond dissociation energy increases along the series $Pd-CH_3 < Pd-C_2H_3 < Pd-C_2H$ by as much as 24.6 kcal mol^{-1} between $Pd-CH_3$ and $Pd-C_2H$ (PCI-80 value). These differences are greater for the metal−carbon bonds than for the corresponding C−H bonds. This has been explained by larger repulsive effects of the metal compared to hydrogen. In contrast, the $Pd-CH_3$, $Pd-C_2H_5$, and $Pd-C_3H_7$ bond strengths are almost identical, as a result of the sd hybridization (vide supra) on the metal. The sd hybridization acts to avoid the repulsion toward carbon. The replacement of one hydrogen atom in $PdCH_3$ by either OH, NH_2, or F also somewhat modulates the metal to carbon bond strengths but not to a very large extent. In particular, almost identical values are found for $Pd-CH_3$ and $Pd-CH_2F$. This points to a negligible charge-transfer effect. The $Pd-CH_2(OH)$ and $Pd-CH_2(NH_2)$ bonds are somewhat weaker than the $Pd-CH_3$ bond (by 7.1 and 1.1 kcal mol^{-1}, respectively) due to some repulsion of the lone pair of the substituent. Quite interestingly, adding a chloride to the system leads to an *increase* of the Pd−C bond strength of $PdCl(CH_2X)$ ($X = NH_2$, OH) with respect to $PdCl(CH_3)$. This increase is accompanied by an inversion at the nitrogen atom (or at the oxygen atom). Siegbahn has explained this feature by a resonance picture involving, in addition to the $CH_2(NH_2)Pd^+Cl^-$ structure, the $(CH_2N^+H_2)PdCl^-$ structure. This second resonance structure gives the characteristics of a metal−olefin system to the system (it has been suggested by a referee that a metallacyclopropane structure would also explain the coordination of N to Pd).

C. π-Complexes

π-Complexes of palladium and platinum are experimentally well-known and appear very often as key intermediates in a variety of transition-metal-mediated or -catalyzed reactions (see section V for the correspondence to theoretical studies). Representative and intensively studied examples include alkenes, alkynes, aldehydes, or ketones, dioxygen complexes. π-allyl systems form another class with specific properties and will be analyzed separately in this review. Recently, more less common systems such as silenes, disilenes, diphosphene or even C_{60} have been shown to make π-complexes with palladium or platinum transition metal fragments. The most recent theoretical investigations have focused either on the analysis of the bonding in the latter systems, or on the substituent effects in the more classical π ligands.

The interaction between a transition-metal complex and a π system is generally described by the Dewar−Chatt−Duncanson mechanism[131,132] where ethylene donates π electrons to an empty σ orbital on the metal. Thus, the π bond is weakened, the π^* orbital is lowered in energy and can accept electrons from a back-donating d_π orbital on the metal. A recent study by Blomberg et al. of the binding of C_2H_4 to the second-row transition-metal atoms[133] shows that this mechanism holds particularly well for the $Pd(C_2H_4)$ system (which is known experimentally[134]). The bonding state is a mixture of d^9s^1 and d^{10} states, d^9s^1 being somewhat dominant. This is seen best in the 4d population which amounts to 9.5 e. The fact that the d population is smaller in the complex than in the ground state of the atom leads to a relatively small correlation effect (26.9 kcal mol^{-1} at the MCPF level). Note, however, that at this level the correlation effect is as large as the binding energy, 26.7 kcal mol^{-1}. Enlarging the basis set and using a CCSD(T) method leads to a binding energy of 30.7 kcal mol^{-1}. Calculations performed later according to the PCI-80 computational scheme[113] increased this value slightly, up to 34.6 kcal mol^{-1}.[107] In the calculations that used an all-electron basis set, the mass velocity and Darwin relativistic effects were accounted for by using first-order perturbation theory. They were found to be rather large, 11 kcal mol^{-1}. The Dewar−Chatt−Duncanson mechanism for the bonding between Pd and C_2H_4 has not been adopted by Nebot−Gil and co-workers, who considered the Pd−C_2H_4 system as a van der Waals complex and made an analysis that concentrated on the dispersion forces.[135] Using a polarized valence double-ζ basis set with a relativistic pseudopotential, they got a very small binding energy at the CI level 6.0 kcal mol^{-1}, which they needed to scale-up to 20.5 kcal mol^{-1} according to an estimate of the dispersion energy at 10 Å. Their results should be, therefore, viewed with caution. The DFT value—39 kcal mol^{-1}—obtained by Fahmi and van Santen[136] (at the NL level and taking into account the spin-free relativistic effects) is much closer to that calculated by Blomberg et al. The geometrical parameters of the PdC_2 unit are also quite alike. Similar results have been obtained very recently at the MC−SCF level by Minaev and Ågren.[137] These authors have also calculated, in the context of their study of the spin uncoupling mechanism for the C−H bond oxidative addition, triplet and quintet states of $Pd(C_2H_4)$.

The study of the binding of bare metals to the single π bond has been extended to the π bond in benzene by Roczak and Balasubramanian in the case of Pt.[138] The MP2 geometry optimization leads to a structure in which the Pt atom binds one of the C=C bonds in an almost perfect η^2 fashion. The equilibrium structure corresponds to a singlet $^1A_1$ ground state. The C=C double bond is quite elongated, from 1.40 Å in C_6H_6 to 1.46 Å in the adduct. The $Pt^+(C_6H_6)$ system was also investigated in its ground and first excited states. The ground state corresponds to a C_{6v} geometry, as found for other metal cations interacting with benzene, especially second-row transition-metal cations.[139] It is unfortunate for the sake of comparison, however, that this study by Bauschlicher et al. does not include the Pd^+ cation.[139]

Two main classes of π ethylene *molecular* complexes of palladium and platinum are known experimentally, with the metal having either the 0 or +2 oxidation state. Protoype examples of these two classes are $[(PPh_3)_2Pt(C_2H_4)]$, **1**,[140,141] and the so-called Zeise's salt $K[PtCl_3(C_2H_4)]$,[142] **2**.

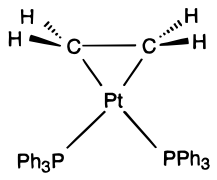

1

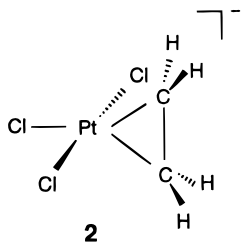

2

The geometrical characteristics of **1** were computationally revisited by Morokuma and Borden about 10 years ago.[143] They performed a partial pointwise geometry optimization at the MP2 level on the $[(PH_3)_2Pt(C_2H_4)]$ model complex (using the small-core ECP of Hay and Wadt[68] and a double-ζ basis set). They compared, in particular, the barrier to rotation and the dissociation energy of an unconstrained ethylene in **1** to those of a highly pyramidalized alkene such as in **3**. Upon pyramidalization, the

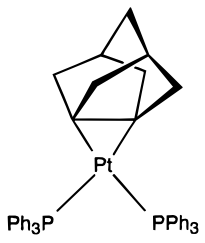

3

binding energy increases to a large extent, by 21.3 kcal mol^{-1}. The barrier to rotation also increases but by only 5−6 kcal mol^{-1}. All these features result from the lowering of the π^* orbital of the double bond (which induces, in turn, an increase of back-donation from the d_π orbital of Pt). The fact that the barrier

Table 3. Binding Energies (kcal mol^{-1}) and Pd−C Bond Distances (Å, in parentheses) of Some Palladium−Ethylene Complexes

	$Pd(C_2H_4)$	$Pd(PH_3)_2(C_2H_4)$	$[PdCl_3(C_2H_4)]^-$	ref
SCF	−0.2 (*a*)			133
		b (2.38)		148
MP2		*b* (2.16)		148
DFT-B3LYP			19.0 (*c*)	161
NL-DFT	39 (2.20[d])			136
		15.9 (2.22)		144
NL-DFT + QR		19.8 (2.18)		144
MCPF	26.7 (2.13)			133
CCSD(T)	30.7 (*e*)			133
		20.9 (*f*)		148
experiment				

[a] The system is not bound at the SCF level. [b] The binding energy is not reported. [c] The Pd−C bond distance is not reported. [d] LDA geometry. [e] MCPF geometry. [f] MP2 geometry, see above.

to rotation is only slightly increased is due to some interaction of the π^* orbital also in the pyramidal structure.

Ziegler and co-workers have assessed the role of the relativistic effects contribution to the computed metal−ethylene bond energies in $[(PH_3)_2M(C_2H_4)]$, M = Pd or Pt.[144] Their methodological procedure is the same as the one used previously for $Pd(CO)_4$ and $Pt(CO)_4$,[91] i.e., they include the relativistic effects at the nonlocal level of the DFT calculations, either through first-order perturbation theory (NL + FO)[92,93] or via the quasirelativistic method (NL + QR).[94] This last method allows one to optimize geometries with an analytical gradient procedure. As expected, the relativistic effects lead to a significant contraction of the metal to carbon bond, more for Pt (0.10 Å) than for Pd (0.04 Å). The result for the C−C bond is a slight increase, because of more π back-donation. The computed structure is in good agreement with the experimental structure of $[(PPh_3)_2Pt(C_2H_4)]$[140,141] and other determinations using relativistic pseudopotentials.[145−148] The computed bond energies at the NL + QR level (19.8 and 22.8 kcal mol^{-1}, respectively) compare well with previous data obtained by Sakaki at the MP4(SDQ) level (with a geometry obtained at the HF level only).[145] They are also in agreement with the more recent values of Frenking.[148] For the same $[(PH_3)_2Pd(C_2H_4)]$ and $[(PH_3)_2Pt(C_2H_4)]$ systems, which were optimized at the MP2 level with a quite flexible basis and a small-core pseudopotential, the CCSD(T) values of Frenking are 20.9 and 28.2 kcal mol^{-1}, respectively, i.e., slightly more than the NL-DFT + QR values of Ziegler. Note that for the corresponding biscarbonyl systems $[(CO)_2Pd(C_2H_4)]$ and $[(CO)_2Pt(C_2H_4)]$ the CCSD(T) values are smaller 14.7 and 21.9 kcal mol^{-1}, respectively.[148] This is most likely due to a decreased π back-bonding of the metal d_π orbitals (which are stabilized by the π^* orbitals of CO). The fact that all these values are much smaller than for the bare Pd and Pt metals arises from the cost of the bending of the two phosphine ligands from a linear geometry in $M(PH_3)_2$ to a bent one in the $[(PH_3)_2M(C_2H_4)]$ complex. There remains, however, some discrepancy with experiment, Table 4: Calorimetric studies for $[(PPh_3)_2Pt(C_2H_4)]$ lead to an estimate of 36 ± 4 kcal mol^{-1} for the Pt−C_2H_4 bond energy,[149] i.e., above the best theoretical values (NL + QR or CCSD(T)) by a few kcal mol^{-1}. Calculations of higher quality (perhaps at the optimization level) should be performed before reconsidering the experimental result.

Ziegler et al. noticed that the values obtained at their highest level of calculation, i.e., NL +QR, are in good agreement (within 1 kcal mol^{-1}) with the ones obtained through a less demanding computational scheme in which the geometries are optimized at the local LDA level and the bond energies are calculated at the NL level with inclusion of relativistic corrections through first-order perturbation theory (NL + FO calculation). They also delineated the various components of the relativistic effects in $[(PH_3)_2Pt(C_2H_4)]$. The greatest influence is seen in the forward donation *and* in the back-donation, which are both increased. As for the metal carbene or metal carbonyl systems, these effects originate from a stabilization of the 6s orbital which in turn leads to a destabilization of the 5d orbitals (by screening the atomic core). The stabilization of the 6s orbital is translated into the stabilization of the a_1 orbital of $Pt(PH_3)_2$, which

Table 4. Binding Energies (kcal mol^{-1}) and Pt−C Bond Distances (Å, in parentheses) of Some Platinum−Ethylene Complexes

	$Pt(C_6H_6)$	$Pt(PH_3)_2(C_2H_4)$	$Pt(PH_3)_2(C_{60})$	$[PtCl_3(C_2H_4)]^-$	ref
SCF		2.5 (2.16)		18.2 (2.30)	145
		a (2.15)			148
		7.4 (2.14)	21.9 (2.08)		153
		−1.5 (*b*)	10.2 (2.11)		147
MP2	57.6 (2.04)				138
		25.8 (2.17)		37.1 (*c*)	145
		a (2.13)			148
		24.7 (*c*)			147
MP4SDQ		20.3 (2.18)		32.8 (*c*)	145
B3LYP-DFT				33.9 (*b*)	161
NL-DFT		13.5 (2.28)			144
NL-DFT + QR		22.8 (2.18)			144
CCSD(T)		28.2 (*d*)			148
experiment		36 ± 4[e]			149
		(2.11[e])			140,141
			(2.13[e])		151

[a] The binding energy is not reported. [b] The Pt−C bond distance is not reported. [c] HF geometry. [d] MP2 geometry. [e] Experimental value for $Pt(PPh_3)_2$.

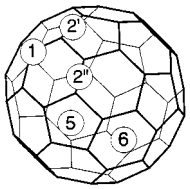

Figure 3. Various sites for the coordination of Pt to C_{60}. (Reprinted with permission from ref 154. Copyright 1994.)

becomes more of an acceptor, and into the destabilization of the d_π orbital of b_2 symmetry, which becomes therefore more efficient for the π backdonation.

In line with the growing experimental research on coordination of Buckminsterfullerene by transition-metal fragments, in particular by platinum (or palladium) bisphosphine complexes,[150] several theoretical studies have been devoted to this topic. In a sense they can be viewed as a combination of the studies carried out on the bonding of Pt to benzene and on the bonding of $Pt(PH_3)_2$ with ethylene that we have reviewed above. The first calculations have dealt with $[(\eta^2\text{-}C_{60})Pt(PH_3)_2]$ as a model of the η^2 coordination of C_{60} to $Pt(PPh_3)_2$, whose structure has been determined by X-ray diffraction.[151] After Fenske−Hall calculations,[152] the first ab initio calculations were reported by Koga and Morokuma.[146] The structure was determined at the HF level, with a quite moderate basis (3-21G for C, P, and H) and the small-core pseudopotential of Hay and Wadt.[68] The computed structure is in good agreement with the experimental one for the PtC_2 unit. More interestingly it reproduces well the lengthening of the coordinated C═C double bond on going from free C_{60} to the bound one. The Pt−C bonds are slightly too short and the Pt−P bonds much too long, most likely as a result of the neglect of electron correlation and/or the lack of polarization functions on phosphorus. The HF binding energy is 21.9 kcal mol^{-1}, compared to 7.4 kcal mol^{-1} for free ethylene. Although electron correlation effects should increase these values by about 20 kcal mol^{-1} (vide supra), it should not affect the *difference* between them too much. That the binding energy is stronger for C_{60} is in line with the previous findings of Morokuma and Borden:[143] that the strain (present in C_{60}) lowers the π^* orbital and increases π backdonation. It would have been interesting to have a comparison with the binding energy to benzene. The fact that the π^* orbital is quite low in energy was obtained in previous calculations of C_{60}[153] and is seen experimentally from the high electron affinity of 2.7 ± 0.1 eV.[150]

Note that these arguments imply that the orbital energy factor, in a fragment molecular orbital interaction analysis, is prevailing over the orbital overlap factor. Lichtenberger et al. have analyzed, again via Fenske−Hall-type calculations, the site preference for the coordination of a bare Pd.[154] The possible sites for the position of the metal are (i) η^1 directly above a carbon atom, (ii) η^2 above two carbons of a pentagon or above two carbons between two pentagons, (iii) η^5 above a pentagon, or (iv) η^6 above an hexagon, Figure 3. Their analysis is based on a comparison between orbital overlap and charge distributions. They conclude that there is a preference for an η^2 coordination above two carbons between two pentagons, i.e., above the (6−6) bond at the fusion between two six-membered rings. This is in agreement with the calculations on the $Pt(C_6H_6)$ system of Roszak and Balasubramanian.[138] Note, however, that the overlap factor does not seem to favor the binding of Pd to C_{60} over the binding to ethylene,[154] at variance with Koga and Morokuma's calculations.[153] It may well be, however, that for $Pt(PH_3)_2$, where the d_π orbital is hybridized toward the double bond, the *differential* overlap factor is less important than for Pd alone, where there is no hybridization present. An analysis somewhat similar to the one of Lichtenberger et al. has been carried out at the extended Hückel level for the $Pt(PH_3)_2$ fragment by Lopez and Mealli.[155]

Koga and Morokuma's analysis of the wave function revealed that nothing could a priori prevent the binding of up to 6 Pt bisphosphine fragments, as exemplified by experiment.[150,156] Poblet and co-workers have carried out a HF study of $(\eta^2\text{-}C_{60})[Pt(PH_3)_2]_n$ systems, with $n = 1$, 2, and 6 for Pt and $n = 6$ for Pd, using a larger basis set than Koga and Morokuma (in particular with polarization functions on phosphorus atoms).[147] The metal was forced to sit above a (6−6) bond, at the fusion of two hexagons for $n = 1$ and 2. For the hexametallic system, the geometry optimization was restrained to T_h symmetry. The computed bond lengths and bond angles are in good agreement with experiment. For $n = 1$, the binding energy is 11.7 kcal mol^{-1} greater than that with $[Pt(PH_3)_2(C_2H_4)]$, thus confirming Koga and Morokuma's results obtained with a smaller basis. A careful analysis of the trends in the binding energies along the series $n = 1$, 2, 6 led to the conclusion that the Pt−C_{60} interaction is highly local. The overall binding energy for the six $Pt(PH_3)_2$ fragments is 30.4 kcal mol^{-1}, much higher than the corresponding value for Pd, 10.9 kcal mol^{-1}. However, without a calculation including electron correlation, one cannot discuss this difference: no minimum was found at the HF level for $[Pd(PH_3)_2(C_2H_4)]$, whereas we have seen above that the NL + QR calculations of Ziegler et al.[144] yielded a binding energy of 19.8 kcal mol^{-1}, i.e., not much different from the binding energy of 22.8 kcal mol^{-1} for the platinum analogue.

Poblet and co-workers have also analyzed the wave function via a Bader-type analysis,[157,158] which is known to be less sensitive to the choice of the basis set than the Mulliken population analysis. The charge transfers computed through this method are of lesser magnitude than the ones obtained through the Mulliken population analysis. However, they confirm that more electron density is transferred from the metal fragment to the organic moiety in $[Pt(PH_3)_2(\eta^2\text{-}C_{60})]$ than in $[Pt(PH_3)_2(C_2H_4)]$ (although the difference is reduced from 0.61e in the Mulliken population analysis to 0.35e in the Bader-type analysis). Both analyses also show that the amount of charge transfer decreases on going from $n = 1$ to 6, but not too much. Poblet has also investigated the reduction of the various $[Pt(PH_3)_2]_n(\eta^2\text{-}C_{60})$ systems. The *relative* electron affinities are in agreement with experiment, a feature already observed by Koga and Morokuma for $n = 1$.[153]

The system $[PtCl_3(C_2H_4)]^-$ (**2**) has been examined by Sakaki and Ieki in the framework of a comparative study of the bonding of ethylene, silene, and disilene with $[PtCl_3]^-$ and $[Pt(PH_3)_2]$.[145] The geometries were optimized at the SCF level. The computed Pt−C bond lengths are too long, Table 4. This is most likely a result of some basis set deficiency to describe the anionic nature of the system and/or of the absence of the counterion (K^+) in the calculations. We note that for the neutral complex $[Pt(PH_3)_2(C_2H_4)]$, the agreement with experiment is much better, Table 4. For other discussions of the influence of the counterion, we refer the reader to the calculations on $[Tl_2Pt(CN)_4]$[159] and on $[Pt_2Cl_2(CO)_4]^{2-}$ [160] that are reviewed further in this article. In the more recent investigation of Strömberg et al.,[161] the electron correlation effects have been taken into account via the DFT-B3LYP method. The calculations used a double-ζ valence basis set and the small-core pseudopotential of Hay and Wadt.[68] Unfortunately no metal to carbon bond distance is given. They should be smaller than the SCF-optimized ones. The binding energy (computed with a larger and polarized basis set) compares well with the MP2 and MP4SDQ values of Sakaki and Ieki, Table 4.[145] The aim of this DFT study was to compare the binding energies of ethylene to the anionic $[PtCl_3]^-$, neutral *cis*- and *trans*-$[M(NH_3)_2Cl_2]$, and cationic *cis*- and *trans*-$[M(NH_3)Cl]^+$ system within the nickel triad M = Ni, Pd, Pt. It has been found that C_2H_4 binds the platinum systems 12−15 kcal mol^{-1} more strongly than the corresponding Pd systems, although this is somewhat modulated by the cis or trans conformation of the bis-chloro and bis-amino systems.[161] The strength of the metal−ethylene bond can be also modulated by constraints on the N−Pd−N angle, as shown by Siegbahn, Strömberg, and Zetterberg in the framework of their study of the insertion of C_2H_4 into the Pd−C bond of $[(NH_3)_2Pd(CH_3)(C_2H_4)]^+$.[162] The N−Pd−N angle which amounts 105.6° in $[(NH_3)_2Pd(CH_3)]^+$ is reduced to 94° when C_2H_4 is bound, due to some steric repulsion between the olefin and the two amine ligands. Thus, when the N−Pd−N angle is constrained to small values, the steric repulsion of the two amines with the incoming olefin is not as large as it would have been for a angle of 105° and the binding energy of C_2H_4 increases from 27.3 to 33.5 kcal mol^{-1} (DFT-B3LYP values) for a N−Pd−N angle of 70°.[162]

Despite its deficiencies, the study of Sakaki and Ieki allows one to compare the bonding capabilities of silene (SiH_2CH_2) and disilene(Si_2H_4) to those of C_2H_4.[145] At both the MP2 and MP4SDQ levels, Si_2H_4 is more strongly bound than C_2H_4 to $[Pt(PH_3)_2]$ by 50 kcal mol^{-1} and to $[PtCl_3]^-$ by 55 kcal mol^{-1}. The silene system (SiH_2CH_2) lies between since the corresponding binding energies range from 29.8 (MP2) to 22.5 kcal mol^{-1} (MP4) for the binding to $[Pt(PH_3)_2]$ and from 35.6 (MP2) to 33.5 kcal mol^{-1} (MP4) for the binding to $[PtCl_3]^-$. The increase in the binding on going from ethylene to disilene is traced back to an increase of both σ donation and π back-donation. The π back-donation is increased so much in $[Pt(PPh_3)_2(Si_2H_4)]$ that the bonding is best described in terms of covalent bonding and no longer through the Dewar−Chatt−Duncanson model. Similar conclusions have been reached by Cundari and Gordon in their HF study of $[Pt(PH_3)_2(Si_2H_4)]$ and $[PtCl_3(Si_2H_4)]^-$.[163] The perpendicular bisphosphine and parallel tris-chloro disilene complexes are found to be transition states for Si_2H_4 rotation and Pt−Cl bond addition across the Si−Si bond, respectively.

The bonding in the $[Pd(PH_3)_2]$ diphosphene complex $[Pt(PH_3)_2(HP{=}HP)]$ has been studied by Sigalas et al., first at the HF level[164] and then at both the DFT and MP2 levels.[165] The geometries have been optimized either at the HF or DFT level (with and without gradient corrections). They are in good agreement with experiment, especially those at the nonlocal DFT level. The η^2 structure has a quite significant rotation barrier, in contrast to the η^1 structure where the diphosphene rotates almost freely. This η^2 mode of coordination is the preferred one (by about 20 kcal mol^{-1} or more, depending on the level of theory).

Some studies have also been devoted to alkyne complexes of either Pd or Pt, including Ziegler's own extension.[144] Calculations were carried out on the $[PdCl(NH_3)(CH_3)(C_2H_2)]$ model system[166] in order to mimic the intermediate expected from the reaction of alkynes with halide-bridged dipalladium complexes.[167,168] Note that experimentally the alkynes have the hydrogen atoms substituted by electron-withdrawing groups.[167] The geometries were optimized at the HF level only, with an all-electron basis and no incorporation of relativistic effects. The computed Pd−C bonds are very long (2.52 Å in the perpendicular form corresponding Zeise's salt). This is consistent with poor π back-donation and a strong electron−electron repulsion of the two doubly occupied π orbitals of C_2H_2 with the $[PdCl(NH_3)(CH_3)]$ fragment. A very small binding energy was computed, 5.8 kcal mol^{-1} after basis set superposition error correction. Clearly more work is needed, in particular at a much higher level of theory, to confirm these results. We may note, however, that Frenking and co-workers found for the $[Pd(CO)_3(C_2H_2)]$ and $[Pt(CO)_3(C_2H_2)]$ systems somewhat similar results. At the MP2 level with a small-core relativistic potential pseudopotential[68] and a quite flexible basis set, very long Pd−C and Pt−C bonds (2.51 and 2.41 Å, respectively) were computed, associated with very shallow energy minima.[108] The CCSD(T) single-point energy calculation gave slightly negative bond dissociation energies. Thus, this seems to confirm the lower level calculations. The geometry of $[Pd(PH_3)(SnH_3)(SiH_3)(MeCCH)]$ has been optimized at both the HF and MP2 levels (with a large-core pseudopotential and a valence double-ζ basis set) in the framework of a theoretical study of the palladium-catalyzed silastannation of alkynes.[169] A very long Pd−C bond (2.68 Å) is found at the HF level but is much shorter (2.35 Å) at the MP2 level. Siegbahn's calculations on the bare metal complex $Pd(C_2H_2)$ are also indicative of a weak binding at the SCF level, the SCF optimized Pd−C bond lengths being too long.[170] At the MCPF or CCSD(T) level, using either the geometry optimized for $Ru(C_2H_2)$ or the MP2

geometry, a definite binding of about 28 kcal mol^{-1} is found. The computed bond lengths that result from the MP2 geometry optimization are not given however, thus preventing a comparison with the SCF geometry optimization.[170] A very recent MP2 geometry optimization of both the perpendicular and planar geometries of $[PtH(SiH_3)(PH_3)(C_2H_2)]$ has been carried out in the framework of the study of C_2H_2 insertion into the Pt−H or Pt−Si bond by Sakaki and co-workers.[171] It also points to quite long Pt−C bonds, especially in the perpendicular form, 2.52 Å (note that in this case the ligand trans to C_2H_2 is SiH_3, i.e., with a rather important trans influence). The planar form is slightly more stable than the perpendicular form and is bound by 17.5 kcal mol^{-1} with respect to $[PtH(SiH_3)(PH_3)]$ and C_2H_2. This value should be reduced by the basis set superposition error, which has not been computed however.[171]

Complexes of Pt(II) with alkynes $[K(18\text{-cr-}6)PtCl_3(MeCCMe)]$ and $[K(18\text{-cr-}6)PtCl_3(EtCCEt)]$ have been recently synthesized and characterized by a crystal structure together with ab initio calculations on the corresponding anions.[172] Experimentally, the Pt−C bond lengths are quite short, 2.14 Å (average value), and the CC triple bond is only slightly elongated with respect to the free alkyne, thus indicative of a very small π back-donation. Unfortunately very few details are given on the calculations: one does even not know which method was used and the computed Pt−C bond lengths are not given.

Related to all these alkyne complexes are the metallacarbyne complexes of Pd(II) that have been analyzed in a joint experimental and theoretical study.[173] The experimental systems are of the type shown in **4**, displaying an unexpected η^1 mode of bonding. They have been modeled by $[Cp(CO)_2MoCH]$-

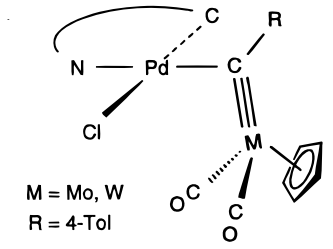

4

$[PdCl_2(NH_3)]$. The optimized SCF structure is in good agreement with the experimental one. An analysis of the wave function (based in particular on fragment electron deformation density maps) shows that the structure can be best rationalized as a Lewis acid−Lewis base adduct ($[PdCl_2(NH_3)]$ being the Lewis acid through its hybridized $d_{x^2-y^2}$ empty orbital and $[Cp(CO)_2MoCH]$ being the Lewis base). In line with this finding, a geometry optimization of the $[Cp(CO)_2MoCH][AlH_3]$ system led to a similar η^1 structure.[173]

The bonding situation is completely different in alkyne complexes of $[Pd(PH_3)_2]$ or of $[Pt(PH_3)_2]$. The $[M(PH_3)_2]$ fragment is expected to be more effective toward π complexation. Ziegler's NL + QR calculations yield binding energies of 29.5 and 30.2 kcal mol^{-1}, respectively (the corresponding nonrelativistic values are 28.7 and 30.2 kcal mol^{-1}, thus pointing to a weak relativistic effect for Pd).[144] In the dicyanoacetylene complex $[Pt(PH_3)_2(NCCCCN]$, studied by Nakatsuji and co-workers,[174] the cyano substituents further activate the triple bond toward complexation. It is therefore not surprising that the HF geometry optimization yields a structure in relatively good agreement with the experimental structures of $[Pt(PPh_3)_2(F_3CCCCF_3]$[175] and of $[Pt(PPh_3)_2(PhCCPh]$,[176] at least for the PtC_2 unit.

As far as the dioxygen complexes are concerned, we have already mentioned the Pd superoxide and peroxide systems studied by Siegbahn.[103] The dioxygen complex of $[Pt(PPh_3)_2]$ has been looked at by Fantucci, using $[Pt(PH_3)_2(O_2)]$ as a model.[177−179] The method used in this study combines the HF model and an electron correlation correction obtained through the LYP functional. The geometry optimization was nevertheless carried out at the HF level, giving good agreement with experiment.[180] Although some calculations were apparently also carried out on the $[Pt(PH_3)_2]$ fragment, no value of the binding energy of O_2 to this fragment is reported. $[Pt(PH_3)_2(O_2)]$ has been investigated much more systematically by Ziegler and co-workers and compared to $[Pd(PH_3)_2(O_2)]$ with the same methodological approach as for $[M(PH_3)_2(C_2H_4)]$.[144] The computed geometries of both systems compare well with experiment.[180] Once the relativistic effects have been incorporated in the calculations, a shorter O−O bond is obtained in the Pd complex, 1.42 Å instead of 1.45 Å in the Pt complex (the experimental values in $M[(PPh(t\text{-}Bu)_2)]_2(O_2)$[180] are 1.37 and 1.43 Å for M = Pd and Pt, respectively). Despite a noticeable contraction on inclusion of the relativistic effects, the calculations fail, however, to reproduce the shorter metal to phosphorus bond for Pt: the computed values are 2.29 (Pd) and 2.33 Å (Pt), the corresponding experimental values are 2.39 and 2.29 Å, respectively. For the Pd−O and Pt−O bonds, the agreement is better, 2.03 Å for both metals computationally vs 2.05 and 2.02 Å experimentally. The binding energies at the NL-DFT + QR level are 15.5 and 21.1 kcal mol^{-1} for the Pd and Pt complexes, respectively, the corresponding NL values being 10.4 and 7.2 kcal mol^{-1}. Thus, as expected, the enhancement due to the inclusion of relativistic effects is much greater for Pt.

There has been some discussion about the preferred mode of coordination of ketene (Ph_2C_2O) to d^{10} bisphosphine fragments. Earlier ab initio calculations of Nakamura and Morokuma suggested an η^2-(C,C) equilibrium structure.[181] However the X-ray crystal structure of the $[dtbpmNi(Ph_2C_2O)]$ system (dtbpm = bis(di-*tert*-butylphosphino)methane, $^tBu_2PCH_2P^tBu_2$) with a P−Ni−P angle of 80° has a η^2-(C,O) structure.[182] This structure has been rationalized in the same article through MO arguments on the basis of extended Hückel calculations for both Ni and Pt systems.[182] One may expect that both coordination modes are close in energy and can interchange easily on the ligand set.[183]

D. Miscellaneous

Other quantum chemical studies have been performed on particular systems, most often in connec-

tion with experimental studies in order to assess a structure, some isomerism, or get some idea about the influence of the surroundings. Due to the development of a user-friendly and efficient quantum chemistry package, in the future one expects to see more and more of such studies.

HF calculations have been carried out on [{$(CH_3)_2$NO)}PdCl(PH_3)], where the dimethyl nitroxide ligand is a model for the TMPO ligand (TMPO = 2,2,6,6-tetramethylpipridinyl-1-oxy).[184] The bonding has been analyzed and compared to that in [{$(CH_3)_2$NO)}-$CuBr_2$]. In the palladium complex, the singly occupied orbital on the PdCl(PH_3) fragment is mostly of metal d_π character. Its interaction with the singly occupied π^* orbital of the dimethyl nitroxide radical gives rise to a strong covalent interaction, in line with the experimental crystal structure of [PdCl(PPh_3)-(TMPO)].[185] The UV photoelectron spectra of *cis*-[Pt-$(CF_3)_2L_2$], where L stands for a variety two-electron donor ligands, have been interpreted with the aid of Xα calculations on the [Pt$(CF_3)_2(C_2H_4)_2$] model system.[186] The Pt−CF_3 bonds have been analyzed and compared to Pt−CH_3 bonds. Xα calculations of the wave function and of the hyperfine interactions for the $[Pt(NH_3)_4(OH)_2]^+$ system taken as a model of bis-(ethylenediamine)platinum bis(hydrogen squarate) complexes have been used to interpret its EPR spectrum.[187] Ahlrichs et al. have performed a conformational analysis, at the DFT level, of a truncated entity of a palladium-coordinated cellulose chain.[188] The palladium porphyrin complex has been optimized through a Car−Parrinello-like approach, using a pseudopotential combined with a plane waves expansion of the molecular orbitals.[189] The optimized geometry is in good agreement with experiment[190] (with a maximum difference of 0.02 Å). Semiempirical calculations, either extended Hückel or Fenske−Hall, have been performed on systems with Pd(II)[191] or Pt(II)[192] to sulfur bonds. Square-planar platinum-(II) complexes containing 7,8-benzoquinoline and various $Ph_2P(CH_2)_nPPh_2$ ligands (dppm, $n = 1$; dppe, $n = 2$; dppp, $n = 3$) have been optimized at the HF level with a relatively small basis set.[193] The Mulliken charges of the various $(CH_2)_n$ bridges have been used to compute the perturbation that in time-dependent perturbation theory accounts for the emission lifetime differences when the number of methylene bridges in the complex increases. A study, limited to the HF level, has been carried out on a number of four-coordinate Pt(II) diimine complexes and five-coordinate ethylenic adducts, where the added C_2H_4 and the diimine lie in the equatorial plane of a trigonal bipyramid.[194] In agreement with experiment, the five-coordinate platinum systems are comparatively more stable toward ethylene dissociation than their palladium analogues. Some rationalization is given via an natural bond orbital (NBO) analysis. Some care should be exercised, however, since the calculations were performed with a rather small basis set, including, in particular, a large-core pseudopotential that may lead to a spurious effect. The authors report that the minimal basis set leads to a negative eigenvalue (corresponding to an antisymmetric stretching of the two M−N bonds) for the second derivative matrix in the symmetric five-coordinate dihalogeno systems. The case of the dichloro complex is particularly striking. When a larger basis set is used, the geometry relaxation of the diimine ligand leads to a nonsymmetrical structure in which one nitrogen atom is quite far, at 2.80 Å, from the platinum atom. Thus, one may wonder whether this structure would not in fact correspond to an intermediate on the pathway of a substitution process (vide infra). Clearly more work is needed on this interesting topic. The system *trans*-methyl-azido-bis(triisopropylphosphine)platinum(II) [Pt$N_3(CH_3)$-$(P^iPr_3)_2$] has been calculated by Frenking in order to shed more light on problems arising with the X-ray crystal structure determination of the Pt−N_3 moiety.[195] An ONIOM-type method, which allows one to combine various levels of theory within a molecule, has been used. In the present case the inner core of the system "Pt$N_3(CH_3)P_2$" is described at the DFT-B3LYP level and the phosphine ligands at the HF level. The computed IR frequencies associated to the N_3 ligand are in good agreement with experiment. On the other hand, the corresponding computed distances and the experimental ones do not agree, thus confirming some artifact in the X-ray crystal structure determination.[195]

There have been a few studies dealing with Pt(IV) or Pd(IV) complexes. The isomerism between the zwitterionic $M(II)^-\cdots H-N^+$ and the neutral N−M(IV)−H forms in palladium and platinum complexes (where N stands for an amine-type ligand) has been addressed recently. Experimentally, isomers of both types have been isolated.[196,197] Earlier calculations, carried out either at the SCF or CASSCF level but with a rather limited active space,[197] indicated the zwitterionic system as being the most stable. However, nondynamical correlation effects associated with the description of the covalent metal−hydrogen bond that is formed upon protonation of the metal reverse this order. They yield the M(IV) form as the most stable one and more for Pt than for Pd (in line with the known greater stability of Pt(IV) complexes).[198−200] The optimized structure of the Pt(IV) complex $[PtMe_2(H)\{(H_2C{=}N{-}NH)_3BH]$,[199] where $[(H_2C{=}N{-}NH)_3BH]^-$ is taken as a model of a tris(pyrazolyl)borate ligand ($[(pz)_3BH]^-$), is in good agreement with an X-ray crystal structure of [Pt-$Me_2(H)\{(3,5\text{-}Me_2pz)_3BH]$[201] which was published subsequently. Studies of the solvation effects on such systems are currently under way.[202,203] The cis−trans isomerism in another Pt(IV) complex, viz. $PtCl_4$-$(pyridine)_2$, has also been studied recently.[204] On the basis of NL-DFT calculations that give good agreement with the experimental structure of the trans isomer, the cis isomer is found less stable by 10.1 kcal mol^{-1}. DFT-B3LYP calculations have been carried out on Pt(II) and Pt(IV) α-diimine complexes of formula [$PtMe_2$(HN=CHCH=NH)] and [$PtMe_4$(HN=CHCH=NH)], in conjunction with detailed spectroscopic and electrochemical studies on systems with substituted α-diimines.[205] The computed orbital sequence points in both cases to a LUMO of α-diimine π^* character, in agreement with the UV spectra and

with the EPR results for the one-electron-reduced species.[205]

Some other studies have been performed that are related to the influence or to the interaction of the surroundings with metal complexes. We have already mentioned the study on the solvation (in dichloromethane) of Pd(IV) complexes.[203] The behavior in acid solution of metal carboxylate complexes, which can act as catalysts for the heterolytic cleavage of a C−H bond, has been addressed:[206] the reaction of palladium diformate [$Pd(O_2CH)_2$] with two formic acid molecules has been shown to yield a diformate−diformic acid [$Pd(O_2CH)_2(HCO_2H)_2$] in which the formate ligand is bound in a η^1 fashion to allow coordination of the carbonyl oxygen atom of HCO_2H.[206] The process is exothermic by 66 kcal mol^{-1} at the HF level, i.e., 33 kcal mol^{-1} per acid molecule. This is much more than the association energy of the formic acid which is estimated to be between 16 and 18 kcal mol^{-1}. Similar features have been also found for palladium trifluoroacetate and trifluoroacetic acid. Hence, the authors conclude that palladium dicarboxylate in trifluoroacetic acid solution will add two acid molecules per metal atom. In the course of a comprehensive study of ligand-field effects in the hydrated divalent and trivalent metal ions of the first- and second-row transition metals, Wahlgren et al. have computed the $[Pd(H_2O)_4]^{2+}$ system at the SCF and CASSCF/MRCI levels.[207] The ground state corresponds to a low-spin square-planar structure. This can be explained by ligand-field theory. Siegbahn and Crabtree have studied, at the DFT-B3LYP level, the relative stability of the cis and trans isomers of [$PdCl_2(H_2O)_2$] surrounded by water molecules (up to 4) to mimic the solvation sphere (when water is a solvent).[208] Solvation effects of the bulk have been accounted for by SCRF calculations (with effects up to the hexadecapole moments of the solute). It is found that the extra water molecules prefer to make hydrogen bonds with the two coordinated water molecules rather than sitting above and below the coordination plane. Without inclusion of the bulk solvation effects, the trans form is more stable than the cis form by 4.7 kcal mol^{-1}, thus by a greater extent than that found experimentally (0.9 kcal mol^{-1}).[209] A similar difference is found when the effects of the bulk are included up the quadrupole moment on either the [$PdCl_2(H_2O)_2$] or [$PdCl_2(H_2O)_6$] systems. That the same results are obtained, whether one adds two or six water molecules, would indicate that it should not be necessary to include water molecules explicitly once the coordination sphere has been saturated. The convergence of the multipolar expansion of the solute is also analyzed.[208]

A qualitative study of the axial bonding capabilities of square-planar d^8-ML_4 complexes (including Pd and Pt complexes) has been made, using extended Hückel calculations and structural correlations.[210] The axial coordination of a Lewis base enhances the nucleophilicity of the metal center (via its d_{z^2} orbital). Conversely, its accepting capability (via its p_z orbital) is increased by the axial bonding of a Lewis acid. The structural implications have also been discussed.[210]

Dolg, Pyykkö and Runeberg[159] have very thoroughly investigated the closed-shell interactions in the d^8-s^2 bonded [$Tl_2Pt(CN)_4$] compound. This system was analyzed previously, via a NL-DFT method (including spin-free relativistic effects and spin−orbit coupling), but the geometry was not optimized.[211] Calculations by Dolg et al. range from HF to MP2 up to CASSCF/MRCI or CASSCF/ACPF with BSSE and spin−orbit corrections. At the highest level of calculation a discrepancy still remains for the Tl−Pt bond length which amounts to 2.88 Å theoretically and 3.14 Å in the X-ray crystal structure.[212] Some estimate of the crystal-field effect has been obtained by putting fractional negative charges around the system to mimic the five cyanides surrounding each thallium atom. The increase of the Tl−Pt bond length obtained on increasing the fractional charge suggests a sizable surrounding effect on the length. The effect of the surroundings has been also considered in a very comprehensive study of the complexes MH_x^{2-} and MCl_y^{2-} (M = Pd, Pt; $x = 2, 4, 6$; $y = 4, 6$) in the crystalline A_2MH_x and A_2MCl_y compounds (A = Na, K; M = Pd, Pt).[213] To this end the anionic systems are embedded in a Madelung potential but with a cutoff that accounts for the short-range repulsion from the nearest neighbors. The quantum mechanical calculations are of DFT type with inclusion of the relativistic effects through first-order perturbation theory. It is shown that the crystal field strongly shifts the $MH_6^{2-} \rightarrow MH_4^{2-} + H_2$ and $MCl_6^{2-} \rightarrow MCl_4^{2-} + Cl_2$ disproportionation equilibria to the right except for $PdCl_6^{2-}$ and $PtCl_6^{2-}$, thus in agreement with the known stability of these systems in the crystal. A similar study has also been performed on the ternary hydrides A_2MH_2 (A = Li, Na; M = Pd, Pt).[214] Finally, we briefly quote—since it is at the borderline of the scope of this review—a careful analysis of the change of the CO stretching frequency in the Pt−CO complex due to the interaction of Pt with zeolite protons.[215] DFT calculations were used on model clusters mimicking some zeolites. They support the experimental hypothesis that the platinum species in mordenite are electron deficient. However, it is also concluded that this concept should be used with care since some other factors are found to influence the C−O frequency shift, such as the formation of additional coordination bonds and the electric field set up by the environment.

Finally one should cite here a few quantum mechanical investigations that have been devoted to cisplatin and its derivatives. In addition to ab initio calculations aimed at developing or improving force field parameters,[216−219] one finds a few studies dealing more specifically with bonding features.[220−222] Some of those have relied on DFT calculations (with Becke−Perdew corrected exchange and correlation functionals)[72,116] using a relativistic pseudopotential for the platinum core and plane waves to describe the valence electrons. This methodological approach was chosen as a first step toward a more difficult goal, viz. the modeling of the interaction of cisplatin with DNA by ab initio molecular dynamics. The first investigation was carried out on cisplatin, transplatin, and water-substituted cisplatin complexes.[221]

The results are in good agreement with the known experimental data, thus validating this methodology. It has been followed by a comparison with carboplatin.[223] A mixed adenine−thymine complex of *trans*-$[Pt(NH_2CH_3)_2]$ with a bridging water molecule has also been examined through this computational approach.[222] In comparison to the parent transplatin, the stronger interaction of the methylated adenine and thymine compared to chloride pushes the $d_{x^2-y^2}$ orbital above some π ligand orbitals of the nucleobases, thus giving to the system the characteristics of a charge-transfer system.

III. Polynuclear Compounds

Many palladium and platinum clusters have been synthesized and structurally characterized, some of them being designed to mimic palladium or platinum surfaces and their associated reactivity. Bare metal clusters are of course the ones that are expected to meet this objective best. Experimentally, there are only a few definite characterizations of Pd_n and Pt_n bare metal clusters (for n being relatively small), and the theoretical studies of such systems are probably more numerous. We shall start by reviewing these studies. We will then switch to the dinuclear molecular complexes according to the various oxidation states of the two metals. Finally, we will consider tri- and polynuclear molecular clusters.

A. Bare Metal Systems

Detailed and extensive investigations, at the CASSCF/MRSDCI + relativistic configuration interaction (RCI) calculations, were carried out on Pd_2 and Pt_2 by Balasubramanian prior to 1990.[224] In most of the subsequent studies, especially for Pd_2, a major goal has been assessment of the accuracy of various DFT schemes through determination of the spectroscopic properties of the ground state of the two systems.

One should, however, quote a study by Blomberg et al. on Pd_2 using the MCPF method, an all-electron basis, and including the spin-free relativistic effects through first-order perturbation theory.[225] As in Balasubramanian's calculations, the $^3\Sigma_u^+$ state made essentially of the $(1\sigma_u)^1(2\sigma_g)^1$ configuration is found to be the ground state. The corresponding dissociation energy of 10.8 kcal mol^{-1} is smaller than in Balasubramanian's work (19.6 kcal mol^{-1}) and in experiment[226] (the experimental value ranges between 17.1 and 26.1 kcal mol^{-1} depending on the technique of evaluation). The computed bond length is greater (Re = 2.54 vs 2.48 Å). Improving the wave function by performing a two-reference ACPF calculation yields a binding energy of 17.0 kcal mol^{-1}.[227] An almost identical value (17.8 kcal mol^{-1}) is obtained when a relativistic pseudopotential is used.

In the course of a study on the CO chemisorption on model clusters of Rh and Pd, Goursot et al.[228] have computed the spectroscopic properties of Pd_2. They used a model potential including relativistic effects and leaving out the 4p orbitals as valence orbitals. The geometry optimization was carried out within the local spin density approximation, but the energy calculations were done with the Perdew correction[116,229] to the exchange and correlation functionals. The $^3\Sigma_u^+$ ground state was obtained. The $^1\Sigma_g^+$ singlet state (made of $(1\sigma_u)^2$, i.e., from two ^{1}S d^{10} palladium atoms), is higher in energy by 9.4 kcal mol^{-1}. The computed spectroscopic values do agree with those of Balasubramanian, especially the Pd−Pd bond distance (Re = 2.46 vs 2.48 Å in Balasubramanian's work).[224] The bond dissociation energy is somewhat higher (31.1 kcal mol^{-1} instead of 19.6 kcal mol^{-1}) but still fits with the experimental estimate.[226]

More systematic studies testing various functionals, the effect of including nonlocal corrections, and the effect of using a relativistic pseudopotential instead of an all electron orbital basis have appeared. Dixon[230] and Seminario[231,232] disagree on the necessity of including relativistic effects for Pd_2. Although Seminario's contention is that nonrelativistic calculations can yield results comparable to the very scarce experiments, his results are somewhat contradictory.[232] The MP4SDTQ calculations (carried out with a large and uncontracted but unpolarized basis set) yield R_e = 2.48 Å, in good agreement with Balasubramanian's result, but a negative binding energy. On the other hand, a correct binding energy (18.8 kcal mol^{-1}) is obtained from the NL-DFT calculations (using the Perdew−Wang 86 exchange correlation functional[116,229]) but at the expense of the accuracy for the Pd−Pd bond length which is then much larger, 2.62 Å. The B3LYP results lie in between, with D_e = 11.7 kcal mol^{-1} and R_e = 2.56 Å. The values computed for the triplet−singlet separation are also quite random. Dixon, on the other hand, advocates the necessity of including the relativistic effects.[230] As expected, longer bond distances are obtained, in good agreement with Balasubramanian's estimate, if nonlocal corrections are included. The use of a relativistic pseudopotential is crucial for getting the triplet below the singlet: the relativistic contraction and lowering of the 5s orbital makes the promotion of an electron from 4d to 5s easier and hence the $(1\sigma_u)^1(2\sigma_g)^1$ configuration is more easily attained. One should also stress here that calculations carried out with the DMol program, which does not incorporate relativistic effects, yield binding energies that are too low,[230] especially at the nonlocal level.[233]

Zerner's INDO calculations on Pd_2, carried out at the HF level for the geometry optimization and at the CIS (i.e., with single excitations only) level for the calculations of the various states,[234] also yield $^3\Sigma_u^+$ as the ground state, as do the NL-DFT calculations of Fahmi and van Santen[136] (with Becke−Perdew corrections and inclusion of the relativistic effects via first-order perturbation theory). The B3LYP functional,[72,235,236] used in conjunction with a small-core pseudopotential by either Toulhoat[233] or Morokuma,[237] gives results that agree with those of Balasubramanian. The bond dissociation energy ranges between 22.2 and 20.6 kcal mol^{-1}, depending on the level of the basis set, and in excellent agreement with experiment.[226] The fact that the B3LYP scheme is not too sensitive to the quality of the basis set was already noticed by Dixon.[230] On the other hand, at the CASPT2 level a quite flexible basis set is necessary in order to obtain correct dissociation energies.[237]

In Pt_2 relativistic effects are far more important than in Pd_2. The difference in the electronic state ordering, ^3D below ^1S for Pt, also has consequences on the state ordering of the dimer. Here too a reference calculation is the earlier one of Balasubramanian at the CASSCF/FOCI + RCI level.[238] In the absence of spin−orbit coupling, the lowest state is $^3\Pi_u$, followed by $^3\Sigma_g^-$ which is almost degenerate at 1.1 kcal mol^{-1} higher, and by $^1\Sigma_g^+$ which lies 5.1 kcal mol^{-1} above $^3\Pi_u$. The ground state is $^3\Sigma_g^-$ (0_g^+) arising from the δ_u^2 configuration. The next excited states are quite low in energy and also arise from δ-type orbitals, viz. $\delta_u^3\delta_g^3$ for $^3\Gamma_u$ (5u) which lies only 3.1 kcal mol^{-1} above the ground state and $\delta_u^3\pi_g^3$ for $^3\Phi_u$ (4u) at 1.8 kcal mol^{-1} above the ground state. The ground-state equilibrium bond length is slightly smaller than that in Pd_2, 2.46 Å instead of 2.48 Å. A recent measurement using STM on graphite gives 2.45 ± 0.26 Å.[239] Spin−orbit coupling also decreases the bond dissociation energy in the ground state from 53.0 to 45.0 kcal mol^{-1}, thus smaller than the experimental estimates which range between 66.4 ± 6.0[240] and 85.6 ± 14.3 kcal mol^{-1},[241] a very recent determination giving a value of 72.4 ± 0.5 kcal mol^{-1}.[89] That Pt_2 is characterized by a cluster of states close in energy has also been found in the CASSCF and GVB + MRCI calculations of Wang and Carter.[242] Their computed Pt−Pt bond dissociation energies are too small, however (26.7 and 26.6 kcal mol^{-1} at the CASSCF for the $^3\Sigma_g^-$ground state and the $^3\Gamma_u$ state. respectively; the GVB/CI increases the value for the $^3\Gamma_u$ state to 36.1 kcal mol^{-1}). The Pt−Pt bond is too long (∼2.7 Å). This may be due to the large-core pseudopotential used[124] and to its associated basis set, although Balasubramanian's contention is that large-core pseudopotentials work satisfactorily. Remember that similar calculations by Smith and Carter[84] on PtCO also led to a bond energy that is too small with respect to experiment (vide supra). The very recent DFT-B3LYP and CASPT2 calculations of Morokuma and co-workers[237] are in better agreement with Balasubramanian. The ground state is found to correspond to the $^3\Sigma_g^-$ state, other states coming from different d hole combination being close in energy. The computed Pt−Pt bond length with their smaller basis set is 2.39 Å at the B3LYP level and 2.44 Å at the CASPT2 level. The best basis set at the CASPT2 level yields 2.41 Å. The corresponding dissociation energies range between 56.2 kcal mol^{-1} at the B3LYP level and 60.5 kcal mol^{-1} at the CASPT2 level with the best basis set. This last value supports the lower estimates for the experimental value.

The Pd_3, Pt_3, and higher homologues Pd_n and Pt_n have been studied quite thoroughly, the palladium systems more than the platinum systems. The first study on Pd_3, carried out by Balasubramanian at the CASSCF/MRSDCI + RCI level, concluded to a $^1A_2$ ground state, with many low-lying, nearly degenerate states between 7 and 10 kcal^{-1} above.[243] The overall separation of these states agrees with the observed photoelectron spectrum of Pd_3^-.[244] The ground-state equilibrium geometry is an acute triangle, with two long bonds of 2.67 Å and a short one of 2.47 Å at the base of the triangle (this corresponds to an angle at the apex of 55°). The ground state is bound by 76 kcal mol^{-1} with respect to the Pd_2 dimer + Pd(^3D) and has an atomization energy of 124 kcal mol^{-1} with respect to Pd(^3D). Using the computed $^1S-^3D$ separation of 14 kcal mol^{-1} for Pd, this yields an atomization energy of about 82 kcal mol^{-1} with respect to Pd(^1S). A more recent calculation of Blomberg et al.,[227] using another relativistic potential to include the spin-free relativistic effects, yields a $^3B_2$ state as the ground state (but different from a low-lying $^3B_2$ state obtained by Balasubramanian).

It is difficult to make a comparison of the above results with the results of the DFT-B3LYP calculations by Seminario on Pd_3[232] since no symmetry assignment is done. A triplet for an equilateral triangular form is said to be the ground state. A singlet with a triangular geometry is found 3.2 kcal mol^{-1} above the ground state. As for Pd_2, the computed Pd−Pd bond length (2.70 Å) seems to be too long, most likely because of the neglect of relativistic effects. Valerio and Toulhouat's calculations[233] that include spin-free relativistic effects via the pseudopotential give shorter bond lengths, e.g., 2.54 Å for the $^3B_2$ state. This $^3B_2$ state, which is computed to be the ground state, has a nonequilateral geometry, the distortion being nevertheless relatively small: the angle θ at the apex of the triangle amounts to 65.6°. $^3B_2$ being the ground state is in agreement with the calculations by Blomberg et al. but at variance with Balasubramanian's results. Note, however, that the open-shell singlet $^1A_2$ cannot be computed within the present DFT calculations. One singlet $^1A_1$ has been computed to lie 5.6 kcal mol^{-1} higher than $^3B_2$. Similar results emerge from Morokuna's study,[245] except for the ground state which is found to be $^3B_1$. However, the $^3B_2$ state is near-degenerate with the $^3B_1$ state. Clearly the close proximity of all these states makes the ground-state assignment especially difficult for Pd_3. However, this is probably of less importance when one studies the reactivity of the cluster. In this case the approach of a reactant should split these states to a greater extent. A final result to be mentioned is that these two DFT studies do agree on the atomization energy, around 60 kcal mol^{-1}, i.e., somewhat less than in Balasubramanian's study.

Wang and Carter extended their investigation on Pt_2 to the Pt_3 cluster using the same methodology.[242] They found a weak d−d coupling that leads to a manifold of states quite close in energy. The $^1A_1$ singlet state (arising from one d^{10} and two d^9s^1 atoms) is the lowest one and has an equilateral triangle structure. Thus, the dominant interactions holding the platinum atoms together are, in their calculations, essentially of s−s type, the d electrons remaining localized on each metal center. The computed bond lengths are quite long (2.79 Å), and the atomization energy (50.3 kcal mol^{-1} at the best level of calculation) seems to be relatively small, as it was for Pt_2. The one valence electron pseudopotential that we mentioned in the context of the studies on Pt−H has been used by the same authors to calculate Pt_3 (and Pt_4).[246] The equilibrium geometry has rather

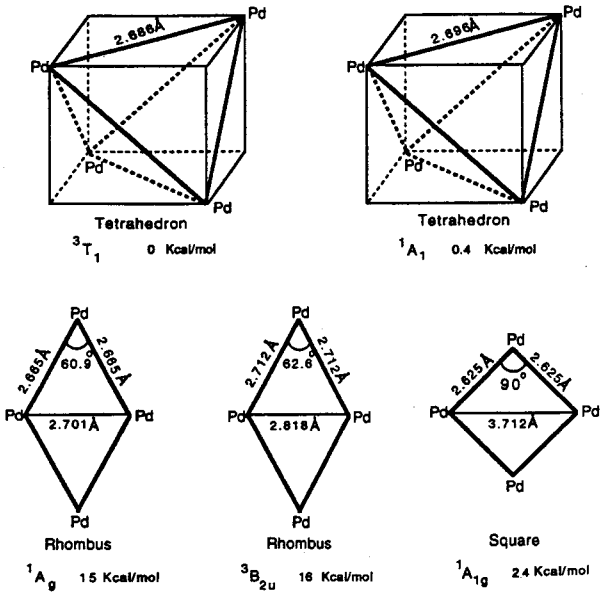

Figure 4. Equilibrium geometries for the low-lying states of Pd_4. (Reprinted with permission from ref 247.) Copyright 1995.

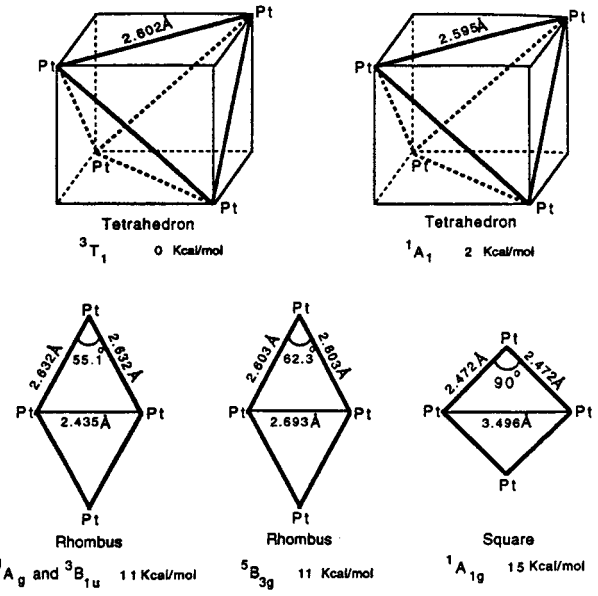

Figure 5. Equilibrium geometries for the low-lying states of Pt_4. (Reprinted with permission from ref 247.) Copyright 1995.

long bonds (two long, 3.05 Å, and a one short, 2.74 Å) and an atomization energy of 49.6 kcal mol^{-1}. As mentioned by Morokuma and co-workers,[245] the fact that these two calculations give such a low value for the atomization energy is probably the result of using a large-core pseudopotential (and also a rather small basis). Their DFT-B3LYP calculations yield shorter bond lengths and a much larger atomization energy (~120 kcal mol^{-1}).[245] The ground state in their case is also a $^1A_1$ state (in C_{2v}) but at variance with Wang and Carter it is made primarily of three d^9s^1 platinums. Here too, low-lying excited states, most of them being triplets, are found very close in energy.

Clusters of higher nuclearity have also been computed. Dai and Balasubramanian[247] chose to use a large-core relativistic pseudopotential and high-level methods, viz. CASSCF/MRSDCI, for investigating the Pd_4 and Pt_4 systems. Their equilibrium geometries for the low-lying states together with the corresponding energy separations are shown in Figures 4 and 5, for Pd_4 and Pt_4, respectively. The ground-state configuration is $^3T_1$, as also found earlier by Goursot et al.[228] The computed atomization energy (relative to Pd in the $^1S_0$ state) is 117 kcal mol^{-1} at the CASSCF/MRSDCI level and 129.7 kcal mol^{-1} when the Davidson correction for the quadruple excitations is included. For Pt_4, a value of 272.2 kcal mol^{-1} (relative to Pt $^3D_3$) has been obtained. In these calculations, as in the calculations of Pd_4 by either Goursot et al.[228] or Fahmi and van Santen,[136] the T_d symmetry was not allowed to relax into a lower symmetry. Zerner and co-workers,[234] as well as Valerio and Toulhouat,[233] have allowed such a relaxation: in both cases a C_{2v} Jahn–Teller-distorted structure is found corresponding to a $^3B_2$ state. The atomization energy computed at the DFT-B3LYP level by Valerio and Toulhouat is much smaller than the one of Balasubramanian, 114.9 kcal mol^{-1}, giving a value per bond much closer to the bulk value and following a smooth trend along the series $n = 1, 3, 4, 6$.[233] One should finally mention that the MRCIS–INDO calculations on the Pd_{13} cluster[234] also yield the less symmetrical D_{5d} structure as being more stable than the I_h icosahedral structure.

The study on PtZr and Pt_3Zr by Wang and Carter has focused on the metal–metal bonding between early and late transition metals.[248] The same methodology as for Pt_2 and Pt_3 was used. PtZr has been analyzed via a CASSCF treatment using optimized geometries, whereas the greater size of Pt_3Zr required the use of GVB-type calculations and a fixed C_{3v} geometry. The most important result from this study—which would most likely survive better calculations, since the difference between the ionization potential of Zr and the electron affinity of Pd is reproduced correctly—is that a significant electron transfer takes place from Zr to Pt, or from Zr to Pt_3. This is at variance with the initial assumption based on the empirical theory of Engel and Brewer[249–251] but could have been expected from the relative work functions. This charge transfer, as well as sd–sd hybrid bonding between Zr and Pt, contributes to the higher stability of these heterometallic systems compared to the homometallic ones.

The binding of atoms or of small molecules to some of these bare metallic clusters has also been addressed. As far as atoms are concerned, Balasubramanian and co-workers have looked at the interaction of the hydrogen atom with Pt_2,[34] Pt_3, and Pd_3.[252] In the platinum study, the spin–orbit effects have been included explicitly after the CASSCF/MRSDCI treatment, via the relativistic configuration interaction (RCI) computational scheme. For Pt_2 + H, all states arising from the Pt_2 ($^3\Sigma_g^-$) + H(^{2}S) were considered. The ground state of $^2A_2$ symmetry in the absence of spin–orbit coupling corresponds to a bridged structure with a Pt–Pt distance of 2.48 Å and a Pt–H distance of 1.70 Å. The $^2B_2$ state is near degenerate, lying only 1.4 kcal mol^{-1} higher. On inclusion of the spin–orbit effects, these two states mix substantially and the splitting between them is slightly increased

to 2.2 kcal mol^{-1}. Both Pt−Pt and Pt−H distances are shortened slightly, by 0.02 Å. The bonding, which is quite covalent, is best described in terms of a three-center four-electron bond. The dissociation energy, 59 kcal mol^{-1}, is smaller than that for Pt−H (72 kcal mol^{-1}, vide supra). In Pt_3H, the interaction of H with the trimetallic cluster takes place preferentially along the C_3 axis.[252] The relativistic effects are found to be more important for the excited states than for the ground state (which is $^2A_2$ in the absence of spin−orbit coupling). The Pt−H bond, 1.80 Å, is longer than that in Pt_2H. The bond dissociation energy, 62.2 kcal mol^{-1}, is also weaker than in PtH. In contrast, in Pd_3H the bond dissociation energy is higher than that in PdH, 71.5 kcal mol^{-1} instead of 55.4 kcal mol^{-1}.[21]

Not surprisingly, the interaction of Pt_3 with Au also leads to C_{3v} geometry with a $^2A_2$ ground state.[253] The optimized structure compares well with X-ray crystal structures of related molecular complexes displaying a Pt_3Au or Pt_3Au_2 core.[254] The study was carried out again at the CASSCF/MRSDCI level with a large-core relativistic potential and inclusion spin−orbit coupling via the RCI technique. As for Pt_3H, the effects of spin−orbit coupling are relatively small in the ground state but significant in the excited states. Valerio and Toulhouat have investigated the interaction of either the sulfur atom or the chlorine atom with Pd_n (n = 2, 3, 4, 6) at the DFT level using the B3LYP functional.[255] The small-core relativistic potential of Hay and Wadt was used with its associated basis and the polarized 6-311G(d,p) basis for S and Cl. The binding has been analyzed as a function of the increasing number of palladium atoms, to mimic chemisorption on small palladium particles. This topic is out of the scope of the present review. We can, nevertheless, mention that a careful analysis of the wave function indicates that the Pd−S or Pd−X bonds are of a charge-transfer type.

The interaction of N_2, CO, and C_2H_4 with Pd_2 and/or Pt_2 has also been examined. We have already alluded above to the calculations by Blomberg and Siegbahn for the Pd_2N_2 system.[225] A relatively large binding energy between Pd_2 and N_2 has been found, the value of 15 kcal mol^{-1} actually computed being—according to the authors—a lower limit of the real result which should be around 20 kcal mol^{-1}. Two structures are found of almost equal stability (within 1 kcal mol^{-1}), the bridge end-on, **5**, and one with a side-on parallel geometry, **6**. The frequencies of N_2

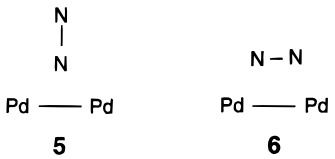

5 **6**

have also been computed and discussed in connection with N_2 chemisorption on palladium surfaces. In both structures the charge transfer to N_2 is low, due to the relatively large ionization potential of Pd from d^9s^1 to d^8s^1. In contrast to Pd_2N_2, the end-on-bridged structure of Pd_2CO in the $^1A_1$ electronic ground state is found to be more stable than the linear end-on geometry by more than 30 kcal mol^{-1} at either the MP2, CASSCF, or CASSCF/MRSDCI level. At this highest level of computation, the difference is 34.6 kcal mol^{-1}.[256] The approach of CO was also studied and found to be almost barrierless, the barrier being only 3.5 kcal mol^{-1}. An analysis of the wave function reveals a small σ donation from CO and a significant back-donation from the two palladium atoms. Similar calculations were performed earlier on Pt_2CO.[257] As in Pd_2CO, the energetically lowest energy structure is the $^1A_1$ state with CO in a bridging position, close to the Pt−Pt bond. Yet, in contrast to Pd_2CO, the wave function is no longer dominated by a single determinant but is highly multiconfigurational near the equilibrium structure. As a consequence, the MP2 value of the dissociation energy is much too high. The most accurate value at the CASSCF/MRSDCI + Q level is 49 kcal mol^{-1}, thus larger than in the Pd_2CO system. There is also a significant barrier, 17.1 kcal mol^{-1} (at the CASSSCF level), to reach the ground-state structure from Pt_2 and CO at infinite separation. This may explain the differences with the Pd surfaces, in particular the preferential formation of the atop sites for small CO coverage on Pt surfaces.

In $Pd_2(C_2H_4)$, the side-on parallel geometry is also found, at the DFT-B3LYP level, to be more stable than the end-on geometry[136] but to a much larger extent: the interaction energies are 31 and 23 kcal mol^{-1}, respectively. This is due to a greater charge transfer and to greater electrostatic attractive interactions. The Pd−Pd bond is lengthened somewhat with respect to Pd_2, 2.74 Å. This value is very similar to the one in Pd_2N_2. In the same study Fahmi and van Santen also analyzed the bonding of C_2H_4 to Pd_n (n = 3−6). For n = 3−5, the side-on parallel bonding leads to a breaking of the Pd−Pd bond that spans the C−C bond, the Pd···Pd distance decreasing on going from Pd_3 (4.23 Å) to Pd_5 (3.04 Å). The binding energies also decrease along the series.

The work on the heterobimetallic cluster has been extended to a study of the interaction of ZrPt with either H or CH_3.[248] As in ZrPt alone, Zr acts as an electron donor in (ZrPt)H or (ZrPt)CH_3. The metal−H and metal−CH_3 bond strengths are increased upon "alloy" formation with the second metal. The increase is largest for the metal−hydride bond, however. Note that one in fact finds a feature that was already noticed by Siegbahn for PdH and PdH_2, namely, preparation of the metal by the first bond formation to the correct covalency for the second bond. The implications of these findings for catalytic reactions of hydrocarbons on alloys are discussed.[248]

B. Dinuclear Molecular Complexes

1. M(0)–M(0) Complexes

The interaction in the dinuclear complexes [Pt_2-(PH_3)$_4$], [PtPd(PH_3)$_4$], and [Pd_2(PH_3)$_4$], which can been classified as being of "aurophilic" type,[258] has been revisited by Sakaki et al. at levels up to MP4SDQ.[259] Experimentally, a diplatinum complex with a bulky ligand on the phosphorus atoms (which increase the kinetic stability) is known[260] and was investigated long ago at the EH level.[261] The calculations of Sakaki use the relativistic small-core pseudo-

potential of Hay and Wadt[68] and a quite large basis set with polarization functions on the metal and phosphorus atoms. The calculations point clearly to the importance of dispersion interactions (in addition to some rehybridization of the d_σ orbital to minimize the $d_\sigma-d_\sigma$ repulsion): The interaction is repulsive at the HF level, and some stabilization with respect to the two monomers is obtained only at the correlated level. At the best level of theory (MP4SDQ with the polarized basis set and correction from the basis set superposition error), the metal−metal bond energy amounts to 4.4, 4.1, and 3.8 kcal mol^{-1} for the Pt−Pt, Pd−Pt, and Pd−Pd systems, respectively. The decrease along the series further supports the crucial role of the dispersion interactions.

Although not being directly relevant to the metal−metal interaction in Pd(0) or Pt(0) complexes, one may cite here extended Hückel calculations carried out by Harvey and co-workers in a framework of flash photolysis studies of $[M_2(dba)_3]$ complexes (M = Pd, Pt; dba = dibenzylideneacetone).[262] These calculations support the experimental assignment of the spectra.

2. M(I)–M(I) Complexes

There have been many more studies pertaining to the analysis of the metal−metal bond in Pt(I) and Pd(I) d^9-d^9 dimetallic or polymetallic clusters. Many of them have been carried out at the extended Hückel (EH) level in conjunction with experimental studies. Thus, the bonding in the $[Pd_2(dmb)_2X_2]$ unbridged complexes (dmb = 1,8-diisocyano-*p*-menthane; X = Cl, Br) has been analyzed via EH calculations on the model complex $[Pd_2(CNCH_3)_4Cl_2]$.[263] Two limiting conformations corresponding to either a perpendicular or a coplanar arrangement of the two *trans*-$[(CNCH_3)_2ClPd]$ d^9 trigonal (C_{2v}) units have been considered. Not unexpectedly, the greater ligand-field effect of the two *trans*-isocyanide ligands orients the d_σ orbital along the C−Pd−C axis in the HOMO as in the LUMO (via a mixing between d_{z^2} and $d_{x^2-y^2}$) and the bonding in the HOMO is achieved through enlarged equatorial lobes of the d_σ orbital. The energy difference between the two forms is not very high, 2.3 kcal mol^{-1}, consistent with the cylindrical σ bonding between the two metals. However, it might also arise from the rather long Pd−Pd bond, 2.72 Å. Such a long bond would prevent large steric interactions between the isocyanide ligands. EH calculations which had been performed earlier on similar bis-platinum(I) complexes, either for $[Pt_2Cl_2(CO)_2(PH_3)_3]$[264] or $[Pt_2(CNH)_2Cl_2]$[265] with a shorter Pt−Pt bond length of about 2.6 Å, yielded much higher barriers ranging between 53 and 85 kcal mol^{-1}. On the other hand, recent experiments show that the $[Pt_2Cl_2(CO)_2(PR_3)_3]$ systems are fluxional.[266] A more thorough EH investigation on $[Pt_2Cl_2(CO)_2(PH_3)_3]$ carried out simultaneously suggests that this fluxionality might be accounted for by the involvement of an intermediate of C_{2h} symmetry having the two carbonyls bridging the Pt−Pt bond.[266] At the EH level, this structure is only 2.4 kcal mol^{-1} higher in energy than the unbridged structure. The barrier to reach it amounts to only 10.5 kcal mol^{-1}. The bonding in bridged species has been analyzed also, either in Pd(I)−Pd(I) complexes bridged by indenyl or isocyanide ligands[267] or in Pt(I)−Pt(I) complexes bridged by sulfur ligands.[268]

As far as ab initio calculation are concerned, a few HF, post-HF, or DFT calculations have been performed. Provencher and Harvey have again considered, in relationship with some photoprocesses observed experimentally, the unbridged $[Pd_2(CNCH_3)_4Cl_2]$ complex and compared it to the bridged $[Pd_2\{CN(CH_2)_4NC\}_2Cl_2]$ system.[269] Their DFT calculations include nonlocal exchange and correlation corrections. An excellent agreement is found between the computed geometry of $[Pd_2(CNCH_3)_4Cl_2]$ and the X-ray crystal structures of $[Pd_2(CN\text{-}t\text{-}Bu)_4Cl_2]$ and $[Pd_2(CNCH_3)_6]^{2+}$. Unfortunately the rotational barrier problem has not been addressed in this study. The same is true for the MP2 calculations of Sakaki and co-workers on $[Pt_2Cl_2(CO)_4]$ and $[Pt_2Cl_4(CO)_2]^{2-}$.[160] The geometry optimization led to an almost perpendicular structure, in agreement with experiment for $[Pt_2Cl_4(CO)_2]^{2-}$.[270] More attention has been paid in this study to the Pt−Pt binding energy in these two systems. The neutral system is bound by as much as 55 kcal mol^{-1} at the MP2 level. In contrast, the dianion is unbound due to Coulombic repulsion between the two $[PtCl_2(CO)]^-$ fragments, unless countercations are lying in the vicinity of the dimetallic unit. The effect of these countercations has been simulated by positive charges and analyzed via perturbation theory.[160] Somewhat related to the bridged structure computed by Mingos as an intermediate for the fluxional process in $[Pt_2Cl_2(CO)_2(PH_3)_3]$ is the structure of the $[Pd_2(dppp)_2]^{2+}$ cation, **7**, which has been analyzed by HF and GVB calculations by van Leeuwen, Orpen, and co-workers on the $[(PH_3)_2Pd]_2^{2+}$ system.[271] An extra bonding interaction

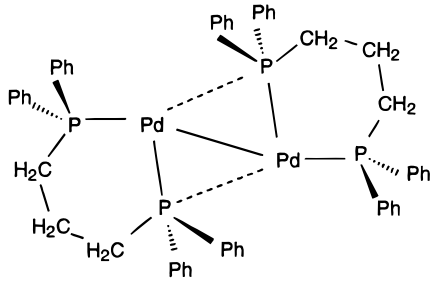

7

arising from overlap between the backsides of the phosphine lone pairs and "unused" Pd d_{xy} lobes is best seen in Figure 6. Interestingly, the proposal that bridging phosphine ligands across a Pt(I)−Pt(I) can exist had been made earlier on the basis of EH calculations on peculiar diplatinum complexes involving gold triphenylphosphine ligands.[272]

The structure of bridged $[Pd_2(\mu\text{-}X)(\mu\text{-}C_3H_5)(PH_3)_2]$ (X = Cl, Br), **8**, has been optimized via MP2 calculations.[273,274] The computed structure is in agreement with experiment.[273,275] The structural features as well as the bonding in this system have been elegantly rationalized by orbital interaction arguments. In fact, this system can be considered as the prototype of a

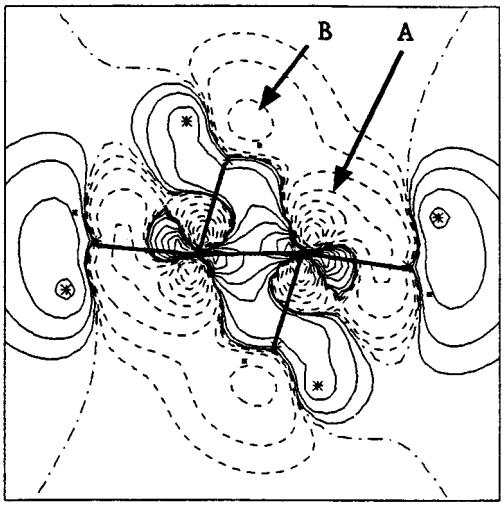

Figure 6. Orbital plot of the metal−metal bonding HOMO of the $[Pd(PH_3)_2]_2^{2+}$ system, showing the overlap between the "unused" Pd lobe (A) and the backside of the phosphine pair (B). (Reprinted with permission from ref 271.) Copyright 1992 American Chemical Society.

series of systems $[Pd_2(\mu\text{-}X)(\mu\text{-}Y)(PR_3)_2]$ where the $[Pd_2(\mu\text{-}X)(PR_3)_2]^+$ cationic fragment is characterized by a

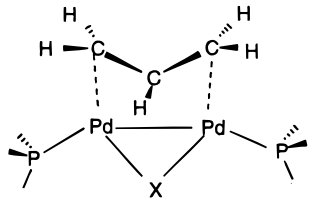

8

HOMO of σ symmetry, and a LUMO and NLUMO of π and σ symmetry, respectively, Scheme 1.[276] It can

Scheme 1

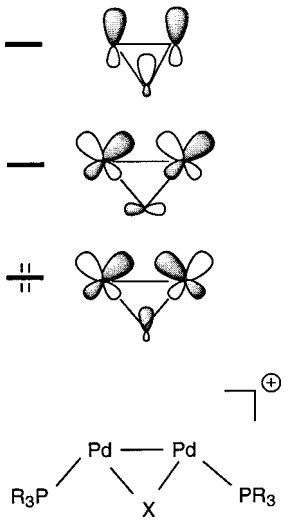

therefore act as a four-electron acceptor. Thus, the structures of the $[Pd_2(\mu\text{-}P^tBu_2)(\mu,\eta^2\text{:}\eta^2\text{-}CS_2)(PPh_3)_2]^+$ cationic complex, **9**,[277] and $[Pd_2(\mu\text{-}SC_6F_5)(\mu\text{-dppm})(PPh_3)_2]$, **10**, a model of which has been calculated recently by HF calculations,[278] have been rationalized along the same lines.[276] Another bridged Pd(I)−Pd(I) complex, viz. $[Pd_2Cl_2(CO)_4]$, has been calculated

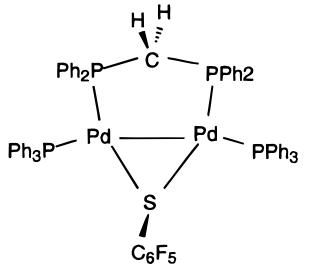

10

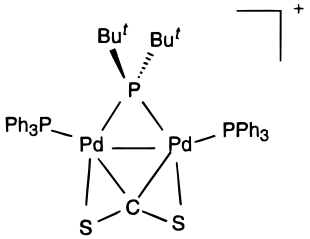

9

at the HF and DFT (in the local spin density approximation) levels: both the planar, **11**, and the hinge conformation, **12**, bridged by two chlorine atoms have been considered and the bonding analyzed. However, it is difficult to discuss the relative

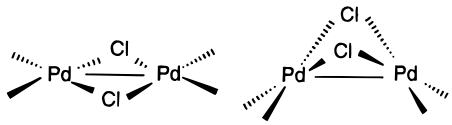

11 **12**

stabilities of these two conformations since no stable molecular structure could be obtained upon geometry optimization.[279]

All the above-mentioned Pd(I)−Pd(I) complexes have a metal−metal bond distance far below 3 Å. Thus, the very long Pd−Pd bond distance found in the X-ray crystal structure of the $[Pd(PPh_3)_2(C_4H_6)]_2^{2+}$ system, in which the $(PPh_3Pd-PdPPh_3)$ unit is sandwiched between two *s-trans*-1,3 diene ligands, has called for a theoretical analysis.[280] This analysis been carried out at the HF and MP2 levels. The MP2 geometry optimization reproduces the experimental structure well. The lengthening of the Pd−Pd bond has been rationalized on the basis of HOMO/LUMO interactions between the $[Pd_2(PPh_3)_2]^{2+}$ unit and the C_4H_6 units. The most noticeable feature is that the orbital involving back-donation from the d_σ metal−metal bonding orbital into the LUMO of $(C_4H_6)_2$ remains practically constant upon Pd−Pd elongation.

3. M(II)–M(II) Complexes

Many theoretical studies that have been devoted to dinuclear Pd(II) or Pt(II) complexes have focused on either analysis of the short Pt···Pt contacts in square-planar Pt(II) d^8 entities that are facing in dimers and in chains or the hinge distortion in bridged dimers. We shall see in the following how these two aspects are in fact quite related to each other.

Scheme 2

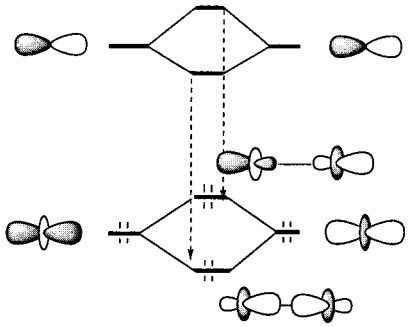

The weakly bonding nature of the $d^8\cdots d^8$ interactions has been recognized by Gray and co-workers[281] and was rationalized using arguments[282] similar to those used to explain $d^{10}\cdots d^{10}$ interactions in bis-platinum complexes (vide supra). These arguments rely on the rehybridization of the d_σ orbitals by p_σ orbitals to minimize the $d_\sigma-d_\sigma$ repulsion.[261,281,283,284] Another view[285] is to consider the bonding as arising from combination of the four electron repulsive interactions between the d_σ orbitals of the two metal atoms with the two attractive donor−acceptor interactions between the d_σ orbital of one metal atom and the p_σ orbital of the other one. When these two attractive interactions are stronger than the repulsive one, then one gets net bonding. These two equivalent views are summarized in Scheme 2.

Alvarez and co-workers carried out the first ab initio calculations on dimers of Pt(II) (and Rh(I)) square-planar complexes, viz. $[PtCl_2(CO)_2]_2$, $[PtCl_2\{HNCH(OH)\}_2]_2$, $H[PtCl_2(CO)_2]_2Cl$, $OC[PtCl_2(CO)_2]_2AuCl$, $[PtCl_2(CO)_2]_2CO$, and $OC[PtCl_2(CO)_2]_2CO$.[286] These systems were selected as models of various known experimental complexes. A relativistic effective core potential and a relatively small basis set were used. The interaction energies were corrected from the basis set superposition error (BSSE), which was in all cases larger than the interaction energy itself, due to the small basis sets used. Thus, the agreement between the optimized MP2 Pt···Pt distances and the experimental ones results most likely from cancellation of errors. Binding energies are reported for $[PtCl_2(CO)_2]_2$ and $[PtCl_2\{HNCH(OH)\}_2]_2$. The staggered conformation of $[PtCl_2(CO)_2]_2$ is found to be unbound once the BSSE has been incorporated. Since the eclipsed conformation of $[PtCl_2(CO)_2]_2$ and $[PtCl_2\{HNCH(OH)\}_2]_2$ may be thought of as resulting from ligand−ligand interactions, pilot calculations were performed for such interactions. They seem to indicate that part of the overall binding can still be traced to metal−metal interactions. An interesting feature of this study, which has been tested by the calculations on the various adducts of $[PtCl_2(CO)_2]_2$, is that the binding of Lewis acid (A) and/or bases (B) at the axial position has an increasing effect on the Pt···Pt bond length along the series $L_4BM-MBL_4 < L_4BM-ML_4 \approx L_4AM-MAL_4 \approx L_4M-ML_4 < L_4M-MAL_4 < L_4BM-MAL_4$. Alvarez et al. have rationalized these features by elaborating further on the hybridization mechanism and its interplay with the pyramidalization of the metal.[287] On the basis of EH and MP2 calculations, a correlation is found between the metal−metal distance and the pyramidality angle at the metal, which in turn can be related to the nature of axial addition.[210] It is shown that addition of a two-electron donor ligand, by decreasing the pyramidality angle, weakens the hybridization and therefore produces weaker (longer) metal···metal contacts. Addition of the Lewis acid has the opposite effect. This study has been extended to a comprehensive analysis, based on EH calculations, of the influence of the equatorial ligands.[285] π-Acceptor ligands, by lowering the p_σ orbital, increase its degree of mixing into the d_σ orbital and thus should contribute to a reinforcement of the metal−metal σ interaction. π-Donor ligands act in the opposite way and should weaken the metal−metal σ interactions. Most of the structural data have been rationalized via this model. The π metal−metal interactions have also been analyzed and provide a basis to explain the deviation from linearity in stacked complexes with mixed ligands.

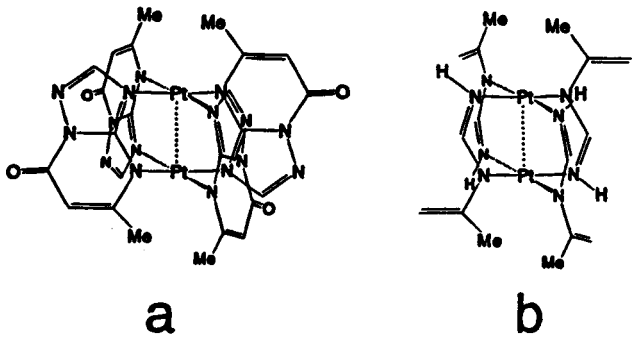

Figure 7. Experimental binuclear Pt(II) triazolopyrimidine-bridged complex (a) and its model $\{Pt_2[NHCHN(C(CH_2)-(CH_3)]_4\}$ (b). (Reprinted with permission from ref 288.) Copyright 1996 American Chemical Society.

A quite refined calculation, at the DFT-B3LYP level, has been done on a model of a platinum binuclear complex obtained from a *cisplatin* analogue.[288] Figure 7 shows the experimental system and the model used for the calculation. The Gaussian-94 LANL2DZ basis set used in this work uses the small-core relativistic pseudopotential of Hay an Wadt[68] and not the large-core one, as incorrectly stated in the article. The optimized geometry agrees with the experimental one, in particular for the Pt···Pt distance which is computed to be 2.751 Å (B3LYP level, the experimental value is 2.744 Å). A very interesting feature of this study is use of the topological analysis of Bader[157,158] to assess the nature of the bonding between the two platinum atoms: a bond critical point is found at the middle of the Pt−Pt vector with a positive value of the Laplacian of the electronic

charge density, thus consistent with a closed-shell-type interaction. However, a negative value of the local energy density at this point indicates some covalent contribution to the interaction. This contribution must obviously arise from the hybridization pattern. The same analysis performed on the HF wave function yields a similar conclusion. All these findings are in line with the conclusions of Sakaki[259] on the $d^{10}\cdots d^{10}$ interactions in the palladium complexes (vide supra) and support (at variance with Pyykkö[258]) the conclusion that such interactions are more than pure dispersion interactions.

Related to this study is the more recent investigation, using NL-DFT calculations (which also include relativistic effects) of the electronic structure of $[M(dmit)_2]_2^n$ ($n = 0, -1$; M = Pt, Pd, Ni; dmit = 2-thioxo-1,3-dithiole-4,5-dithiolato) units involved in stacks.[289] The bonding has been shown to arise primarily from ligand−ligand attractive interactions. These attractive interactions are supplemented, especially in the case of Pt (and to a lesser extent in the case of Pd), by metal−ligand and metal−metal interactions. The metal−metal interactions are of the same nature as the ones just discussed above. A slight bending away of the ligands relieves part of the steric repulsion (in the Pt case), as does the slipping of the two units. The delicate balance between all these factors has been assessed via an interaction energy analysis.[289]

Somewhat related to the $d^8\cdots d^8$ cofacial dimers are $d^8\cdots d^{10}$ heterobimetallic complexes where a gold or a silver cation is facing a square-planar d^8 platinum complex. There has been an investigation of such complexes but at the extended Hückel level only.[290] The experimental spectra and the photochemistry have been discussed on the basis of the nature of the molecular orbitals. More refined calculations would be necessary to make firmer conclusions.

The bonding and the structure of edge-sharing dimers of square-planar complexes were first addressed by Alvarez and co-workers. They analyzed via EH calculations the bonding in the planar d^8-d^8 $[Pt_2L_4(\mu\text{-}XR_n)]$ systems.[291] The generalized orbital interaction diagram of Figure 8 shows how the so-called framework molecular orbitals are formed from the σ and π valence orbitals on both the metals and the bridging groups. For d^8 metals such as platinum or palladium, one has eight valence electrons that give rise to four doubly occupied orbitals, thus accounting for the four metal-to-bridging ligands bonds. Lledós has used these orbitals to rationalize via both EH and ab initio calculations the hinge distortion in platinum(II) dimers with a Pt_2X_2 ring (X = S, SR).[292] The argument is based on the allowed mixing, upon folding of the Pt_2X_2 ring, of some of these orbitals with orbitals of d_δ type. It is rather weak, however, and some counter examples have been found.[293,294] For instance, the structure of the $[Pt_2Se_2(PPh_3)_4]$ complex was found to be planar both in the X-ray crystal structure and via a geometry optimization carried out at the HF level (but not at the MP2 level).[293] In fact, it was recognized later in a joint study that this hinge distortion could be analyzed like the $d^8\cdots d^8$ interactions in stacked platinum dimers.[294]

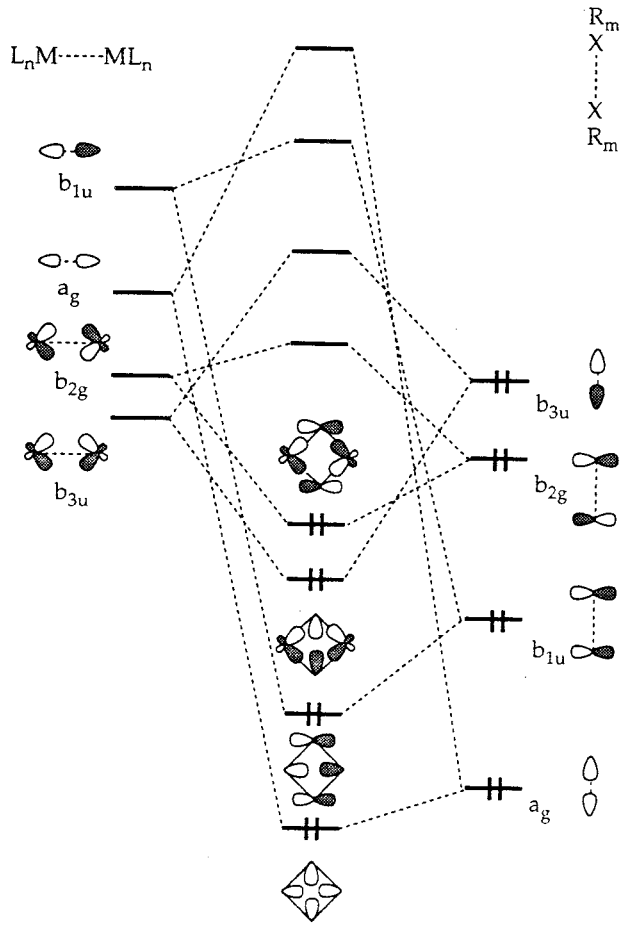

Figure 8. Schematic orbital interaction diagram between two ML_n fragments (left) and two XR_m bridges (right) to form a $[M_2L_{2n}(\mu\text{-}XR_m)_2]$ complex. The orbitals are labeled according to their representation in the D_{2h} group. Only the in-plane framework orbitals are considered; the nonbonding d orbitals are omitted. (Reprinted with permission from ref 291.) Copyright 1994.

The only difference is that the two d_σ orbitals (as the two p_σ orbitals) now make an angle smaller than 180°, see **13**. Thus, Lledós, Alvarez, and co-workers

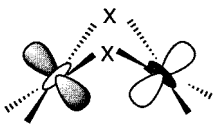

13

were able to provide a rationale for many experimental structures on the basis of the attractive metal$\cdots$metal interactions shown in Scheme 2, eventually modulated by various ligand effects of electronic and steric nature, and with the aid of MP2 geometry optimizations.[294,295] Quite noteworthy, their view of the bonding is supported by a topological charge density analysis that was carried out on a bent dirhodium(I) complex: there, as in the *cisplatin* analogue dimer that we mentioned previously, a bond critical point between the two metal atoms characteristic of a direct coupling is found.[296]

There have been a few other calculations dealing with M(II)−M(II) complexes of palladium and platinum. The bonding in a diplatinum system resulting from the dimerization, upon one electron−one proton

electroprotic transformation, of two Pt(II) bis-chelate radicals has been unravelled. It corresponds to the coupling of the two unpaired electrons of the chelate rings and to some $d_{z^2}-d_{z^2}$ interaction.[297] Marks et al. have carried out ab initio calculations (at the HF level) on cofacial dimers of palladium bis(glyoximates) to rationalize the temperature-dependent conductivity of low-dimensional, partially oxidized material $Pd(dpg)_2^{0.20+}(I_5^-)_{0.20}$ (dpg = diphenylglyoximato).[298] DFT-B3LYP calculations on the bipyrimidine-bridged bis-Pt(II) system $[Me_2Pt(bpym)PtMe_2]$ have shown that the LUMO is essentially a bipyrimidine π^* orbital, thus accounting for the radical anion character of the one-electron-reduced species.[299] There is no significant interaction of the metal fragments across the π-conjugated bipyrimidine ligand. The study has been extended to the Pt(IV)−Pt(IV) $[Me_4Pt(bpym)PtMe_4]$ complex, whose DFT structure is in good agreement with the experimental X-ray crystal structure.[299] The single metal−metal bond in $L_4M-M'L_3$ dimers of d^8 metal ions, with the structural motif shown in **14**, has been rationalized via molecular orbital interactions based on extended Hückel calculations.[284,300,301] In one case, corresponding to the systems of the type $L_4Pt-PdL_2Y$ (Y being a trans halogen substituent), an inverse halogen dependence of the ^{195}Pt chemical shift vs orbital energy differences has been found and is indicative of the transmission of electronic effects via the metal−metal bond.[301] The single bond in $L_4Pt-M'L_2$ d^8-d^{10} dimers with the structural motif shown in **15** also has been analyzed via EH calculations.[284] The bonding characteristics in the phosphido-bridged $[Pt_2(\mu\text{-}P^tBu_2)_2(H)(PH^tBu_2)]^+$ system (where H is a terminal hydrido ligand) and in the *phosphine*-bridged $[Pd_2(\mu\text{-}P^tBu_2)_2(\mu\text{-}PtH^tBu_2)(PH^tBu_2)_2]^+$ system have been compared via HF and DFT calculations.[302] The Bader population analysis clearly shows three center Pd···H−P interactions in the latter case.

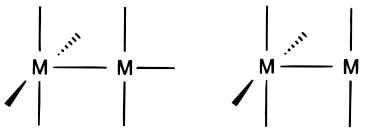

14 **15**

4. M(III)–M(III) and M(II)–M(IV) Complexes

There is a wide variety of dinuclear Pt(III)-Pt(III) dinuclear complexes with bridging ligands across the single metal−metal bond, e.g., sulfates (SO_4^{2-}), hydrogen phosphates (HPO_4^{2-}), pyrophosphites ($H_2P_2O_5^{2-}$), or acetates (O_2CCH_3).[303] In the latter case the bonding has been analyzed via quasirelativistic-Xα calculations on the analogous tetraformate complex $[Pt_2(\mu\text{-}O_2CH)_4(H_2O)_2]^{2+}$.[304] The computed molecular orbital sequence does indeed correspond to a metal−metal single bond with the σ^* orbital being the lowest unoccupied orbital. As expected, the quasirelativistic corrections stabilize the orbitals with significant 6s character and raise those with significant 5d character, thus further strengthening the metal−metal σ bond via increased mixing of 6s and 5d. These results have been used to interpret the observed electronic spectrum of the corresponding tetraacetate complex.[304]

The first dinuclear complex of palladium(III) was recently isolated, owing to the use of the dinitrogen-donor ligand hpp (the anion of 1,3,4,6,7,8-hexahydro-2*H*-pyrimido[1,2-*a*]pyrimidine) and its X-ray crystal structure solved.[305] The $[Pd_2(hpp)_4Cl_2]$ system has a very short Pd−Pd bond of 2.391 Å. A HF geometry optimization (with an all-electron valence double-ζ basis set supplemented by polarization functions on all atoms) led to an optimized bond length of 2.402 Å. Not surprisingly the metal−metal interaction corresponds to a $\sigma^2\pi^4\delta^2\delta^{*2}\pi^{*4}$ configuration.[305]

The system $[(H_2PCH_2CH_2PH_2)Pt(\mu\text{-}SCH_3)_2PtIMe_3]$ has been computed as a model of the experimental complex $[(Ph_2PCH_2CH_2PPh_2)Pt\{\mu\text{-}SCH(CH_2CH_2)_2NMe\}_2PtIMe_3]$, whose X-ray crystal structure is characterized by the folded nature of the central $Pt^{II}(\mu\text{-}S)_2Pt^{IV}$ ring, the anti conformation of the alkyl chains of the thiolate ligands, and the position of the iodine atom in the inner region of the hinged Pt_2S_2 ring.[306] The calculations were carried out at the DFT-B3LYP level with a small-core relativistic pseudopotential.[68] Various isomers have been considered, the most stable one computed to be the anti(I-*endo*), in agreement with the experimental structure. This has been ascribed to some attractive interaction between iodine and the unsaturated Pt(II) center: Note, however, that the calculations seem to overemphasize this interaction: the computed Pt···I distance amounts to 3.38 Å, whereas it is 3.86 Å in the experimental structure. This is due to a greater folding of the Pt_2S_2 core and to a larger Pt−I bond in the calculations. The transition states for the interconversion between the most stable isomers have been determined and discussed in connection with the NMR data.[306]

C. Tri and Polynuclear Molecular Complexes

Many studies have been devoted to the $[M_3(\mu_3\text{-}CO)(dppm)_3]^{2+}$ systems (M = Pd;[307] M = Pt[308]) and their various adducts or derivatives. The interest for such systems stems from the fact that they can be considered for their chemical properties as mimicking either a Pt_3 or Pd_3 unit on a platinum or palladium surface. Moreover, they display a very interesting stoichiometric and catalytic activity.[309] Most of the theoretical studies, essentially of extended Hückel type, arise from the Puddephatt group and from the Harvey group and are intimately linked to the experimental aspects. Puddephatt has rationalized the structures of the $[Pt_3(\mu_3\text{-}H)L(dppm)_3]^+$ and $[Pt_3(\mu_3\text{-}CO)L(dppm)_3]^{2+}$ systems, in particular the fact that the capping ligand is asymmetrically bound.[310] The factors that contribute to the terminal mode of binding for the two isocyanide ligands on a single platinum atom of $[Pt_3(CNR)_2(dppm)_3]^{2+}$ have been delineated.[311] The interactions of either $[Re(CO)_3]^+$ or $[ReO_3]^+$ with the $[Pt_3(dppm)_3]$ fragment have been compared in the framework of a study aimed at characterizing models for oxide interactions in bimetallic catalysts.[312]

Harvey and co-workers have paid more attention to the tripalladium complex (although in some in-

stances the triplatinum complex was considered as well) and have focused on the photophysical and electrochemical properties. They first correlated the electronic spectra of $[Pd_3(\mu_3\text{-}CO)(dppm)_3]^{2+}$ and $[Pt_3(\mu_3\text{-}CO)(dppm)_3]^{2+}$ to the orbital sequence obtained from an extended Hückel calculation.[313] More refined calculations of DFT type, made in collaboration with Ziegler, have led to a firmer assignment of the spectra. The nature of the lowest electronic states $^3A_2$ (which corresponds to a $\sigma \rightarrow \sigma^*$ transition) and ^1E has been assessed. The authors have used these results, in particular the expected Pd···Pd lengthening upon excitation, to elaborate further on the host−guest chemistry of these systems in the excited states.[314] Subsequent optimizations (again at the DFT level) of the $[Pd_3(PH_3)_6(\mu_3\text{-}CO)]^{2+}$ system for the ground state $^1A_1$ and for the excited states $^3A_2$ and ^3E showed indeed a lengthening of 0.186 Å in the $^3A_2$ state (and of 0.289 Å in the ^3E state). This has been confirmed by an analysis of the emission band.[269] In relation with this host−guest chemistry, Harvey et al. have also considered the mixed-metal trinuclear system $[Pd_2Co(\mu_3\text{-}CO)_2(dppm)_2(CO)_2]^{2+}$. They have computed at the DFT level the molecular orbital sequence and used this sequence to predict the nature of the lowest transitions of the UV spectra of related complexes.[315] The same group has finally investigated the photoinduced oxidative degradation of the $[Pd_3(\mu_3\text{-}CO)(dppm)_3]^{2+}$ cluster by chlorocarbons and by the chloride ion,[316] as well as its electrochemical reduction.[317] Since many of the arguments were of geometrical type, the geometries of the adducts $[Pd_3(PH_3)_6(\mu_3\text{-}CO)\cdots Cl]^+$, $[Pd_3(PH_3)_6(\mu_3\text{-}CO)(\mu_3\text{-}CO)\cdots Cl{-}CH_3]^{2+}$, of the oxidized form $[Pd_3(PH_3)_6(\mu_3\text{-}CO)]^{3+}$, and of the reduced forms $[Pd_3(PH_3)_6(\mu_3\text{-}CO)]^+$ and $[Pd_3(PH_3)_6(\mu_3\text{-}CO)]$ have been determined at the DFT level (including nonlocal exchange correlation corrections).[316,317]

Some other studies have dealt with clusters that can be considered as or are related to building blocks of Chini's clusters. Such clusters consist of triangular $[M_3(CO)_6]_n^{2-}$ units ($n \geq 1$; M = Ni, Pt) stacked along the 3-fold axis of symmetry.[318] In conjunction with an experimental study of the liquid structure of $[Pt_3(CO)_6]_2^{2-}$ which shows that this system adopts, as in the solid state, an eclipsed conformation of the two $[Pt_3(CO)_6]^{2-}$ triangular units (in contrast to the Ni analogue where the liquid and the solid structures have a different arrangement), both the eclipsed (D_{3h}) and staggered (D_{3d}) conformations have been calculated.[319] The calculations were carried out within the DFT formalism, with and without nonlocal corrections. The structural parameters obtained from the B3LYP calculations are in good agreement with experiment. At this level of theory the energy difference between the two conformations D_{3h} and D_{3d} is only 0.1 kcal mol^{-1}. In fact, these two conformations turn out to be transition states and the true minimum that corresponds to a twisting angle of about 30° lies 1 kcal mol^{-1} lower. The reduced radial distribution functions corresponding to the atom−atom distance obtained from the calculations and from experiment match quite well. The monocluster $[Pt_3(CO)_6]^{2-}$ could be isolated and characterized by IR, NMR, and liquid X-ray scattering. The B3LYP computed structure is again in agreement with experiment.[319] The $[Pt_3(CO)_6]$ neutral system has also been recently investigated at the NL-DFT level.[320] As in many previous studies,[321] the ground state corresponds to the $(a'_1)^2(a'_2)^0$ configuration. The vibrational spectrum has been computed and discussed in connection with CO chemisorption on platinum surfaces.[320] In the context of Chini's clusters, one should also mention hexaplatinum complexes involving $[Pt_6(\mu_2\text{-}CO)_6(\mu_2\text{-}dppm)_3]$ as elementary unit, where the three dppm ligands hold together two triangular units. The study by the Puddephatt group includes some extended Hückel calculations.[322,323] Yamamoto and Yamazaki have analyzed, through extended Hückel calculations, the mixed cluster $[HgPt_6(2,6\text{-}Me_2C_6H_3NC)_{12}]$ in which Hg is sandwiched between two $[Pt_3\{\mu_3\text{-}(2,6\text{-}Me_2C_6H_3NC)\}_3(2,6\text{-}Me_2C_6H_3NC)_3]$ units.[324]

The bonding in mixed linear trinuclear mercury platinum clusters of general formula $[\{Pt(diphosphine)(isocyanide)\}_2Hg]^{2+}$, **16**, has also been analyzed via extended Hückel calculations.[325] Note that these

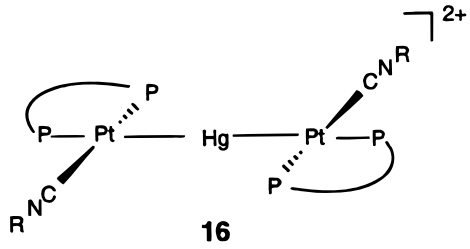

16

clusters were originally, but erroneously, formulated as $[\{Pt(diphosphine)(isocyanide)\}_2Pt]^{2+}$ and analyzed as such.[326] Related to these systems are systems in which Hg is substituted by a linear or a bent d^{10} ML_2 unit (in this case the metal−metal bonds are supported by triphosphine ligands acting either in a bidentate or tridentate way).[327] Thus, a comparison of the orbital interaction diagrams of the $[\{Pt(PH_3)_2(CNH)\}_2Hg]^{2+}$ and $[Pt_3(PH_3)_6(CNH)_2]^{2+}$ model systems clearly shows the similarity in the respective bonding patterns, a doubly occupied $d_{x^2-y^2}$ orbital on PtL_2 playing the role of the 6s orbital of Hg.[327] Interestingly, the $[Pd_4(dmb)_4(PPh_3)_2]Cl_2$ system (dmb = 1,8-diisocyano-*p*-menthane) and its polymers have been recently synthesized and analyzed via extended Hückel calculations by Harvey and co-workers.[328] These $[L_3M{-}ML_2{-}ML_2{-}ML_3]^{2+}$ type systems (M = Pt) can be seen as the next members of a series starting with the $[L_3M{-}ML_2{-}ML_3]^{2+}$ systems that we just mentioned. In the tetranuclear complexes, the bonding arises from a two-electron bonding interaction between dp hybrids localized on the ML_2 end of each $[L_3M{-}ML_2]^+$ moiety.[328]

Quasirelativistic Xα calculations have been performed on Pd_6Cl_{12} and the molecular orbital sequence obtained from these calculations discussed by comparison to the sequences obtained for $PdCl_2$ and $PdCl_4^{2-}$.[329] This system makes aggregates with a variety of π systems, from benzene to fullerene C_{60}. The composition of the orbitals, especially the empty ones, has been used as an indicator to suggest that

the π system can act as a donor in a charge-transfer state.

IV. Reactivity Studies

There have been a few reviews or books dealing with the theoretical aspects of organometallic reactivity already.[14,16,330−332] In the following we will focus on reactions involving more specifically palladium or platinum.

1. Oxidative Addition and Reductive Elimination

Reactions Involving One Metal Center. As said in the Introduction, this class of reaction was investigated from a theoretical point of view quite early, especially for H−H, C−H, or even C−C bonds with either naked metal atoms or with the $M(PH_3)_2$ fragment (M = Pd, Pt).[55,333−338] Thus, a coherent picture has emerged. It emphasizes the covalent nature of the M−H or M−C bond in the oxidative addition product and the competition between the d^9s^1 and d^{10} states of the metal atom, at least when the M^0/M^{II} (M = Pd, Pt) pair of formal oxidation states is involved. In particular, the formation of the two M−H or M−C bonds requires the promotion of the metal to the d^9s^1 state. The more accessible this state, the more exothermic or the less endothermic the oxidative addition and the lowest the corresponding energy barrier are. This is why oxidative additions are generally easier with Pt than Pd systems. Conversely, the reductive elimination process is easier for Pd than for Pt. As far as the geometries are concerned the reactions

$$H_2 + Pt(PH_3)_2 \rightarrow Pt(H)_2(PH_3)_2$$

and

$$Pt(H)(CH_3)(PH_3)_2 \rightarrow Pt(PH_3)_2 + CH_4$$

were the first organometallic reactions for which transition states were determined through a gradient geometry optimization.[333,335] One distinctive feature was the presence of an early transition state for the oxidative addition of H_2. The theoretical investigations that were carried out before 1990 have been reviewed.[331,339]

The subsequent studies have aimed at (i) a more precise determination of the kinetic and thermodynamic parameters, (ii) a comprehensive assessment of all parameters involved in the reaction, including the steric ones when bulky ligands are present, (iii) a comparison of the reactions on Pd and Pt with reactions on other metals, (iv) an extension to the oxidative addition of bonds other than H−H, C−H, or C−C, and (v) a step toward the heterogeneous regime by looking at reactions on Pd and Pt clusters and surfaces.

Hay has compared, on the $H_2 + Pt(PH_3)_2 \rightarrow Pt(H)_2(PH_3)_2$ reaction, the performance of his two sets of pseudopotentials,[68,124] the large-core ones which were used in earlier investigations and the small-core ones which have been used in this study.[340] In addition to the explicit treatment of the 5s and 5p electrons, the small core pseudopotentials are norm conserving, i.e., they preserve the valence electron density about Pt. Since the large-core pseudopotentials overestimate the bond energies, the exothermicities that were obtained from the previous studies are too high. The small-core pseudopotential have been used by Morokuma and co-workers in their benchmark study of the $H_2 + Pt(PR_3)_2 \rightarrow Pt(H)_2(PR_3)_2$ reaction (R = H, Me, ^{t}Bu, and Ph) with their newly developed "integrated MO + MM" method.[79] At the highest level of geometry optimization, the calculations for the MO part of the system were of MP2 type with a valence double-ζ basis set, polarized for the ligands. We shall not discuss here the performance of this approach, which is the subject of another article of the present thematic issue. From a chemical point of view, some points are worth mentioning: The energy barrier is low and similar for H (3.8 kcal mol^{-1}), Me (3.9 kcal mol^{-1}), and Ph (1.3 kcal mol^{-1}) and as expected much higher for ^{t}Bu (14.5 kcal mol^{-1}). In this latter case the steric effects lead to a twist of H_2 in the transition state, the H−H−Pt−P angle being 32.2°. The lower barrier for R = Ph is due to some inter-phenyl attractive interactions. This is best seen from a decomposition analysis of the energy into a MO and a MM part. The product is found to be predominantly cis for R = H, Me, and Ph and trans for R = ^{t}Bu, again as a result of the steric effects. Finally the value of 20.4 kcal mol^{-1} computed for the barrier of the reverse reaction, i.e., the reductive elimination of H_2 from $[(H)_2Pt(PMe_3)_2]$, is in excellent agreement with the experimental value in a noncoordinating solvent,[341] 20.0 ± 0.5 kcal mol^{-1}.

A detailed examination of the articles written by Siegbahn, Blomberg, and co-workers about their comprehensive investigation of the C−H bond oxidative addition[342−345] to the second-row transition metals allows one to compare this process for C−H bonds involving either sp^3, sp^2, or sp carbon atoms. The first studies have been performed for the oxidative addition of CH_4,[346−348] with basis sets and methods being improved over the years. We shall therefore discuss only the results of their latest calculations,[348] together with those of the studies on the oxidative addition of C_2H_4[348] and of C_2H_2[170] for which they used the same methodology. The geometries were optimized at the SCF level with a small-core relativistic pseudopotential[68] and valence double-ζ basis sets. For the energy determination, larger basis set were employed (with polarization functions on all atoms including palladium) either at the MCPF level or at the CCSD(T) level, starting from the SCF wave function as a zeroth order wave function. In the CCSD(T) calculations which served as benchmark calculations for the entire row, the basis sets were especially large and several polarization functions on each atom were added. The main energetic results with some geometric features are summarized in Table 5. More details about the optimized geometries of the molecular precursors, transition states, and products may be found in the original publications.

As seen from Table 5, the optimized geometries are quite similar for the three reactions. It has been argued that the SCF level is sufficient for geometry optimization, since in the most interesting regions

Table 5. Comparative CCSD(T) and MCPF Results for the C−H Bond and C−C Bond Oxidative Addition to Palladium

	Pd + CH_4	Pd + C_2H_4	Pd + C_2H_2	Pd + C_2H_6[e]
		Molecular Complex		
ΔE (kcal mol^{-1})[a]	(−4[c])	−30.7 (−26.7)	−28.3 (−27.2)	
M−C (Å) [b]	2.5 [c]	2.13		
		Transition State		
$\Delta E^{\ddagger}$ (kcal mol^{-1})[b,d]	10.6 (15.0)	0.3 (4.7)	−4.1 (−1.1)	23.1 (31.8)
M−C (Å)[b]	2.10	2.01	1.97	2.17
M−H (Å)[b]	1.54	1.53	1.53	
∠C−M−H[b]	57.1°	61.8°	57.7°	
∠C−M−C[b]				58.3°
		Products		
ΔE (kcal mol^{-1})[b,d]	5.6 (9.3)	−2.2 (1.5)	−5.4 (−3.6)	−0.2 (+7.2)
M−C (Å)[b]	2.03	1.98	1.95	2.03
M−H (Å)[b]	1.53	1.54	1.50	
∠C−M−H[b]	82.7°	80.5°	79.2°	
∠C−M−C[b]				89.9°
ΔE_{elim} (kcal mol^{-1})	5.0 (5.7)	2.5 (3.2)		

[a] CCSD(T) values, the MCPF values are in parentheses; no ZPE correction is included; negative values correspond to exothermic reactions. [b] SCF optimized geometries; thus, a negative energy barrier corresponds to a barrierless reaction at the CCSD(T) and/or MCPF level. [c] With an assumed geometry taken from the corresponding rhodium system. [d] Computed to the separated substrate and Pd (^{1}S). [e] C−C bond oxidative addition.

of the potential energy surface (including the transition state and the product) the SCF and MCPF surfaces are quite parallel. Moreover, due to the flat character of the surfaces in these regions, discrepancies between SCF- and MCPF-optimized geometries should have very small effects. Although one can agree on these arguments, it is nevertheless somewhat puzzling that in every case the transition-state geometry is product-like, also in the case of the exothermic reactions Pd + C_2H_4 and Pd + C_2H_2. Note that these reactions are exothermic only at the CCSD(T) level. It is therefore likely that the product-like geometry is a consequence of the endothermic nature of all reactions at the SCF level, which is the level of optimization. Siegbahn and Svensson have carried out a systematic investigation of the geometry optimization step for second-row transition metals, comparing the SCF, MP2, and QCISD levels, but essentially for stable structures.[349] A transition state was considered only in one case, for the reaction Pd + H_2O → Pd(H)(OH). However, this reaction is exothermic at both the SCF and QCISD levels. It is therefore not surprising that in this case a minimal variation for the transition state is found. Calculations carried out later by Sakaki et al. for the oxidative addition of the Si−H and the Si−Si bonds on Pd(PH_3)$_2$ and Pt(PH_3)$_2$ showed large differences between the MP2- and SCF-optimized values.[350] But, as pointed out by one referee, the "softer" character of the Si systems compared to the C system should lead to stronger geometric responses to changes in the reaction energy. Indeed, the relative energies computed from the SCF and MP2 geometries differ by less than 2.0 kcal mol^{-1}. This justifies the original assumption of Siegbahn et al., at least for model systems that do not involve bulky substituents where the difference in the structure might have more influence on the energies.

As far the energies are concerned, the endothermicity (for the Pd + CH_4 reaction) or the quite low exothermicity (for the Pd + C_2H_4 and Pd + C_2H_2 reactions) has been ascribed (as in Goddard's work) to the d^{10} nature of the ground state of the palladium atom and to the relatively high d^{10}−d^9s^1 splitting. On the other hand, that there are no electrons in the 5s orbital leads to a minimal repulsion with the incoming substrate and explains why the energy barriers are relatively moderate for CH_4 or very low for C_2H_4 (there is no barrier for C_2H_2). The general trend that the energy barrier decreases on going from CH_4, to C_2H_4, to C_2H_2 (and that the stability of the product increases) is traced to a steric effect: the sideways orientation necessary for an efficient interaction between the metal and the C−H bond is more easily reached by ethylene and acetylene than by methane.[170,348] Hybridization effects (which relate the strength of a C−H bond to the degree of 2s mixing in that bond) were put forth in these studies but were discarded later.[130] Note here that an alternate explanation based on spin uncoupling inside the ethylene was provided very recently by Minaev and Ågren.[137] Specifically, upon displacement along the asymmetric Pd−C vibration mode, there is a strong spin uncoupling induced by the low-lying ^{3}D (d^9s^1) state of Pd. The $^3(\pi\pi^*)$ excited triplet state of ethylene can mix into the $^3(\sigma\sigma^*)$ excited triplet state, which at the transition state is localized on the C−H bond. For methane there is no involvement of a $^3(\pi\pi^*)$ triplet state and thus no possibility of mixing with the $^3(\sigma\sigma^*)$ state. This leads to a higher activation barrier. Either these arguments or the steric argument provide a rationalization of the fact that stronger C−H bonds (C(sp)−H > C(sp^2)−H > C(sp^3)−H) are also more easily activated. According to Siegbahn, the difficulty to observe C−H bond oxidative addition reactions of either alkenes or alkynes can be explained instead by the strong stability of the Pd−C_2H_4 or Pd−C_2H_2 molecular precursor complexes. These molecular complexes act as thermodynamic sinks. A similar feature is also found at the NL-DFT level by Fahmi and van Santen: in their calculations the molecular complex is bound by 39 kcal mol^{-1}, the reaction Pd + C_2H_4 → Pd(H)(C_2H_3) is exothermic by 6 kcal mol^{-1} with a transition state 3

kcal mol^{-1} below the separated reactants. The good agreement with the benchmark values of Siegbahn and co-workers[348] has been taken as an argument to use the DFT method to study the C−H activation on the palladium dimer.[136]

Table 5 also shows the results that were obtained by Siegbahn and Blomberg for the C−C bond oxidative addition of ethane to Pd.[351] As expected from previous work,[55] the energy barrier is much higher than that for the C−H bond oxidative addition, because two CH_3 groups (instead of one) have to undergo a costly tilting in order to orient themselves favorably. Blomberg and Siegbahn noticed, however, that among the second-row metal atoms, palladium is the one which has the lowest barrier for breaking the C−C bond, since it is the only one to have an s^0 ground-state configuration. The presence of such an s^0 state is more important for the C−C bond than for the C−H bond oxidative addition, because the repulsion of the metal will involve the nonbonding electrons of *two* methyl groups. The reaction is almost thermoneutral. Interestingly, the two methyl groups in the $Pd(CH_3)_2$ product make an angle of 90°, i.e., the ideal angle for a d^9s^1 hybridization. An additional interesting feature of the study is the comparison of the oxidative additions of the C−C bond in ethane (C_2H_6), cyclopropane (C_3H_6), and cyclobutane (C_4H_8). The corresponding barriers at the MCPF level are 23.1, −10.6, (i.e., barrierless), and 6.9 kcal mol^{-1}, the reaction energies being, respectively, −0.2, −22.4, and −19.6 kcal mol^{-1}. It has been argued that the oxidative addition of cyclopropane proceeds without energy barrier because of the strong strain of the metal−carbon bonds in the metallacyclobutane adduct (the C−M−C angle amounts to 69.5°).[351] Although one can easily understand that the strain in the cyclopropane *reactant* should lead to low barriers, it is difficult to see how the strain in the metallacyclobutane *product* can induce a low barrier. One would follow such arguments more easily when considering the barrier for the reverse process, the reductive elimination: in this case the greater strain of the metal−carbon bonds in metallacyclobutane (C−M−C angle = 69.5°) compared to metallacyclopentane (C−M−C angle = 85.3°) readily accounts for a lower barrier in the former case (11.8 kcal mol^{-1} compared to 26.5 kcal mol^{-1}).

According to Siegbahn, Blomberg, and co-workers, the accuracy of these CCSD(T) calculations is about ±5 kcal mol^{-1}. In studies carried out in conjunction with gas-phase kinetic measurements, further refinements were brought to these values by adding the zero-point vibrational energies to all stationary points and using the so-called PCI-80 computational scheme.[107,109] In this scheme[113] the correlation effects are scaled, assuming that the MCPF technique recovers 80% of these effects at the stationary points. Some of the results of the corresponding calculations are summarized in Table 6. The comparison with Table 5 shows that using the PCI-80 scheme and incorporating the zero-point energy effects increase the binding energies and lower the energy barriers quite uniformly, by about 5 kcal mol^{-1} with respect to the CCSD(T) values and somewhat more (∼ 10−12 kcal mol^{-1}) with respect to the MCPF results. Thus, the comparative results obtained previously for palladium still hold, at least as long as the comparison is restricted to the C−H and C−C bond oxidative addition.[107] There is one problem, however, arising from the comparison with the Pd + H_2 reaction. The MCPF calculations yield an *exothermicity* of 7.3 kcal mol^{-1} for the PdH_2 product.[352] If the PCI-80 would further decrease this value, for PdH_2 one would get a result at variance with the previous study of Balasubramanian in which the PdH_2 system is about 5 kcal mol^{-1} *above* Pd(^{1}S) + H_2.[57] Some clarification on this point is needed.

Table 6. PCI-80 Energy Results for the C−H Bond and C−C Bond Oxidative Addition to Palladium and Platinum

	Pd + CH_4	Pd + C_2H_4[b]	Pd + C_2H_6	Pt + CH_4
		Molecular Complex		
ΔE (kcal mol^{-1})[a]	−5.1	−34.6	*c*	−2.1
		Transition State		
$\Delta E^{\ddagger}$ (kcal mol^{-1})	3.6	−4.4	19.5	1.2[d]
		Products		
ΔE (kcal mol^{-1})	−2.3	−7.2	−5.5	−32.0
$\Delta E^{\ddagger}_{elim}$ (kcal mol^{-1})[e]	5.9	2.8	25.0	33.2

[a] The ZPE corrections are included; the spin−orbit corrections are taken into account for the platinum complexes; the values are relative to the free substrate and the metal atom in its ground state, i.e., Pd (^{1}S) and the lowest component of the Pt d^9s^1 ($^3D_3$); negative values correspond to exothermic reactions. [b] C−H bond oxidative addition. [c] Only an η^2-CH complex is reported with a binding energy of 6.6 kcal mol^{-1}. [d] This value refers to the crossing point between the singlet and the triplet surface, see text. A transition state on the singlet surface has been obtained at the SCF level, 10.5 kcal mol^{-1} below the separated reactants. [e] Barrier for the reverse reaction, i.e., the reductive elimination process.

The platinum results for the reaction Pt + CH_4 are also of interest.[109] The corresponding calculations were carried out with a large basis set and a newly developed relativistic effective core potential. This RECP not only treats the 5s and 5p electrons explicitly, but also the 4d electrons, which are described by one contracted orbital. The spin−orbit effects were taken into account via the total quenching model (i.e., assuming that the energy lowering due to spin−orbit effects takes place only for the platinum atom). The geometries were optimized at the MP2 level. The corresponding energy profile is shown in Figure 9. A salient feature is the crossing of the triplet and singlet surfaces at the beginning of the reaction. The crossing takes place at a very low energy, 1.2 kcal mol^{-1} above the reactants Pt (^{3}D) + CH_4. The spin−orbit interaction between these two states is not taken into account in the total quenching model. It should further lower the barrier arising from the crossing. The very low barrier is in agreement with the experimental findings. The very deep well for the Pt(H)(CH_3) intermediate and the very high barrier associated with the subsequent H_2 elimination (which is in fact nothing other than the reverse of a σ-bond metathesis reaction) leads to the result that Pt(H)(CH_3) is most likely the final product of the gas-phase reaction. The effectiveness of the reaction of Pt with CH_4 (and small alkanes) is therefore a consequence of the d^9s^1 ground state

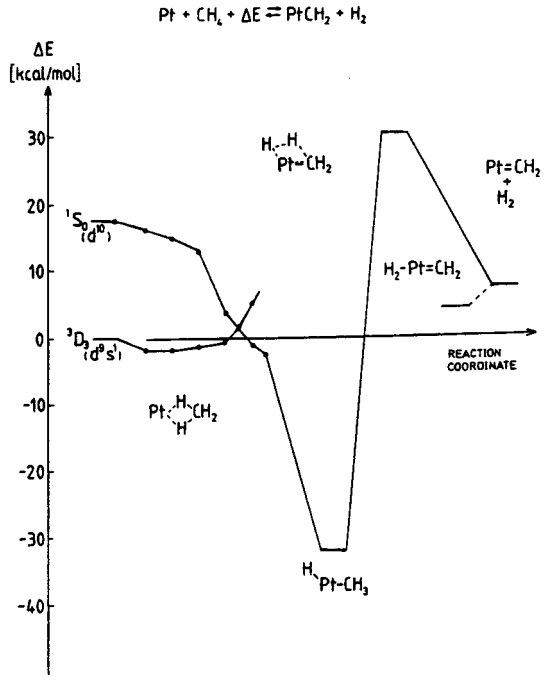

Figure 9. Potential energy profile for the reaction between platinum and methane. (Reprinted with permission from ref 109.) Copyright 1995 American Chemical Society.

combined with a relatively low d^{10} state. As stated before, the d^9s^1 state is well suited for the formation of two covalent bonds. Moreover, the presence of the low-energy d^{10} state diminishes long-range repulsion and allows the correlation in spin with the H−Pt−CH_3 complex.[109] All these theoretical results, either on the palladium or platinum systems were shown to fit nicely with the experimental results within RRKM theory.[107,109]

Finally, two points of methodological interest, emerging from a recent and comprehensive study on the C−H activation reaction of CH_4 with all transition-metal atoms from the three transition rows are worth being mentioned.[353] The first one is that DFT-B3LYP calculations compare very well with the PCI-80 results for this reaction. The second point is that the total quenching model, which assumes that the major spin−orbit effect arises from the Pt atom, also works very well: the additional molecular spin−orbit effects, which were obtained via a parametrized one-electron spin−orbit Hamiltonian as in the work of Schwarz et al. on Pt−H (vide supra),[44] are very small, 0.5 kcal mol^{-1}.[353]

There have been a few other studies dealing with the reaction of methane with Pd or Pt and with the corresponding cations Pd^+ or Pt^+. Hada and Nakatsuji have carried out symmetry-adapted cluster CI (SAC−CI) calculations of the reaction Pt + CH_4 but found unrealistically high barriers.[354] This may arise from the use of large-core pseudopotentials and/or relatively small basis sets. In their MCPF calculations on the same reaction, Swang et al. used a relatively large basis set, and for Pt a relativistic pseudopotential that keeps the 5s, 5p, and 4d orbitals frozen and describe the inner shells by a local potential. They did not incorporate spin−orbit effects.[355] Taking into account these differences with Siegbahn and Blomberg's calculations, both sets of results are in good agreement. In their study of the reaction of second-row transition-metal cations with CH_4, Blomberg, Siegbahn, and Svensson did not find any reactive channel for Pd^+. Only an η^2 molecular complex could be identified, with a stabilization energy of 17.0 kcal mol^{-1} (MCPF calculations including zero-point vibrational corrections and relativistic effects through first-order perturbation theory).[356] This large value is the result of a charge-induced dipole interaction and of the d^9s^0 ground state of the cation that minimizes the electron−electron repulsion. That no oxidative addition product could be found is in line with the previous results of Balasubramanian et al. for $[PdH_2]^+$, where only a molecular adduct between H_2 and Pd^+ was found.[63,65] Pt^+ behaves quite differently, since it reacts quite readily in the gas phase with CH_4.[357] Schwarz and co-workers have investigated this reaction theoretically and experimentally.[358] The calculations were carried out at the DFT-B3LYP level (with a relativistic small-core pseudopotential for Pt[68] and a polarized double-ζ basis set for the ligands). As with Pd^+, CH_4 forms an adduct with Pt^+ but it is somewhat more stable, the binding energy being 28.3 kcal mol^{-1}. However, the reaction proceeds further through a very low barrier toward the hydridomethyl complex H−Pt^+−CH_3 (which is below the adduct by an extra 11.5 kcal mol^{-1}). H−Pt^+−CH_3 then evolves via steps, which might be rate determining, first to the dihydrido methylene intermediate H_2Pt^+−CH_2 and then to the dihydrogen methylene complex $(H_2)Pt^+$−CH_2, prior to the final dissociation of H_2. That Pt^+ can form, in contrast to Pd^+, a hydridomethyl complex with CH_4 is traced to the much lower $d^9s^0 \rightarrow d^8s^1$ promotion energy in Pt^+ (17.6 kcal mol^{-1}) compared to Pd^+(74.4 kcal mol^{-1}). The computed ΔG_{298K}, −8.3 kcal mol^{-1}, compares well with the experimental value, -3.2 ± 1 kcal mol^{-1}. A similar energy profile has been obtained at the PCI-80 level in a collaborative effort with Siegbahn, Blomberg, and co-workers, except for the barrier toward the hydridomethyl complex which disappears at the higher level.[359]

Many of the results that have been discussed above for the C−H oxidative addition (and reductive elimination) of methane on the bare Pd and Pt metal atoms are also found in the studies that have been devoted to the reaction of CH_4 with zerovalent PdL_2 and PtL_2 molecular complexes. Sakaki and co-workers have analyzed the ability of the $Pd(PH_3)_2$ and $Pt(PH_3)_2$ systems to undergo the oxidative addition in two different situations: either with two unconstrained PH_3 ligands as a model of two monodentate phosphines such as PPh_3 or with constraints in the geometry optimization that simulate the use of a chelating bidentate bisphosphine such as 1,2-bis(dicyclohexylphosphine)ethane (dcpe = $[(C_6H_{11})_2PCH_2CH_2P(C_6H_{11})_2]$) and bis(di-*tert*-butylphosphino)methane (dbpm = $[(t\text{-}Bu)_2PCH_2P(t\text{-}Bu)_2]$).[360,361] In the most recent study the geometries were optimized at the MP2 level and the energies calculated at the MP4SDQ level, using the small-core pseudopotential of Hay[68] and a valence double-ζ basis set (polarized in some instances). A small molecular precursor is found in every case but with an almost negligible stabilization

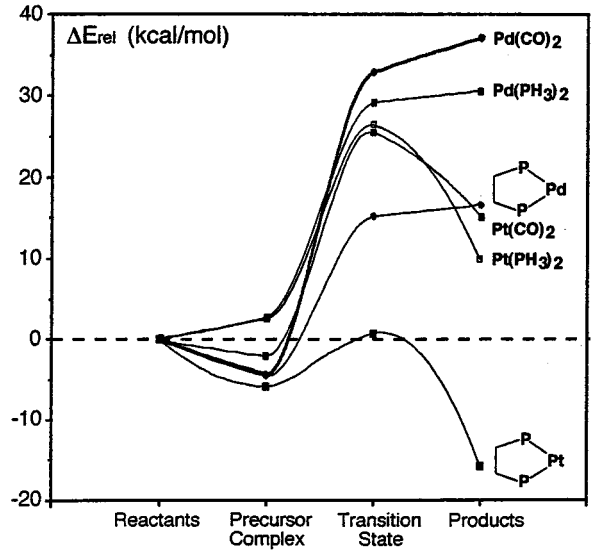

Figure 10. Potential energy profiles (at the MP4SDTQ// MP2 level) for the reaction of CH_4 with various ML_2 complexes, M = Pd, Pt. (Reprinted with permission from ref 362.) Copyright 1997 American Chemical Society.

for $Pd(PH_3)_2$ and $Pt(PH_3)_2$; in contrast, the systems that model the chelating phosphine lead to a definite stabilization energy of a few kcal mol^{-1}. As with the bare metals, the activation energy for C−H bond oxidative addition is computed to be larger for Pd than for Pt. The difference amounts to about 7 kcal mol^{-1} when starting from the linear $M(PH_3)_2$ systems that model the nonchelating case. It is much more important for the systems that model the chelating ligand: for the Pd(dcpe) model system the computed activation energy is 20.0 kcal mol^{-1}, to be compared with 3.8 kcal mol^{-1} for the Pt(dcpe) model system (MP4SDQ values). This differential effect, which is in agreement with the known experimental data, is traced to the ability of the $M(PH_3)_2$ skeleton to distort.[361] A distorted ML_2 skeleton has its d_π orbital high in energy. This orbital can therefore interact quite strongly with the σ^*_{C-H} orbital. Similar features have been obtained more recently by Su and Chu in their comparison of the energy profiles for the reaction of CH_4 with $M(PH_3)_2$, $M(CO)_2$, and $M(H_2PCH_2CH_2PH_2)$.[362] Figure 10 summarizes their results and clearly shows that for the Pt system with the chelating diphosphine ligand there is almost no reaction barrier. Rather than using molecular orbital interaction arguments, Min and Su base their reasoning on valence-bond-type arguments using the curve crossing model of Pross and Shaik.[363] They relate the size of the barrier to the singlet to *triplet* state separation in the ML_2 system: Thus, a bent system will have a smaller separation leading to a lower barrier; the singlet−triplet separation is also smaller in the Pt systems compared to the Pd systems, therefore accounting for a smaller barrier in the former. The effects of the ligands can be explained in the same way. One should note that the singlet−triplet separation can be correlated with the destabilization of the d_π orbital and the stabilization of the d_σ orbital, both factors leading to a smaller barrier in a molecular orbital interaction explanation.

As seen from Figure 10, chelating diphosphine ligands that have a small bite angle lead to a decrease of the activation barrier. However, for CH_4 the barrier remains relatively high and the overall reaction is endothermic. Sakaki and co-workers have analyzed[364] why on introduction of electron-withdrawing substituents such as CN the energy barrier for this reaction is noticeably decreased and the reaction becomes exothermic, accounting for its observation in experiments.[365] They found that the main factor lies in the conjugation of the π^* orbital of CN with the σ^* orbital of C−H. This stabilizes the σ^* orbital, thus leading to an increased charge transfer to this orbital.

Hill and Puddephatt have considered in a recent study based on EHMO and DFT-B3LYP calculations the reductive elimination of CH_4 or C_2H_6 from various five-coordinate Pt(IV) complexes (and the reverse reaction, the oxidative addition of the C−H bond as well).[366] As expected, C−H reductive elimination and oxidative addition are much easier than C−C reductive elimination and oxidative addition. Their conclusions generally agree with experimental knowledge, except for the comparison between NH_3 and PH_3 as ligands. At variance with experiment where the reductive elimination appears to be much easier with phosphine than with amine as a ligand, a similar activation energy of 25 kcal mol^{-1} is computed in both cases. Perhaps the model chosen for the phosphine, here PH_3, is inadequate from an electronic and/or a steric point of view. The primary product of the reductive elimination is found to be a molecular adduct between CH_4 and a T-shaped Pt(II) tricoordinate complex, with an η^2 coordination mode. In this adduct one Pt−H bond is 2.07 Å and the Pt−C bond is 2.59 Å. The other Pt−H bond is longer, 2.38 Å. One should note here that somewhat similar structures have been obtained for adducts of CH_4 with T-shaped tricoordinate complexes of Pd(II)[367] and Rh(I).[368,369] The structure of the ethane adduct corresponds again to an η^2 coordination mode, since one hydrogen atom on one carbon is 2.24 Å away from Pt whereas another hydrogen from the second carbon atom is much further from Pt, at 2.60 Å.

Despite its importance in cross-coupling reactions, to our knowledge there has not been an ab initio study of the reductive elimination of propene from vinyl−methyl palladium complexes. An extended Hückel study, using the *cis*-$[Pd(PH_3)_2(CH_3)(CH{=}CH_2)]$ system as a model, has put forth a mechanism involving a methyl migration toward the coordinated vinyl ligand rather than a concerted elimination.[370] The two transition states, which have been approximately determined, are quite alike however. Thus, considering the approximate nature of both the theoretical method and the transition-state determination, no definite conclusion can be drawn. One should point out that a comparison with the reductive elimination from $[Pd(PH_3)_2(CH_3)_2]$ shows a much higher barrier for the latter process.[370] This is not surprising if one recalls the results of Fahmi and van Santen[136] and of Siegbahn et al.[348] As computed from Table 5, the barrier for the reductive elimination reaction from $[Pd(H)(C_2H_3)]$ is 2.5 kcal mol^{-1}, whereas it amounts to 23.3 kcal mol^{-1} for the reductive elimination from $[Pd(CH_3)_2]$ (CCSD(T) val-

ues). A similar value of 6 kcal mol^{-1} for the reductive elimination from [Pd(H)(C_2H_3)] has been computed at the DFT-NL level by Fahmi and van Santen.[136]

The oxidative addition of bonds other than the C−H bond has been also considered. We have already mentioned, in the context of the Pd−NH_3 and Pd−OH_2 bare metal−ligand systems, the studies of Blomberg, Siegbahn, and co-workers for the oxidative addition of the N−H and O−H bonds to the palladium atom.[81,82] At the CCSD(T) level, the Pd + NH_3 and Pd + H_2O reactions are endothermic, by 3.6 and 9.6 kcal mol^{-1}, respectively. At the same level of calculation, the value for Pt + CH_4 is 5.6 kcal mol^{-1}, see Table 5. The larger endothermicity for the H_2O reaction has been ascribed to the presence of one more lone pair on H_2O compared to NH_3, thus leading to more electron−electron repulsion. The more diffuse character of the ammonia lone pair compared to the water lone pair, which was influential for the long-range electron donation mechanism in the two molecular complexes, is of less importance for the product due to the shorter M−N (and M−O) distances.[82] The barriers for the oxidative addition are in the order CH_4 (10.6 kcal mol^{-1}) < NH_3 (12.6 kcal mol^{-1}) < H_2O (21.6 kcal mol^{-1}). It should be noted that in the transition state, as in the products, the geometry of $PdNH_2$ is pyramidal and that of PdOH is bent as a result of the *covalent* nature of the Pd−N or Pd−O bonds in the transition states and in the products.

The oxidative addition of the O−H bond to palladium and platinum *complexes* has also been investigated. For palladium the process leading from a square-planar Pd(II) to an octahedral Pd(IV) has been examined (at the MP2 level with a valence double-ζ basis set and a relativistic small-core pseudopotential) on the *cis*- and *trans*-[Pd(H)$_2$(NH_3)$_2$] model systems.[367] Both the energy barrier and the reaction energy were found to be quite dependent on the stereochemistry of the product, the facial arrangement of the three hydrogens atoms yielding a greater exothermicity and a smaller barrier. In the most favorable case, i.e., H_2O + *cis*-[Pd(H)$_2$(NH_3)$_2$] → *fac*-[Pd(H)$_3$(OH)(NH_3)$_2$], the barrier is 28.8 kcal mol^{-1} and the reaction is exothermic by 23.4 kcal mol^{-1}. The thermodynamics of the addition of H_2O on a more realistic system involving a tris(pyrazol-1-yl)-borate complex of Pd(II) has been investigated also in the framework of a theoretical study of the reduction of water to H_2 by such complexes.[371] Here too the thermodynamics is greatly influenced by the stereochemistry of the product. A recent study of Su and Chu has addressed the possibility of the O−H oxidative addition of methanol to the zerovalent PtL_2 system, focusing again on the influence of the bite angle of the two ligands.[372] As for the C−H bond oxidative addition,[361,362] the DFT-B3LYP calculations show that the small bite angle of either the dppm or the dppe ligand promote the oxidative addition, by strongly reducing the barrier of the reaction and by increasing its exothermicity. The σ-donor ability of the ligand also plays a role.[372]

At this stage one should not forget that in some instances σ-bond metathesis reactions with a metal−ligand bond might be competitive with the oxidative addition to the metal.[373] Such reactions have been investigated for Pd(II) and Pd(IV) complexes and the corresponding transition states determined and discussed either for H_2 or O−H addition.[367,374] The Shilov reaction,[375] viz. the activation of an alkane C−H bond by Pt(II) complexes in aqueous solution, has been shown by Siegbahn and Crabtree to take place via a σ-bond metathesis between the C−H bond and the Pt−Cl bond, with some extra water molecules participating to the coordination sphere.[376] The computed DFT-B3LYP energy barrier from the η^2-CH_4 molecular precursor is 27 kcal mol^{-1}, in very good agreement with the experimental estimate.[375] The importance of the presence of a lone pair in the reacting moiety to induce the heterolytic cleavage (or recombination) of H_2 has been recognized.[367,373] Also related to this process is the elimination of H_2 from a system having a so-called M−H···H−X "dihydrogen bond".[377] The report of the first theoretical determination of the transition state for such a process postulated in the mechanism of the reduction of water to H_2 mediated by a tris(pyrazol-1-yl)borate complex of Pd(II), Figure 11, has been published recently.[371] A σ-bond "metathesis-like" pathway between a B−S bond and a Pd−alkyne bond has also been put forth by Morokuma and co-workers[378] as a key step in the mechanism of the alkyne thioboration catalyzed by Pd complexes. In this case the hypervalent nature of the sulfur atom is thought to play an important role, since the corresponding transition state for the reaction between a B−B bond and a Pd−alkyne bond in the alkyne diboration process is much higher in energy.[378]

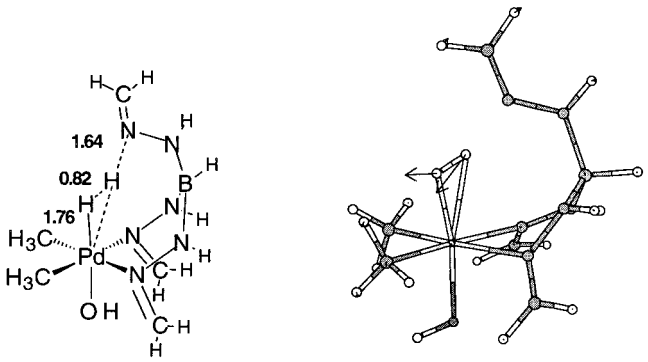

Figure 11. Transition state for the H_2 elimination from the Pd−H···H−N dihydrogen bond in [Pd(Me_2)(H)(OH){pz_2-(pzH)BH}]. Bond distances are in Å, angles are in degrees.

The addition of Si−H and Si−X bonds to Pd(PH_3)$_2$ and Pt(PH_3)$_2$ complexes has been treated quite extensively by Sakaki and co-workers over the years.[350,360,379−381] One of the goals of these studies was to compare the Si−H and Si−X oxidative additions to the C−H and the C−C bond oxidative additions. Although it is sometimes difficult to make a strict comparison from one article to another, due to some slight changes in the basis sets that have been used, one can nevertheless grasp a quite coherent picture. We have previously mentioned the study of the correlation effects on the geometry optimization showing that although the geometries can vary to a rather large extent upon introduction of electron correlation at the MP2 level, the effect on the relative

Table 7. Comparative Energy Results (in kcal mol^{-1}) for the C−H, Si−H, C−C, Si−Si, and Si−C Bond Oxidative Addition to Palladium and Platinum

reaction	precursor	transition state	products	ref
	Pd Complexes			
$Pd(PH_3)_2 + CH_4$[a]	−0.7	36.9	34.1	361
$Pd(PH_3)_2 + SiH_4$[a]	−2.3	0.5	−6.6	350
$Pd(PH_3)_2 + C_2H_6$[b,c]	−1.4	56.8	30.5	380
$Pd(PH_3)_2 + Si_2H_6$[a,d]	−3.0	13.3	−17.1	350
$Pd(PH_3)_2 + SiH_3CH_3$[b,e]	−2.5	16.3	8.1	380
	Pt Complexes			
$Pt(PH_3)_2 + CH_4$[a]	−0.8	29.9	9.9	361
$Pt(PH_3)_2 + SiH_4$[a]	−2.2	2.4	−21.9	350
$Pt(PH_3)_2 + C_2H_6$[b,c]	−1.1	66.0	5.2	380
$Pt(PH_3)_2 + Si_2H_6$[a,d]	−3.1	17.5	−34.8	350
$Pt(PH_3)_2 + SiH_3CH_3$[b,e]	−2.3	24.9	−14.1	380

[a] MP4SDQ//MP2 result. [b] MP4SDQ//HF result. [c] C−C bond oxidative addition. [d] Si−Si bond oxidative addition. [e] Si−C bond oxidative addition.

energies is not substantial.[350] Table 7 summarizes the results of the best calculations corresponding to MP4SDQ energies computed on either HF-optimized geometries (MP4SDQ//HF) or on MP2-optimized geometries (MP4SDQ//MP2). The oxidative addition of Si−H proceeds much more easily than the oxidative addition of C−H, with almost no energy barrier and a rather large exothermicity for either Pd or Pt. The Si−Si oxidative addition is also much easier than the C−C oxidative addition and slightly easier than the Si−C bond oxidative addition, Table 7. The substituent effects on Si for the oxidative addition reaction $[Pt(PH_3)_2] + HSiX_3 \rightarrow [Pt(H)(SiX_3)(PH_3)_2]$ (X = H, Cl, Me) have been analyzed in the framework of a theoretical investigation of the catalytic cycle for platinum-catalyzed hydrosilylation of alkenes.[381] The energy barrier is almost insensitive to the substituents due to the reactant-like nature of the transition states. In contrast, the reaction exothermicity increases in the order Me (16.8 kcal mol^{-1}) < H (21.9 kcal mol^{-1}) < Cl (32.3 kcal mol^{-1}), MP4SDQ values. All these features have been rationalized in terms of the various bond energies.[381]

Sakaki et al. have had more difficulties rationalizing the fact that the oxidative additions involving a Si−X bond have lower activation energies for Pd than for Pt, in contrast to what was expected from the known results on C−H oxidative addition. Their explanation is based on an energy decomposition analysis combined with a careful inspection of difference density maps for the Si−Si bond oxidative addition. For this reaction (and this should hold for the other oxidative additions of Si−X as well), the early transition state (i.e., reactant-like) is characterized by a greater amount of exchange repulsion (i.e., electron−electron repulsion) for Pt than for Pd.[350] Indeed, the Pt 6s population of $Pt(PH_3)_2$ is greater than the Pd 5s population of $Pd(PH_3)_2$. Sakaki has related this effect to the smaller energy gap between 5d and 6s in $Pt(PH_3)_2$ compared to the gap between 4d and 5s in $Pd(PH_3)_2$. One finds again the argument of Siegbahn, Blomberg, and co-workers that the s^0 state is important when a large electron−electron repulsion (as the one provided here by the two silyls) is expected. One might argue that this proposal disagrees with the conclusion of Su and Chu[362] that one can correlate the activation barrier with the singlet to triplet energy difference. However, in the case of the C−H bond oxidative addition, which was the one considered by Su and Chu, the transition states are more product-like. Thus, a lower triplet that favors the product also favors the transition state.

For the oxidative addition of SiH_4, a comparison between $M(PH_3)_2$ (M = Pt, Pt) and $[MCl(CO)(PH_3)_2]$ (M = Rh, Ir) has been made.[382] An explanation has been provided for the greater reactivity of the diphosphine palladium and platinum systems over the Vaska-type complexes. Sakaki has also investigated the oxidative addition of BX_2-BX_2 to $Pd(PH_3)_2$ and $Pt(PH_3)_2$ and compared it to the oxidative addition of the C−C and Si−Si bonds.[383] An interesting feature is the participation, in addition to the σ^* orbital, of the unoccupied π and π^* orbitals to the stabilization of the transition state. This explains why the reaction is relatively easy despite the stronger B−B bond. At the MP4SDQ//MP2 level, the reaction of $B(OH)_2-B(OH)_2$ with $Pt(PH_3)_2$ is exothermic by 22.2 kcal mol^{-1} with respect to the reactants. The energy barrier is 4.1 kcal mol^{-1} relative to the reactants and 13.3 kcal mol^{-1} relative to the molecular precursor complex. In the case of palladium, the reaction goes uphill from the precursor complex. The transition state and the cis product could be located during the MP2 geometry optimization, but when the energies are recomputed at the MP4SDQ level they lie 0.2 and 1.6 kcal mol^{-1} above the reactants, respectively. A similar behavior has been observed by Morokuma and co-workers in the course of their study of the alkyne and alkene diboration catalyzed by platinum and palladium diphosphine complexes.[384,385] They find, however, for the cis product of the oxidative addition of $B(OH)_2-B(OH)_2$ to $Pd(PH_3)_2$ a very shallow energy well, 0.1 kcal mol^{-1} below the transition state. As in Sakaki's calculations, the overall reaction is endothermic (by 5.0 kcal mol^{-1}).[385] The oxidative addition of the S−B bond to Pd(0) complexes is even less likely to occur, due to the weaker nature of the Pd−S bond compared to the Pd−B bond. Indeed, in their study of the Pd-catalyzed thioboration of alkynes, Morokuma and co-workers could not find any energy minimum that would correspond to the product of this oxidative addition.[378]

Reactions with Metallic Clusters. A good starting point to analyze the reactions of H_2 and CH_4 with palladium and platinum clusters is the 1991 study that Balasubramanian performed for the $Pt_2 + H_2$ reaction.[386] In this work, potential energy curves were obtained using the same methodology as the one used in his previous studies of PtH and Pt_2 (vide supra), viz. CASSCF calculations followed by MRSDCI and relativistic CI calculations including spin−orbit coupling.[34,238] Owing to this high level of theory, limitations had to be made when scanning the potential energy surfaces. The more severe ones are probably the restrictions to a few predefined approaches with an imposed symmetry and in particular for every approach a coplanar arrangement of Pt_2 and H_2, see **17a−d**. According to these calculations, the most

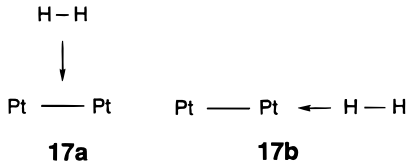

17a **17b**

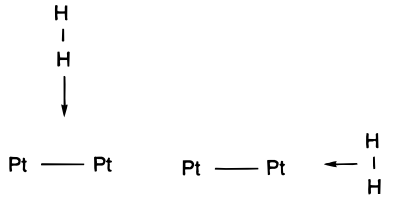

17c **17d**

productive pathway is **17a** for the $^1A_1$ state (C_{2v} symmetry). This pathway leads, after a spontaneous rearrangement of the *cis*-product **18**, to the trans product **19**, which is found to be 3 kcal mol^{-1} lower in energy. The overall reaction is found to be exo-

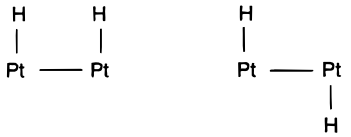

18 **19**

thermic, by 30.7 kcal mol^{-1} with respect to the $^1\Sigma_g^+$ state of Pt_2 (which is the lowest state of Pt_2 that correlates with $^1A_1$ of Pt_2H_2 in the absence of spin−orbit coupling). The barrier for this approach amounts to about 21 kcal mol^{-1}. The spin−orbit coupling stabilizes **19** by about 2.8 kcal mol^{-1}. The effects are much larger, however, in the dissociation limit region, ∼27 kcal mol^{-1}, where the state of Pt_2 is found to be a mixture of triplet [$^3\Sigma_g^-(0_g^+)$] and singlet [$^1\Sigma_g^+(0_g^+)$]. The overall exothermicity is therefore strongly reduced to about 5−6 kcal mol^{-1}. The other approaches, **17b**−**d**, were also investigated but were found less favorable, at least for the $^1A_1$ state. It is nevertheless interesting to mention (with respect to the subsequent studies) that in approach **17d** a molecular complex of H_2 was found, **20**, lying slightly below the separated reactants (no stabilization energy is given, but from the reported energy curve a value of 2−3 kcal mol^{-1} can be estimated). The

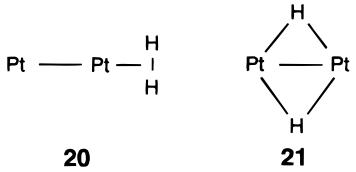

20 **21**

reaction in this approach proceeds via a very high barrier (∼75 kcal mol^{-1}) to the dibridged intermediate shown in **21**, this intermediate being 22 kcal mol^{-1} above **19**. Somewhat similar results have been obtained subsequently by Poulain et al.[387] In their MCSCF + MRCI calculations, constrained approaches of H_2 were again considered. Moreover, the Pt−Pt bond lengths were not optimized, to avoid reconstruction effects of the surface. Thus, their calculations pertain more to surface studies. They also favor the parallel approach **17a**. For approach **17d**, keeping the H−H distance fixed leads to a molecular adduct, stabilized by 4 kcal mol^{-1}. However, on relaxation of the H−H distance, the oxidative addition takes place, yielding a Pt−PtH_2 dihydride structure. The reaction energy for this addition on one Pt end is less than the one obtained previously for Pt + H_2.[54] This points to some deactivating effect of the second platinum atom. It is interesting to note here that a deactivating effect of Ru in PtRu with respect to Pt_2 has been proposed for the same approach on the basis of NL-DFT calculations.[388]

So far the most extensive study on the Pt_2 + H_2 reaction has been the one of Musaev, Morokuma et al.[237] Since they were primarily interested in the cluster chemistry, they have performed full geometry optimizations using the DFT-B3LYP method after a careful assessment of its performance (against CASPT2 calculations for Pt_2, vide supra) and of the basis sets to be used. The full geometry optimization for singlet and triplet states leads to a reaction mechanism which is dramatically different from the previously discussed mechanisms that were based on the limited potential energy surface scans. Some of the steps of Musaev Morokuma et al. mechanism, however, have their analogue in these limited scans. One should also note that spin−orbit coupling effects were not taken into account in this study, although we have seen that they may be important for the platinum systems. The reaction mechanism for Pt_2 + H_2 is best summarized in Figure 12, together with the schematic potential energy profiles for the CH_4 attack (vide infra). According to this reaction mechanism, the H_2 attacks begins at one platinum atom, yielding a dihydrogen complex **Pt_2_X_Mol** whose ground state is a triplet $^3A'$ (at 14.3 kcal mol^{-1} below the ground-state reactants) and with a *nonplanar* geometry at platinum. This nonplanar geometry is due to the involvement of the d_δ orbitals in the binding. The singlet $^1A'$ planar structure lies 8.2 kcal mol^{-1} above the nonplanar structure. Then H−H cleavage takes place *on a single platinum atom*, leading to a strongly pyramidal $PtPtH_2$ dihydride (**Pt_2_X_Com1**), the $^1A'$ state now being slightly more stable than the $^3A'$ state. The activation energy is negligible for both states. The final step, which also has a low barrier, is a 1,2 shift of hydrogen from one platinum atom to the other, leading to the final product (**Pt_2_X_Com2**) with one hydride on each platinum, the structure being gauche rather than cis planar or trans planar (the two planar structures being transition states). The relative stabilities and the structures of the intermediates have been rationalized via molecular orbital interaction arguments. Perhaps a discussion of the 1,2 shift, which is interesting not only from a theoretical point of view but also with respect to surface hopping, might have been appropriate.

The oxidative addition of H_2 on Pd_2 has been analyzed in the same study.[237] Musaev, Morokuma et al. found in this case only one singlet $^1A'$ minimum, 36.6 kcal mol^{-1} below the ground-state reactants. No transition state could be characterized on the singlet

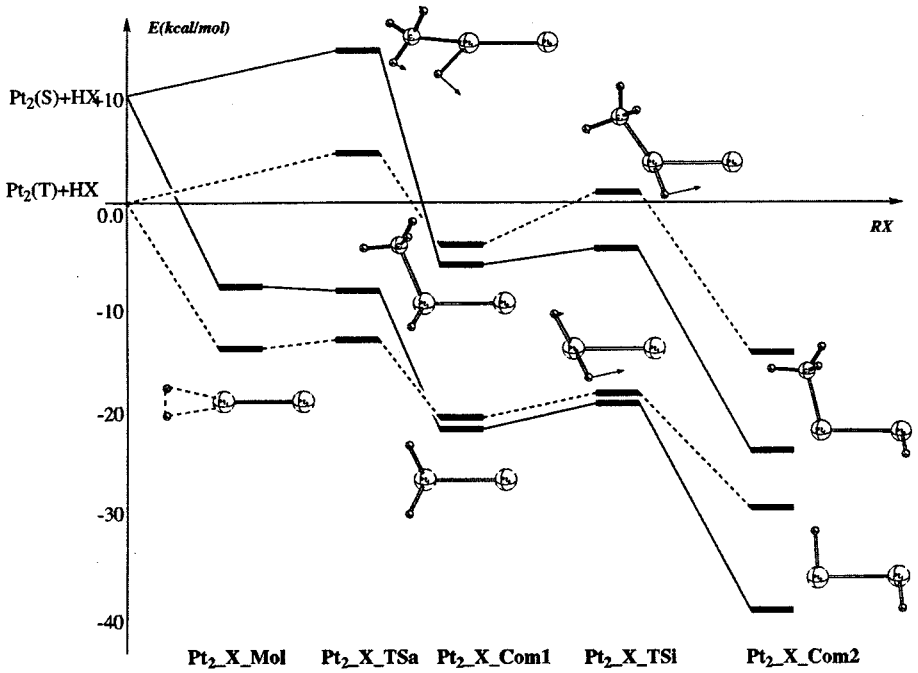

Figure 12. Schematic energy profile for the H_2 (lower line) and CH_4 (upper line) activation on Pt_2. Solid lines are for singlet electronic states and dotted lines for triplet states. (Reprinted with permission from ref 237.) Copyright 1998.

surface. The triplet electronic states were computed to be much higher in energy. Remember that the ground state of Pd_2 is the triplet $^3\Sigma_u^+$. Thus, in the H_2 activation process an intersystem crossing mechanism is involved. The structure of the minimum corresponds to a dibridged structure, as in **21**, although it is not perfectly planar but slightly distorted, the H−Pd−Pd−H dihedral angle being 168.5°. Note that similar features were already found by either Blomberg et al.[227] or Poulain and coworkers.[389] An analysis of trajectories using a reaction-path Hamiltonian[390] based on semiempirical CNDO calculations also agrees with these results.[391] The computed MCPF reaction energy of Blomberg et al. (35.1 kcal mol^{-1}) is very similar to the above DFT-B3LYP value. Thus, the H_2 activation process is much more effectively done by Pd_2 in comparison to Pd alone, in contrast to the Pt_2 case. All these results have been rationalized also using molecular orbital arguments.

The oxidative addition of methane on Pt_2 and Pd_2 has also been the subject of various studies. For $Pt_2 + CH_4$, Musaev, Morokuma et al. point to a mechanism very similar to the one delineated for $Pt_2 + H_2$, Figure 12.[237] There is, however, a higher barrier on the singlet surface for the initial oxidative addition on the platinum atom, 10.7 kcal mol^{-1}. The barrier is lower for the triplet, 2.6 kcal mol^{-1} only. The first intermediate, the second transition state, and the final product are more stable on the singlet-state surface, Figure 12. The final product on this surface is 25.1 kcal mol^{-1} below the reactants, the corresponding triplet minimum being 9.0 kcal mol^{-1} higher, i.e., still rather low with respect to the reactants. Hence, starting from the ground-state triplet of Pt_2, the activation of H_2 can take place either on the triplet surface where the barrier in the entrance channel is low or the system can cross over to the singlet electronic state in the vicinity of the first intermediate. Musaev, Morokuma et al. also argued that for Pt alone the $Pt + CH_4$ reaction could not start spontaneously from the ground state of the Pt atom and that it would be slow due to the necessity of intersystem crossing. This would in turn explain an experimental observation that CH_4 is activated by Pt with a rate which is slower than Pt_{2-5} by nearly an order of magnitude.[392] We have seen, however, in Siegbahn and co-workers' study that a very low crossing point was found for the $Pt + CH_4$ reaction, Figure 9.

For $Pd_2 + CH_4$, the calculations of Blomberg et al. used MCPF calculations.[227] The optimizations were performed at the Hartree−Fock level with constraints (in particular C_s symmetry), either for the intermediate or for the optimization of the transition state. From a methodological point of view it is worthwhile to note the effect of f polarization functions which yield lower barriers and more stable products. The product was found to have a geometry similar to that of the H_2 oxidative addition. Under C_s symmetry, a transition state for the C−H cleavage was localized on the singlet surface. A low barrier of 6.5 kcal mol^{-1} was obtained. The full optimization procedure of Musaev, Morokuma et al.[237] led to somewhat different results, since an alternative pathway involving an asymmetric approach of CH_4 with respect to the two palladium atoms, via the transition state **22** shown in Figure 13, has been put forth. The energy barrier between the molecular precursor and the transition state is only 3 kcal mol^{-1}. The approach is driven by the preference for CH_3 to a make a directional bond, due to the sp^3 hybridization. The asymmetric product **23** is found very close in energy to the symmetric one **24**, Figure 13. One should note here the previous calculations carried out by Broclawik et al. at the DFT-BLYP level (i.e., with nonlocal exchange and correlation corrections).[393] The computed geometries for the molecular

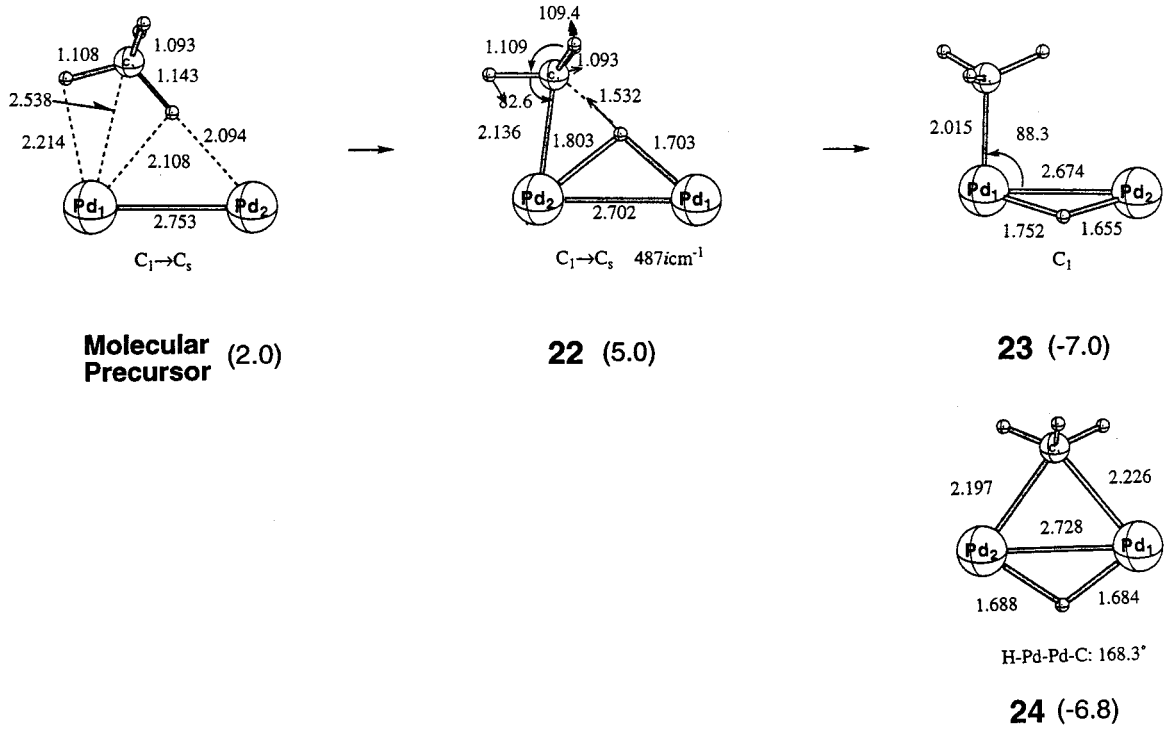

Figure 13. Computed pathway for the reaction of $CH_4 + Pd_2$. (Reprinted with permission from ref 237.) Copyright 1998.

precursor and for the transition state are quite similar to those of Musaev et al. They obtain an energy barrier of 5.2 kcal mol^{-1}. The computed geometry of the final product is the symmetrical one also found by Blomberg et al. For the same reaction $Pd_2 + CH_4$ Mamaev et al. again performed an analysis of trajectories using a reaction-path Hamiltonian based on semiempirical CNDO calculations.[394] Their results are closer to the ones of Musaev et al. than to the ones of Blomberg. They get, in particular, a transition state corresponding to an asymmetric attack of the two palladiums.

Some work has been finally devoted to the reactivity of the Pd_3 and Pt_3 clusters. The initial studies, either of Balasubramanian et al. on $Pd_3 + H_2$ and $Pt_3 + H_2$[395] or of Poulain et al.[389] on $Pd_3 + H_2$, suffer from the same shortcomings as their studies on the dimers, namely, the use of limited potential energy surface scans. For the in-plane approach of H_2 parallel to one metal−metal bond, Balasubramanian concludes to a smaller barrier for Pt compared to Pd. On the other hand, the reaction energy is greater for Pd_3 compared to Pt_3.[395] A different picture has been obtained by Musaev, Morokuma et al.[245] after a full geometry optimization. Many intermediates and transition states are involved, and we refer the interested reader to the original paper. It is worth mentioning, however, some salient features and results. The reaction of H_2 on Pd_3 is very facile: it takes place without an energy barrier, leading directly to the product. For the addition of CH_4 on Pd_3, two activation pathways are found as with Pd_2. The two processes are exothermic but they have relatively high barriers, 18.0 and 14.6 kcal mol^{-1}, respectively. That these barriers are much higher than those for Pd_2 is in agreement with the experimental findings.[392] For the systems $Pt_3 + H_2$ and $Pt_3 + CH_4$, the reactions follow the same pattern as for Pt_2, viz. cleavage of the H−H bond or C−H bond on one single atom followed by a 1,2 shift of hydrogen. No activation barrier was found for H_2, and a smaller barrier compared to Pt_2 was found for the C−H activation.

The increase of the number of intermediates close in energy and of isomerization pathways on going from Pt_2 to Pt_3 points to the increased complexity of this type of microscopic analysis and perhaps to its limitations. Although Musaev, Morokuma et al. conclude with their belief in the possibility of unravelling the size-dependent effects of such clusters, one may worry that some of these intermediates and pathways might be missed for clusters of higher nuclearity. In a sense the problems to be solved should be somewhat similar to those associated with the global energy minimum search in very large molecules.

2. Migratory Insertion and Deinsertion, β-Hydride Elimination

This reaction is a very important step (sometimes the rate determining one) in many palladium- and platinum-mediated or -catalyzed processes. The most frequently encountered reactions involve the insertion of either CO or olefins into metal hydride, metal methyl, or metal alkyl bonds and their respective inverse reactions. As for the oxidative addition, their basic electronic features were unravelled prior to 1990. It was shown, in particular, that the actual mechanism involves a migration of the σ-donor ligand (H, CH_3, or the higher alkyl) to the ligand with π properties (the olefin or CO).[14] The theoretical studies that were carried out in the last 10 years have focused on a precise comparison between transition metals within a row, on the influence of the alkyl chain length, and on the comparison of the insertion into the metal−hydrogen or the metal−carbon bond with the insertion into the metal−Si bond. The recent

finding that the elements of the nickel triad can be active in polymerization of olefins[396,397] and alternating copolymerization of carbon monoxide and olefins[398−400] has also attracted the interest of theoreticians.

The Olefin Insertion Reaction. Siegbahn has performed a detailed comparative study of the olefin insertion reaction into the metal−hydrogen and metal−carbon bonds for the entire second row of transition metals.[401−403] This study has been first restricted to the monovalent M−H and divalent MH_2, MHCl, and MHF systems.[402,403] Unfortunately in the palladium case the comparison between the monovalent and divalent systems is hampered by the fact that the π complex of PdH_2 does not correspond to a dihydride interacting with C_2H_4 but rather adopts a geometry corresponding to a zerovalent Pd(η^2-H_2)(η^2-C_2H_4) complex (this is due to the preference, mentioned earlier, of PdH_2 for a molecular dihydrogen complex). The calculations were, as in many Siegbahn's studies of this type, carried out at the MCPF level. The barrier heights for the insertion are given and analyzed with respect to the separated metal hydrides PdH, PdHCl, or PdHF and ethylene and not with respect to the molecular precursor in which the ethylene is bound to the metal. This was dictated by some simplification for analyzing trends, but the results are therefore more relevant to data in the gas phase than to data in solution. For palladium, relatively low barriers are found, arising from a competition between the d^{10} state of palladium which cannot form the covalent d-bond, which is present in the transition state but has the weakest repulsion with respect to the incoming ligand, and the d^9s^1 state which can form this d-bond but has a greater electron−electron repulsion arising from the s electrons. One again finds a rationalization quite similar to that for the oxidative addition. When a halide ligand is present, the metal will resemble a metal cation with a d^9 ground-state configuration more, hence the barrier is reduced. The similarity of the barrier heights for the C_2H_4 insertion into the Pd−H bonds of PdHF and PdHCl is also in line with this argument.[403] The insertion into the metal−methyl bond of $PdCH_3$ is found to be more difficult that the insertion into the metal−hydride bond of PdH, the corresponding barrier with respect to the separated reactants being higher by 13.7 kcal mol^{-1}. As for the oxidative addition of the C−H bond, this is due to the increased directionality of the methyl bond.[401]

The calculations that were carried out later by Siegbahn, Zetterberg et al. on the insertion of C_2H_4 into the metal−carbon bond of the corresponding cationic $[PdCH_3]^+$ and $[PdC_2H_5]^+$ systems were done at the DFT-B3LYP level and at the PCI-80 level for a few test calculations.[162] Thus, one cannot strictly compare the cationic systems to the neutral ones. The results obtained for the cationic systems are summarized in Table 8. We have already mentioned that experimentally Ni and Pd cationic complexes were found to be very active for the polymerization of olefins. For the bare metal systems, the π ethylene complex is strongly stabilized, with a binding energy as large as 43.9 kcal mol^{-1} for $[Pd(CH_3)(C_2H_4)]^+$ (the corresponding value for $[Pd(C_2H_5)(C_2H_4)]^+$ is 36.0 kcal mol^{-1}). This large stabilization has been ascribed to a large effect of a charge-induced dipole interaction between Pd^+ and the highly polarizable C_2H_4 ligand. Due to this strong binding one finds, starting from this π complex, a substantial barrier (18.3 kcal mol^{-1} for the methyl migration and 25.1 kcal mol^{-1} for the ethyl migration) and an endothermic insertion process (by 3.1 and 10.3 kcal mol^{-1}, respectively). This seems to contradict the experiments, especially the computed value of the barrier for the ethyl migration, since in the [(phenanthroline)Pd(C_2H_5)(C_2H_4)]$^+$ complex a $\Delta H^{\ddagger}$ value of 18.5 kcal mol^{-1} was measured.[404] In fact, the computed energy barriers and reaction energies vary substantially with the coordination pattern. When two amine ligands are added to give $[(NH_3)_2Pd(C_2H_5)(C_2H_4)]^+$, i.e., a more reasonable model of the experimental system, a barrier of 19.3 kcal mol^{-1} is obtained and the reaction is now exothermic by 7.6 kcal mol^{-1}. The corresponding values for the $[(NH_3)_2Pd(CH_3)(C_2H_4)]^+$ system are 18.0 and 7.5 kcal mol^{-1}, Table 8. Two factors have been shown to contribute to these changes: (i) a delocalization of the positive charge over the ammonia ligands and (ii) the lack of a β-agostic interaction that was present in $[Pd(C_2H_5)(C_2H_4)]^+$ due to the coordinative unsaturation. Some changes can also be due to the variation of the N−Pd−N angle. We mentioned in the subsection on π-complexes the increase of the binding energy of ethylene on closing the N−Pd−N angle. This increase is *not* correlated to an increase in the energy barrier, however. In the [(HN=CH−CH=NH)Pd(CH_3)(C_2H_4)]$^+$ system, where the chelating diimine has a bite angle of 76°, the binding energy of C_2H_4 is increased compared to $[(NH_3)_2Pd(CH_3)(C_2H_4)]^+$ but the insertion barrier is lowered from 18.0 to 16.4 kcal mol^{-1}. The origin of this lowering is traced mainly to a reduced steric repulsion, although the loss of π back-donation (due to the competition between the olefin and the π orbitals of the diimine ligand) and/or the increased charge on palladium may also contribute.[162] The β-hydride elimination from the alkyl product of the insertion was also investigated and found to be an easy process, thus accounting for the formation of branching products in the polymerization processes.

Table 8. Comparative Energy Results (in kcal mol^{-1}) for the Insertion of C_2H_4 into the Pd−C Bond of Cationic Alkyl Palladium Complexes[a]

system	C_2H_4 binding energy[b]	barrier height[c]	reaction energy[c]
$[Pd(CH_3)(C_2H_4)]^+$	−43.9	18.3	3.1
$[Pd(NH_3)_2(CH_3)(C_2H_4)]^+$	−27.3	18.0	−7.5
$[Pd(HN(CH)_2NH)(CH_3)(C_2H_4)]^+$	−29.8	16.4	−7.0
experiment[d]		18.5 ± 0.1[e]	
$[Pd(C_2H_5)(C_2H_4)]^+$	−36.0	25.1	10.3
$[Pd(NH_3)_2(C_2H_5)(C_2H_4)]^+$	−14.9	19.3	−7.6
experiment[f]		19.4 ± 0.1[e,g]	

[a] At the DFT-B3LYP level; negative values correspond to an exothermic process. [b] With respect to the reactants. [c] With respect to the C_2H_4 molecular precursor. [d] $[Pd(phen)(CH_3)(C_2H_4)]^+$ system, see ref 404. [e] $\Delta G^{\ddagger}$ value at −25 °C. [f] $[Pd(phen)(C_2H_5)(C_2H_4)]^+$ system, see ref 404. [g] The experimental $\Delta H^{\ddagger}$ value is 18.5 ± 0.6 kcal mol^{-1}.

The same authors have also extended their study of the migratory insertion in $[(HN{=}CH{-}CH{=}NH)Pd(R)(C_2H_4)]^+$ ($R = CH_3$, C_2H_5) and of the subsequent β-H elimination process to the platinum (and nickel) cases.[405] When $R = CH_3$, the barrier for migratory insertion is much higher in the platinum case, 25.5 kcal mol^{-1} instead of 16.4 kcal mol^{-1} in the nickel case. This accounts for the experimental observation that the platinum system is not effective for polymerization. The subsequent β-H elimination process from the three coordinate $[(diimine)M(\sigma\text{-propyl})]^+$ complex is less endothermic for Pd (with a computed endothermicity of 4.8 kcal mol^{-1}) than for Ni (the computed endothermicity being 11.0 kcal mol^{-1}). This is in line with the larger extent of branching experimentally found for Pd compared to Ni.[396] From a computational point of view, it worth mentioning that in this study[405] no specific transition state could be found for this elimination process (at variance with the previous report of the same authors[162]).

Sakaki and co-workers compared the insertion of C_2H_4 into the Pt−H bond to the insertion into the Pt−SiH_3 bond for the square-planar $[PtH(SiH_3)(PH_3)(C_2H_4)]$.[406] The geometries have been optimized at the HF level and the relative energies computed at the MP4SDQ level. From these calculations, insertion into the Pt−SiH_3 bond appears generally to be more difficult than insertion into the Pt−H bond. The greater energy barrier found for the insertion into the Pt−SiH_3 bond arises primarily from the 20 kcal mol^{-1} energy difference between the C−H bond (which is formed during the insertion into the Pt−H bond) and the C−Si bond (which is formed during the insertion into the Pt−SiH_3 bond) and from the directionality of SiH_3 (similar to CH_3, vide supra). This can be modulated, however, by other factors such as the respective trans influence of the spectator ligands. For instance, a barrier of only 4.4 kcal mol^{-1} is computed for the insertion of C_2H_4 into the Pt−H bond, when SiH_3 is trans to H; when PH_3 is trans to H, the barrier rises to 20.6 kcal mol^{-1}.[406] A similar trans influence has been found in the pentacoordinate system $[Pt(H)(PH_3)_2(X)(C_2H_4)]$, in which X (either Cl or $SnCl_3$) is trans to the migrating hydrogen atom.[407] For the stronger trans-director ligand $SnCl_3$, a much lower barrier is computed, 11.8 kcal mol^{-1}, instead of 33.9 kcal mol^{-1} for Cl (MP4SDQ//MP2 values).[407]

Coussens, Meier, and co-workers have investigated, via HF, MP2, and DFT calculations and Car−Parrinello type molecular dynamic simulations, the insertion of C_2H_4 into the Pt−H bond of *cationic* $[Pt(H)(PR_3)_2(C_2H_4)]^+$ systems (R = H, Me, Cl).[408] Both MP2 and DFT calculations predict a low barrier (between 1.6 and 2.7 kcal mol^{-1}) for the $[Pt(H)(PH_3)_2(C_2H_4)]^+ \rightarrow [Pt(PH_3)_2(C_2H_5)]^+$ reaction. Yet the barrier is high enough to prevent the observation of C_2H_4 insertion within the 400 fs time span of the molecular dynamics simulation. In contrast, the reaction is completed within 100 fs when the phosphine ligand is either PMe_3 or PCl_3. The authors of the paper warn that too much significance should not be put on this difference, since the real experiments take place in solution where the true rate is at least diffusion limited and most likely affected by the solvent. Yet these studies do indicate that the insertion step is not rate limiting in a multistep process. From a theoretical point of view, one should also note that such calculations pave the way to dynamic simulations in transition-metal chemistry.

More recently, Coussens et al. extended their investigation to the insertion of propene into the Pt−H bond of $[Pt(H)(PR_3)_2(C_3H_6)]^+$.[409] In this case, the theoretical approach was restricted to quantum mechanical calculations of HF, MP2, or DFT type, using fairly large basis sets. The DFT calculations (using the B3PW91 hybrid exchange correlation functional) seem, on the basis of a comparison with QCISD calculations, to give slightly better results than the MP2 ones. The differences are relatively small, however. From a chemical point of view, the insertion barrier decreases in the order PH_3 (∼2−3 kcal mol^{-1}) > PMe_3 (∼1−2 kcal mol^{-1}) > PF_3 (∼0.5−1 kcal mol^{-1}). In agreement with experimental data, the linear propyl products are favored over the branched one. The energy difference between the two forms decreases in the order $PMe_3 > PH_3 > PF_3$. The double-bond isomerization of propene has also been investigated. In noncoordinating solvents, the "isopropyl rock" exchange (i.e., the direct exchange of β-hydrogens in the β-agostic isopropyl complex)[410,411] has been identified. The isomerization pathway occurring via association and dissociation of a solvent molecule has been studied, using CH_3CN as a solvent molecule, and was found to involve somewhat higher barriers.[409]

The Alkyne Insertion Reaction. There have only been very few studies devoted to this process. We have already mentioned the study of the insertion of C_2H_2 into the PdCH_3 bond of the $[PdCl(NH_3)(CH_3)(C_2H_2)]$ model system.[166] The geometries of the intermediates were optimized though a gradient optimization technique at the SCF level; a reaction path was determined at the same level, assuming the $C_{CH_3}-C_{C_2H_2}$ distance as the reaction coordinate. Interestingly, the transition state that has been obtained in this way is quite similar to the one obtained by Natatsuji for the insertion of MeOCCH into the Pd−H bond of $[PdH(PH_3)(SiH_3)(MeOCCH)]$ via a gradient geometry optimization.[169] The energies on the reaction path were recomputed at the CASSCF-MRSDCI level. At that level the reaction is exothermic by 22 kcal mol^{-1} and has a barrier of 17 kcal mol^{-1} to overcome.[166] It was hypothesized in this article that electron-attracting substituents on the acetylene should lower the energy barrier by lowering the π^* orbital. This has been shown to be the case by Nakatsuji and co-workers in their study of the insertion of various alkynes RCCH (R = CN, H, CH_3, and OCH_3) into either the Pd−Si or Pd−Sn bond of the $[Pd(PH_3)(SnH_3)(SiH_3)(RCCH)]$ model system.[169] The barrier for the insertion into the Pd−Si bond, which is governed by donation from the HOMO of the palladium fragment into the LUMO of the alkyne, is lowest when R = CN, which corresponds to the lowest LUMO of the alkyne.[169] This study was also aimed at unravelling the electronic and steric factors of the regioselectivity of the silastannation of alkynes

Scheme 3

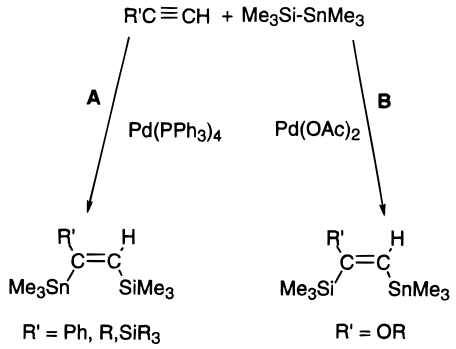

catalyzed by palladium phosphine complexes, Scheme 3. It was found that for the model catalyst (i.e., with PH_3 instead of PPh_3) insertion into the Pd−Sn or Pd−Si bond always proceeds via the addition of Si or Sn on the unsubstituted carbon atom. Moreover, the addition of Sn is slightly preferable over the addition of Si. This results from the fact that whatever the substituent is, the two most stable transition states for the alkyne insertion are **25a** and **25b**, **25a** being more stable than **25b** by ∼2−4 kcal mol^{-1}. The

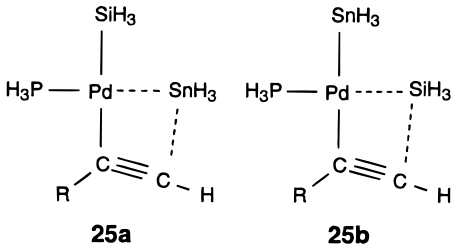

orientation of the alkyne in **25a** and **25b** is governed by the donation of the HOMO of the alkyne (which is always polarized on the terminal carbon atom) into the vacant p orbital localized on Sn or Si. That the reaction should proceed via transition-state **25a** explains the regioselectivity observed for path B of Scheme 3 but not the regioselectivity observed for path A. However, a geometry optimization of transition-state **25a** with PPh_3 instead of PH_3 yields a stabilization of 12.6 kcal mol^{-1} when the alkyne is rotated by 180°, thus accounting for path A when Pd(PPh_3)$_4$ is used as a catalyst.[169]

Sakaki and co-workers have extended their comparative study of the C_2H_4 insertion into the Pt−H bond and into the Pt−SiH_3 bond of [Pt(H)(SiH_3)(PH_3)(C_2H_4)] to the C_2H_2 case.[171] Similar results are found, the insertion into the Pt−H bond proceeding with a much lower barrier than the insertion into the Pt−Si−H_3 bond (12.8 instead of 20.9 kcal mol^{-1}). A comparison between the ethylene and the acetylene cases, using a vibronic coupling model, is made.

The CO Insertion Reaction and Other Insertion Reactions. Most of the studies that have been carried out since 1990 have focused on the interplay between the CO insertion step itself and the steps that take place immediately before and/or after the insertion, i.e., the steps that involve a rearrangement of the coordination sphere via ligand substitution reactions or isomerization reactions.[412−415] One should nevertheless mention the study of Blomberg et al. of CO insertion into metal−hydrogen and metal−methyl bonds for the bare second-row transition metals, including palladium.[416] As for the ethylene insertion that was reviewed above, the barrier heights (which have been obtained via MCPF calculations) are analyzed with respect to the separated PdH, $PdCH_3$, and CO and not with respect to the [Pd(CO)H] or [Pd(CO)(CH_3)] molecular complex in which the CO is bound to the metal. In the absence of additional ligands, these insertion reactions proceed directly, without prior binding of CO to the metal. The inserted products Pd(COH) and Pd($COCH_3$) are more stable than the separated reactants by 4.9 and 10.9 kcal mol^{-1}, respectively, but *less* stable than the [Pd(CO)H] and [Pd(CO)(CH_3)] molecular complexes by 25.6 and 33.2 kcal mol^{-1}, respectively. The corresponding barriers from the separated reactants are 7.7 and 13.5 kcal mol^{-1}. The larger barrier in the methyl case is ascribed, as for the oxidative addition and the ethylene insertion, vide supra, to the greater directionality of the metal−alkyl bond. Thus, the CO insertion into the metal−methyl bond appears to be favored thermodynamically but not kinetically. It is also argued, using similar arguments to those used for the ethylene insertion, that adding covalent ligands that increase the oxidation state should further favor the insertion into metal−hydride bond compared to metal−alkyl bond.[416]

Indeed, a calculation of Koga and Morokuma finds that at the MP2//HF level the CO insertion into the Pd−CH_3 bond of [Pd(H)(CH_3)(CO)(PH_3)] is slightly more difficult than the insertion into the Pd−H bond, the respective energy barriers being 10.2 and 7.4 kcal mol^{-1}.[417] On the other hand, the endothermicity is greater in the hydride case, 6.7 instead of 4.3 kcal mol^{-1} for methyl. For the insertion into the Pd−H bond of [Pd(H_2)(CO)(PH_3)], there is no barrier and the reaction is 9.4 kcal mol^{-1} uphill. Thus, from these calculations the hydride migration may not be as difficult as previously believed. However, as we shall see in the following, CO insertion reactions are rather sensitive to basis set effects. The calculations were carried out with a relatively small basis set and with a large-core pseudopotential. Different conclusions might therefore emerge if a more saturated basis set would be used in conjunction with a small-core pseudopotential.

The above study assumed a square-planar Pd(II) complex in which CO and either hydride of the alkyl are cis to each other. In many carbonylation reactions, however, CO is not initially bound to the metal and the precursor complex is a complex containing either a terdentate ligand, **26**, or a bidentate ligand and another monodentate ligand, **27**. The question

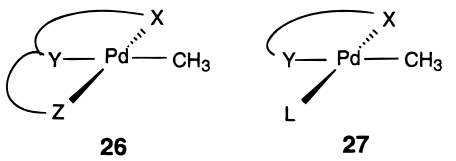

then arises of the mechanism of the substitution of one metal−ligand bond by a metal−CO bond and of its coupling with the CO insertion. Does it take place

Scheme 4

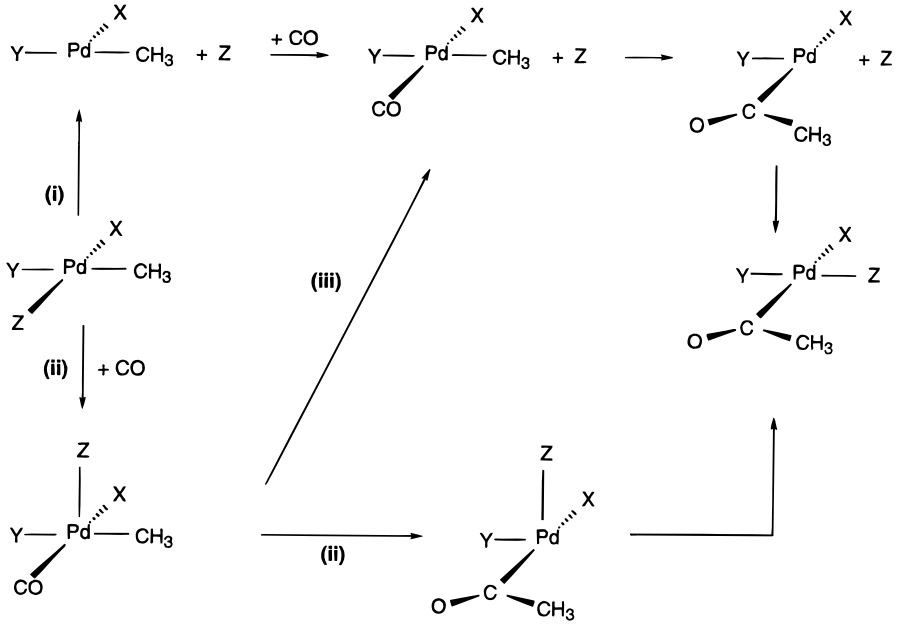

via a dissociative mechanism, see path i of Scheme 4, where one metal−ligand bond is cleaved, CO comes, and then inserts into the metal−alkyl bond, or as in path ii, does it involve an associative mechanism in which a five-coordinate intermediate is first formed on CO addition, the CO insertion taking place in this five-coordinate intermediate? Or does the five-coordinate intermediate relax to the four-coordinate carbonyl complex prior to insertion, path iii. In the case of a bidentate or terdentate ligand, will a dissociated arm remain in the immediate vicinity of the metal and participate to some extent to the insertion reaction? In the specific case of a bidentate ligand, what is the most reactive pathway, the one involving the dissociation of one arm (especially if the ligand is hemilabile) or the one involving the dissociation of the monodentate ligand?

The first three questions have been addressed for a cationic Pd(II) complex bearing terdentate nitrogen-donor ligands in a joint experimental and theoretical study.[412] The calculations were carried out on the $[Pd(NH_3)_3(CH_3)]^+ + CO$ model system, using an all-electron valence double-ζ basis set. The geometries were optimized at the SCF level. The relative energies were calculated at the SCF and MP2 level, the Pd−NH_3 dissociation step and the CO insertion step also being computed at the CASSCF and CASSCF/MRSDCI levels. From these calculations the purely dissociative and associative pathways, paths i and ii, can be ruled out. No transition state for the CO insertion having NH_3 strongly bound to Pd is found. On the other hand, the calculations suggest a path in which after concerted exchange of NH_3 for CO via a five-coordinate transition state, the amine ligand stays in the vicinity of the Pd coordination sphere and stabilizes the transition state through a loose association. One dissociated arm of the experimental terdentate ligand might play this role. The neutral system in which one NH_3 ligand was replaced by CH_3 behaved somewhat similarly. The association of NH_3 with the systems hardly exists, however. The insertion barrier is also quite similar (15.4 instead of 18.8 kcal mol^{-1}, in the cationic system, MP2//SCF values). Thus, the greater reactivity experimentally observed in the cationic systems compared to the neutral ones has been tentatively ascribed to a different trans influence of the ligand trans to the migrating methyl.[412]

Very recently, MP2//HF calculations by Groen et al. on the $[Pd(HN{=}CHCH_2N{=}CHCH{=}NH)(CH_3)]^+ + CO$ model system, where the terdentate ($HN{=}CHCH_2N{=}CHCH{=}NH$) ligand was free to dissociate one of its arms, **I** in Figure 14, do not contradict the previous proposal.[415] As seen from the HF-optimized geometries of Figure 14, the CO insertion into the Pd−methyl bond takes place in a four-coordinate complex (see the sequence **III** → **IV**(TS) → **V** of Figure 14) having a dissociated arm in the vicinity of palladium. Definite conclusions regarding the step prior to insertion, viz. the CO incorporation **I** → **II**(TS) → **III**, Figure 14, could not be drawn from these MP2//HF calculations. At the HF level, a small barrier (3 kcal mol^{-1}) is found, but it disappears when the energies are computed at the MP2 level. The MP2//HF insertion barrier, computed with an all-electron basis and a valence double-ζ basis set, is 11.5 kcal mol^{-1}. Interestingly, a calculation done in the same study with the ($HN{=}CHCH_2N{=}CH_2$) bidentate model ligand yields a somewhat higher value of 14.1 kcal mol^{-1}.[415] The DFT-B3LYP calculations of Morokuma et al. carried out with the (HN=CHCH=NH) diimine ligand yield a comparable value, 15.0 kcal mol^{-1}.[418] Groen et al. ascribe their lower value in the case of the terdentate ligand to some steric effect and not to the presence of the dissociated arm.[415]

Yates and co-workers have performed, also in close connection with experimental investigations, a very comprehensive study of the carbonylation mechanism of the neutral $[Pd(HN{=}CHCOO)(PH_3)(CH_3)]$ system, **28**, taken as a model of palladium−alkyl complexes of picolinic acid derivatives **29** that have been shown to undergo rapid carbonylation.[413,414] Quite large

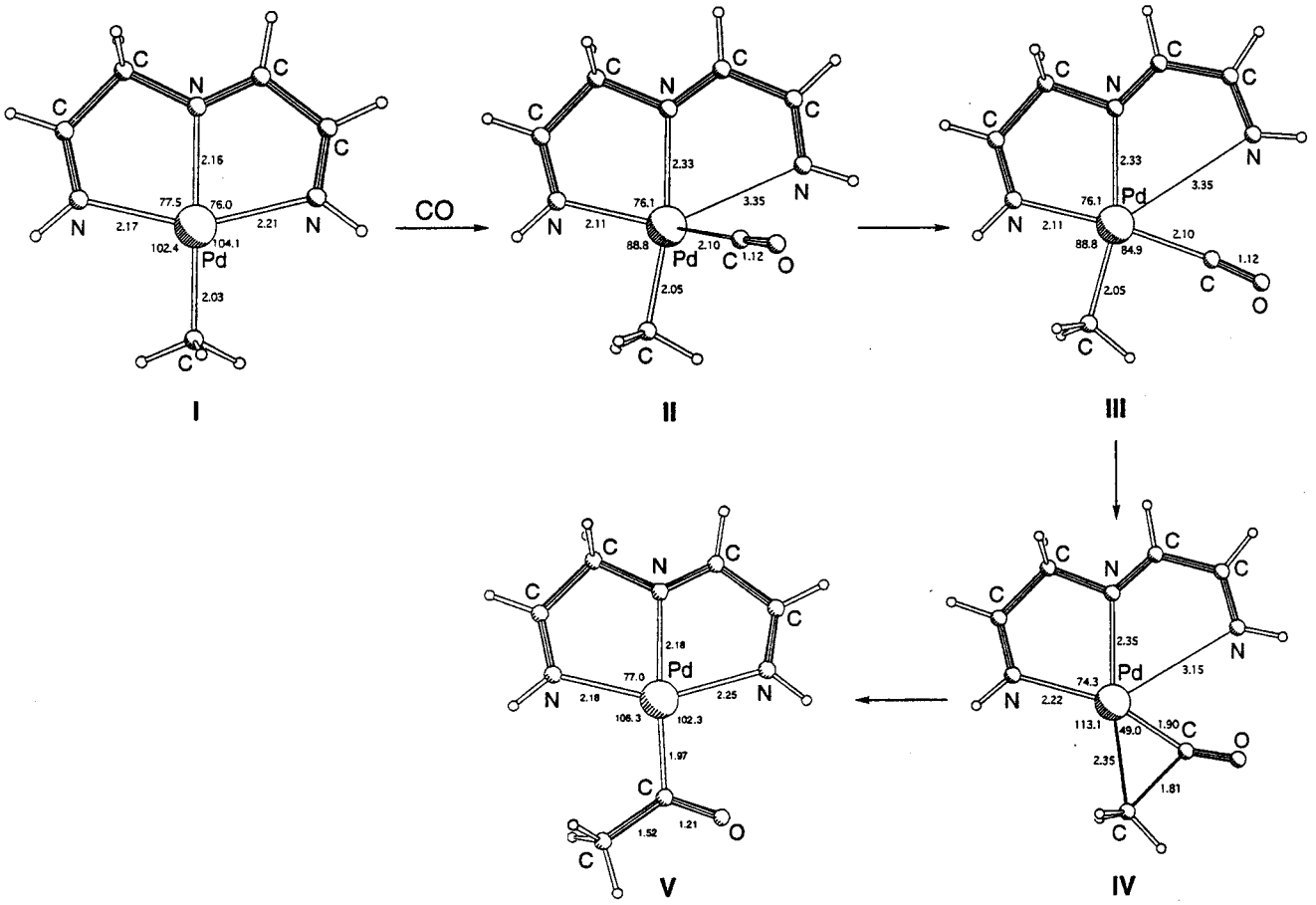

Figure 14. Computed reaction pathway (at the SCF level) for the reaction $[Pd(HN{=}CHCH_2N{=}CHCH{=}NH)(CH_3)]^+ + CO \rightarrow [Pd(HN{=}CHCH_2N{=}CHCH{=}NH)(COCH_3)]^+$. (Reprinted with permission from ref 415.) Copyright 1998.

basis sets were used for computing the energies at the MP2 level on geometries optimized either at the DFT-BLYP level or at the MP2 level. Both the *cis*-(N,P) and *trans*-(N,P) isomers have been considered. The calculations show that the dissociation of PH_3 is unlikely and that upon CO approach from **28**, a

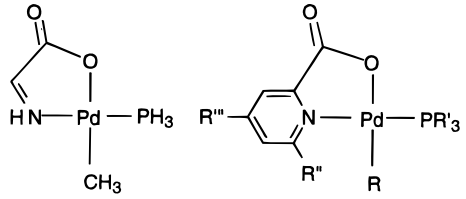

28 **29**

five-coordinate square-pyramidal $[Pd(HN{=}CHCOO)(PH_3)(CH_3)(CO)]$ intermediate, with the nitrogen atom at the apex of the palladium atom, is formed after some rearrangement, **30**. According to the BLYP and MP2 calculations, the nitrogen atom is more strongly bound in **30** than in the neutral $[Pd(NH_3)_2(CH_3)_2(CO)]$ system[412] (vide supra), the computed Pd−N bond distance being much shorter, 2.722 Å at the BLYP level, 2.351 Å at the MP2 level, and 3.11 Å at the SCF level in the $[Pd(NH_3)_2(CH_3)_2(CO)]$ system. Yates et al. ascribe this feature to some increased π back-donating ability or to the inclusion of correlation effects. But one may wonder whether the chelating nature of the ligand is also not of importance for keeping N closer to Pd. Yates et al. then considered various pathways for the CO insertion starting either from **30**, **31**, **32**, or **33**. The most

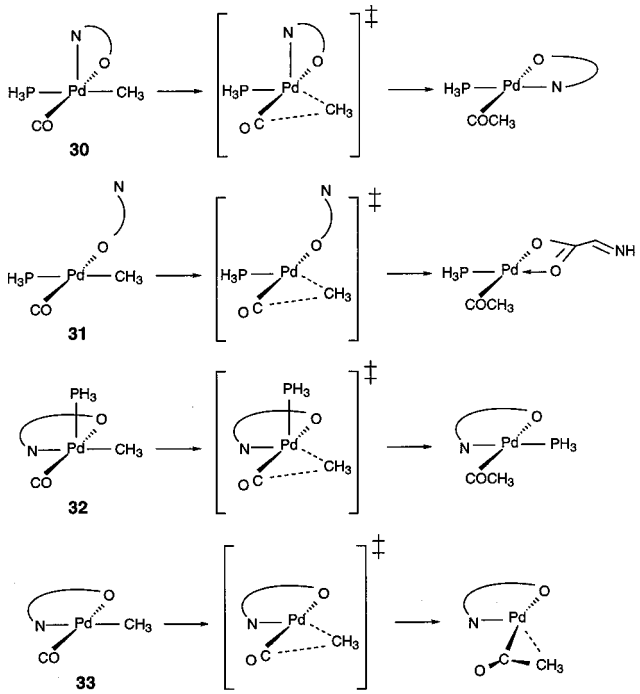

favorable is, as in the cationic system analyzed by Markies et al.,[412] the one starting from **30**, in which the donor nitrogen is weakly bound. Quite notewor-

thy, this result was found to be rather sensitive to the quality of the basis set. At the best level of calculation the computed barrier is 14 kcal mol^{-1}. Note that in the pathway starting from **31**, the imine and the carbonyl groups of the bidentate ligand exchange their role. In a very recent article, Yates et al. allude to calculations performed on a cationic analogue,[419] where the bidentate ligand is the neutral (HN═CHCHO) model ligand instead of the anionic $(HN═CHCOO)^-$ ligand used before. A similar mechanism seems to operate, one difference being that in the five-coordinate $[Pd(HN═CHCHO)(PH_3)(CH_3)(CO)]^+$ intermediate the O atom is now at the apex of palladium, instead of N in the neutral system. One can think that this is due to a stronger electrostatic interaction of oxygen in the cationic system.

To close this section, one should also mention a study of the insertion of $SnCl_2$ into the Pt−Cl bond of *cis*-$[Pt(Cl)_2(PH_3)_2]$.[420] The geometries of the separated reactants, transition state, and products (cis and trans) were optimized at the HF level and their energies recomputed at the MP2 level. These energy calculations point to an exothermic reaction and to the absence of an energy barrier from the reactants. One should perhaps wait until a DFT or a MP2 geometry optimization has been performed to assess this feature definitively. Moreover, it should be stressed that no determination of a molecular precursor adduct is reported in this study.

3. Nucleophilic Attack on a Coordinated Ligand

Nucleophilic Attack on the Allyl Ligand. The nucleophilic attack on an allyl ligand is a key step of many transformations of organic compounds catalyzed or mediated by allylpalladium complexes.[8] This is, for instance, the case in allylic substitution reactions,[421−426] bis-oxidation of conjugated dienes,[427,428] isomerization of allylic compounds, etc. These reactions are also characterized by some regio- and/or stereoselectivity induced by either the ligands on the metal or the substituents on the allyl ligand. Much work has been done to unravel these mechanistic issues, which could be also more complicated due to the possible interference of the $\eta^3 \leftrightarrow \eta^1$ interconversion.[1,429] Thus, the theoretical work that has been carried out on allyl complexes since 1990 has mostly dealt with a deeper understanding of their reactivity aspects.

Some of these aspects, however, rely on a precise assessment of the ground-state properties of the π-allyl complexes. Thus, in a collaborative effort, Norrby, Åkermark, Blomberg, and co-workers have developed molecular mechanics parameters[430] that allow the calculation of systems with quite large and complex ligands on the palladium atom as with substituents on the allyl ligand.[431,432] To this end, MCPF calculations (using the same computational recipe as for the naked palladium ligand systems, vide supra) have been carried out on the $[(\eta^3\text{-}C_3H_5)\text{-}Pd]^+$ system. From this study the binding appears as being quite covalent between a Pd^+ cation in its $d^9\ ^2D$ ground state and an allyl radical, one indicator being the electronic population of Pd that remains close to 9. The covalent interaction takes place between the nonbonding π orbital of the allyl radical and the metal d_π orbital of appropriate symmetry. There is also some donative interaction between the doubly occupied π orbital of the allyl and the empty 5s and 5p orbitals on palladium. Calculations also performed on $[Cl_2Pd(\eta^3\text{-}C_3H_5)]^-$ and $[(NH_3)_2Pd(\eta^3\text{-}C_3H_5)]^+$ show that this bonding pattern, schematically drawn in Figure 15, is retained in the bis-ligated system.[430] It is also rather similar to the previous ones that were based on extended Hückel calculations.[433−436] The covalent nature of the bonding which is emphasized here appears most clearly from the topological charge density analysis[157,158] made by Szabo on the MP2 wave functions of several $[L_2Pd(\eta^3\text{-}C_3H_5)]$ systems (L = none, F^-, Cl^-, NH_3, $CH_2═CH_2$, PH_3).[437] Critical points characteristic of covalent bonding have been found between Pd and the *three* carbon atoms. That the Pd−C bond is described in terms of a covalent bond is quite important since ligands that enforce this covalent type of binding will strengthen the Pd−C bond and make it therefore less prone to being cleaved on addition of a nucleophile. Indeed, the calculations (also carried out at the MP4 level) show that F, Cl, and NH_3 (considered by Szabo as pure σ-donor ligands) strengthen these palladium−carbon bonds and weaken the C−C allyl bonds whereas the opposite effect is found for the π acceptors $CH_2═CH_2$ and PH_3 (the phosphine being considered by Szabo as a π acceptor, see however our previous discussion). On the basis of these arguments it can be easily understood why, for instance, π acceptors activate the complex toward nucleophilic addition.[437]

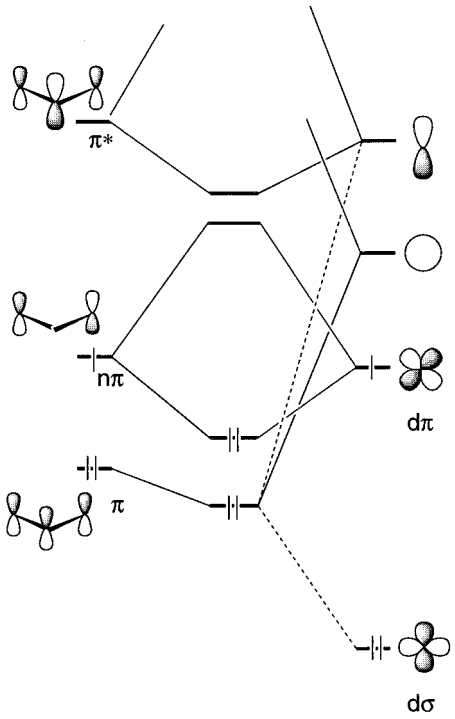

Figure 15. Schematic molecular orbital interaction diagram between the valence orbitals of the allyl ligand and the metal orbitals of appropriate symmetry.

A similar pattern was found by Sakaki et al.[274] In addition, these authors discuss the origin of the large dihedral angle of 110−125° between the π-allyl plane and the PdL_2 plane and of the downward shift of the

Scheme 5[a]

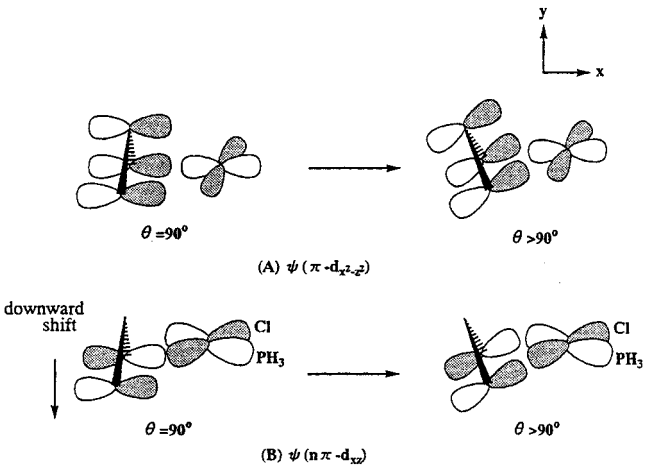

[a] Reprinted with permission from ref 274.

π-allyl skeleton below the PdL_2 plane. The large dihedral angle is due to a repulsive interaction—which is not accounted for in the picture of either Norrby et al.[430] or Szabo[437]—between a doubly occupied d_σ orbital and the π orbital. To weaken this interaction, which is shown by the lower broken line in Figure 15, the π-allyl ligand tilts, making a dihedral angle of >90°. However, since this tilting would also weaken the attractive covalent interaction between n_π and d_π, the allyl ligand shifts downward, Scheme 5.[274]

A comparison between Pd and Pt has been made by Sakaki et al.[438] in the case of the $[M(H)(PH_3)(C_3H_5)]$ systems (M = Pd, Pt). Both display the same geometry, i.e., an asymmetric bonding due the large trans effect of the hydride ligand. The asymmetry is greater for Pd compared to Pt. The M−P and M−C bonds are slightly shorter for Pt (except the M−C bond trans to phosphorus). The interconversion between the η^3-C_3H_5 and the η^1-C_3H_5 isomer has been also considered. The η^3 isomer is found much more stable than the η^1 isomer: when electron correlation is included, e.g., at the MP4SDQ level, the energy difference amounts to 8.6 kcal mol^{-1} for Pd and 13.0 kcal mol^{-1} for Pt. The addition of an extra phosphine ligand lowers this value to 3.1 kcal mol^{-1} in the case of $[Pd(H)(PH_3)_2(C_3H_5)]$. It even leads to a reversal in the stability order for Pt, since the η^1 isomer of $[Pt(H)(PH_3)_2(C_3H_5)]$ is found to be more stable than the η^3 isomer by 8.6 kcal mol^{-1}. Although Sakaki et al. do not comment on this point, one may speculate that this reversal is due to the greater covalent bonding between the metal and the cis ligands H and η^1-C_3H_5 in Pt compared to Pd.

In the bonding pattern of Figure 15, the π* orbital of the ligand is high in energy, above the $n_\pi-d_\pi$ antibonding combination that is generally considered as being the LUMO. That this $n_\pi-d_\pi$ orbital is the LUMO is often used as a rationale to account for the fact that the nucleophilic addition usually takes place on a terminal carbon atom. However, as elegantly explained by Carfagna et al.,[439] the situation is not as clear-cut as it seems. The bending and the shift of the allylic ligand that we mentioned above brings the anti hydrogen atoms (or substituents) rather close to the metal, thus raising some repulsive interactions. To relieve these interactions, the CH_2 groups distort: the anti hydrogens deviate from the allyl plane away from it (by 30° or more) whereas the syn hydrogens are pinned toward it. The consequence of this distortion, which is seen both in crystal structures[440] and in the optimized geometries[437,441,442] and which can be viewed as a disrotatory-like movement of the CH_2 groups, is dual: first there is a stronger interaction between d_π and n_π, which destabilizes the antibonding $n_\pi-d_\pi$ combination. Concomitantly, the π* orbital is stabilized, because of a reduced overlap between the p orbitals on the carbon atoms. As a result, the two levels come close to each other, much closer than one might have expected on reasoning with a planar allyl ligand, and the probability of a nucleophilic attack on the central carbon atom (the one with the greatest lobe in π*) is increased.[439] In fact, further calculations of Szabo, combined with an experimental investigation, have shown that a proper choice of the ancillary ligands can indeed orient the nucleophilic addition toward the central carbon atom.[443,444] A bidentate σ-donor ligand such as TMEDA raises the d_π orbital to such an extent that the π* orbital is below $n_\pi-d_\pi$ and becomes the LUMO, hence favoring attack at the central carbon atom. On the other hand, a π-acceptor ligand, such as $CH_2{=}CH_2$, favors the attack on the terminal carbon atoms. These calculations, carried out at the MP2 level, were corroborated by the experimental observations.[443,444]

Ward used EH calculations in an attempt to rationalize the observed regioselectivity of the nucleophilic attack on [Pd(allyl)(phosphine)(imine)] complexes.[445] With PH_3 and either NH_2^- or $H_2C{=}NH_2$ as a model of the phosphine and the imine, respectively, he finds (at variance with the ab initio calculations) a rather strong involvement of the allyl π* orbital in the orbital mixing pattern. According to his calculations, this π* orbital mixes into the $d_\pi-n_\pi$ combination and polarizes it on the carbon atom trans to the phosphine ligand, **34**. One therefore

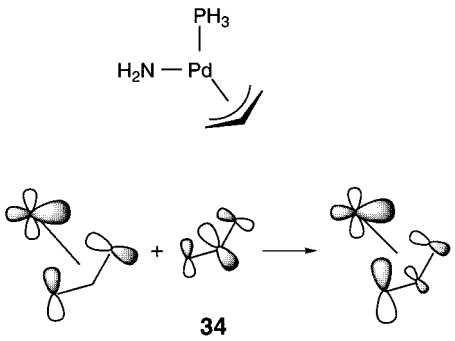

34

expects that the nucleophilic addition will take place on this carbon atom, as experimentally found and as rationalized by Szabo on the basis of covalency arguments.[437] One should point out, however, that the phase relationship for the mixing in **34** results from the fact that in the d_π orbital of the Pd(phosphine)(imine) fragment, which is the LUMO of this fragment, the lobe trans to the imine atom is greater than the lobe trans to the phosphorus atom due to the greater σ-donor strength of the imine.

Scheme 6

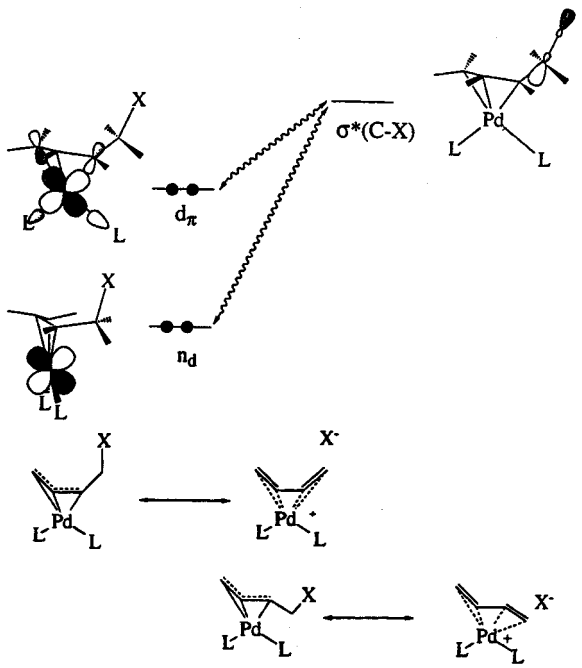

Thus, one intuitively expects the Pd−C bond trans to the imine to be stronger and is therefore brought back to Szabo's type of arguments.

Szabo has extended the scope of his investigations to analysis of the effects of β substituents and to their interrelation with the effects of the ancillary ligands.[441] The calculations, of MP2 and MP4SDQ type with a small-core pseudopotential, were carried out on a whole series of systems, viz. $[PdL_2(CH_2CHCHCH_2X)]$ ($L = Cl^-$, F^-, PH_3; X = Cl, OCH_3, H) where CH_2X takes a syn or an anti position. Consideration of both configurations allowed one to compare reactions occurring in cyclic (η^3-allyl)palladium where the anti position is imposed to reactions occurring in acyclic systems where the syn position is also possible. The major result of this study is the characterization of a new type of interaction between the β substituent and the palladium atom. More precisely, both the in-plane d_π orbital and a lower d orbital can interact in a bonding way with the σ^*_{C-X} orbital, Scheme 6. This interaction makes the allylic system similar to a butadiene complex, either cis or trans according to the anti or syn configuration of the allyl, Scheme 6. The result is a deactivation of the more substituted carbon atom and an activation of the less substituted one toward nucleophilic addition. The stronger the σ-donor capability of the ligand, the more regioselective the reaction is. We have seen, however, that the nucleophilic addition is activated by ligands that are either poor σ donors or π acceptors. Thus, a compromise has to be found between the β substituent effects and the activating effects of the ancillary ligands. The best compromise is to use bidentate ligands with a σ donor trans to the substituted allylic termini. Calculations performed later at the DFT-B3PW91 level yielded very similar results both for the geometries and for the energies.[442]

These calculations were in fact part of a combined experimental and theoretical investigation, aimed at testing the theoretical proposal.[442] They were performed on complexes bearing a β-methoxy-substituted cyclic allyl ligand, such as η^3-cyclohexenyl, η^3-cycloheptenyl, and η^3-cyclooctenyl. The experiment, which was based on comparison of the rates of the deuteriomethanolysis of the various cyclic complexes, unambiguously showed the validity of the theoretical proposal. A careful analysis of the geometrical features confirmed that a strict antiperiplanar conformation of the Pd−C_3 and C_4−O bond is necessary to maximize the strength of the β-substituent effects. Extension to the β-acetoxy-substituted (η^3-cyclohexenyl)palladium complexes with the acetoxy substituent in either the anti or syn position yielded similar conclusions.[446]

One should notice that the theoretical investigations of Szabo pertaining to the trans nucleophilic addition, i.e., the addition of an external nucleophile, do not include a transition-state determination. His conclusions rely only on the combination of computed ground-state properties with experimental observations. Thus, the determination of such a transition state by Blöchl and Togni,[447] using Blöchl's methodology[448] based on first-principle molecular dynamics within the projector augmented wave method,[449] is of major interest. The calculations were first carried out for the $[Pd(PH_3)(pyrazole)(C_3H_5)] + NH_3$ reaction. The optimized structure of the reactants, transition state, and product are shown in Figure 16. In the $[Pd(PH_3)(pyrazole)(\eta^3\text{-}C_3H_5)]$ reactant, the Pd−C bond trans to N is shorter than the bond trans to P by 0.035 Å, a feature explained by Blöchl and Togni as resulting from the greater trans influence of the phosphine. However, it also corresponds to a stronger σ covalent bond, as discussed by Szabo (vide supra). The attack was studied for the two terminal positions. The transition state for the attack trans to the pyrazole is 1.9 kcal mol^{-1} higher in energy than the one for the attack trans to the phosphine, the activation energies being 11.9 and 10.0 kcal mol^{-1}, respectively. The influence of the steric effects and its interplay with the electronic effects have also been investigated on one of the systems used in the experiments,[450] **35**. The simulations indicate that

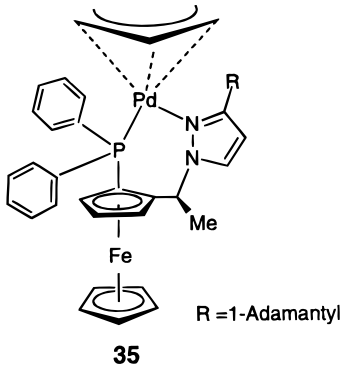

35

although both electronic and steric effects are at work, the site selectivity is dominated by steric effects that force the allyl ligand to rotate out of the P−Pd−N plane.[447]

The comparison between the attack of the neutral nucleophile NH_3 and the attack of anionic nucleophiles such as F^- and CN^- has now been done for

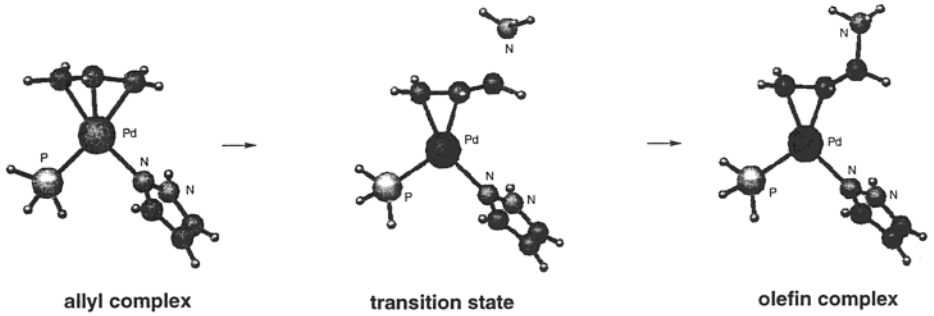

Figure 16. Optimized reactants, transition state and product for the nucleophilic addition of NH_3 on the allyl ligand of the $Pd(PH_3)$(pyrazol)(allyl) model system. (Reprinted with permission from ref 447.) Copyright 1996 American Chemical Society.

the $[Pd(NH_3)_2(\eta^3\text{-allyl})]$ system.[451] These two nucleophiles were taken as models of an electronegative anion and a stabilized carbon anion, respectively. Since the gas-phase reaction of anionic nucleophiles appears to be barrierless, the study was performed with a continuum solvation model, either the PCM/DIR [452] or SM2 model[453] for water solvation. Dichloromethane was also used as a solvent in the PCM/DIR solvation model. The results rely on DFT-B3LYP calculations carried out with a polarized valence double-ζ basis set and a small-core pseudopotential, except in the case of the SM2 solvation model which uses semiempirical AM1 wave functions. The transition-state determination was not based on gradient calculations but used a two-dimensional potential energy surface fit. It should be pointed out, however, that calibration calculations for the gas-phase $[Pd(NH_3)_2(\eta^3\text{-allyl})] + NH_3$ reaction yielded a good agreement between the transition-state geometry obtained via a gradient determination and the transition-state geometry obtained via the two-dimensional fit. The agreement with the transition state geometry determined by Blöchl and Togni (vide supra) was also quite satisfactory. The results of the calculations in CH_2Cl_2 show an increase in the reaction barriers in the order $CN^- > NH_3 > F^-$, from 6.9 to 17.2 kcal mol^{-1}, the value for NH_3 being 7.9 kcal mol^{-1}. Note that the corresponding gas-phase value is 2.1 kcal mol^{-1}. Thus, solvation leads to an increase of the reaction barrier, as expected from the charge delocalization and the increase of the cavitation work in the transition state. The PCM/DIR solvation model yields results that are more satisfactory than the SM2 ones, essentially because of the lack of parameters for palladium solvation in the latter case. Thus, the solvation energies within the SM2 model were obtained from consideration of the allyl cation−nucleophile system, without the $Pd(NH_3)_2$ moiety.

Szabo very recently investigated the cis migration of the coordinated chloride ligand to the η^3-allyl ligand in the $[PdCl(BQ)(\eta^3\text{-}C_3H_5)]$ system (BQ = *p*-benzoquinone, $C_6H_4O_2$), Scheme 7.[454] Such a reaction can also be viewed as a reductive elimination, since one goes from Pd(II) to Pd(0). It takes place experimentally in some catalytic transformation where benzoquinone is usually used as a cocatalyst to activate the η^3-allyl intermediate toward nucleophilic attack and to regenerate a Pd(II) complex in order to maintain a catalytic cycle. The calculations were carried out at the DFT-B3PW91 level, with a relativistic small-core pseudopotential for Pd[68] and a polarized basis set on the heavy atoms of the ligands. The effects of substitution of the benzoquinone on the Cl migratory aptitude were also studied by considering F, Cl, and CN as substituents. The cyclohexenyl was taken as a test for substitution on the allyl. The reactants, transition states, and products were fully optimized. The calculations showed that the steric effects induced by the η^2 coordination of the benzoquinone ligand facilitate the displacement of Cl toward the allyl ligand. The reaction in the unsubstituted system is slightly endothermic, by 2.5 kcal mol^{-1}, the barrier at the transition state amounting to 15 kcal mol^{-1}. The geometry of the transition state shown at the left of Figure 17 is characterized by a strong elongation of the Pd−C bond which is cis to Cl, from 2.16 Å in the reactant to 2.54 Å in the transition state. The fact that this is most likely due to the necessity for the relatively large Cl atom to maximize its interactions is best seen from the comparison with the structure of the transition state obtained by Sakaki et al.[438] for the reductive elimination process $[Pd(H)(PH_3)(\eta^3\text{-}C_3H_5)] \rightarrow [Pd(PH_3)(\eta^1\text{-}C_3H_6)]$, Figure 17, right. In this process, which corresponds to a cis migration of H toward the allyl ligand instead of the cis migration of Cl, it is the Pd−C bond trans to H which is elongated (from 2.47

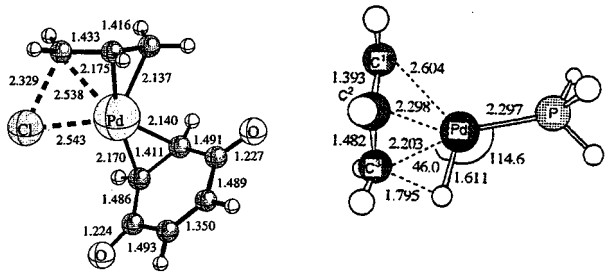

Figure 17. Transition state for the cis migration of Cl to the η^3-allyl ligand (left) and for the cis migration of H (right) in η^3-allyl Pd complexes. (Reprinted with permission from refs 454 and 438. Copyright 1998 and 1996 American Chemical Society).

Scheme 7

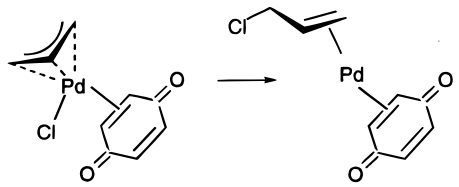

Å in the reactant to 2.60 Å in the transition state). The substitution effects are as expected from the previous studies: electron-withdrawing substituents lower the energy barrier, down to ~10 kcal mol^{-1} for the two CN's of 5,6-dicyanobenzoquinone (DDQ), which is also not too bulky. Alkyl substituents on the allyl can further decrease this value to 6.5 kcal mol^{-1}. These results have also been verified by experimental studies.[454]

Nucleophilic Addition on a Coordinated Olefin. This reaction is also very important in organometallic chemistry and in homogeneous catalysis.[455] It is, in particular, the first step of the catalytic cycle of the Wacker process.[456,457] Recently there has been a review of the theoretical studies pertaining to this topic.[458] In an attempt to get a detailed understanding of all steps involved in the process, Siegbahn first concentrated on the nucleophilic addition step. The reaction energy obtained from the gas-phase model reaction $[PdCl_2(C_2H_4)] + OH^- \rightarrow [PdCl_2(C_2H_4OH)]^-$ is not realistic, the computed exothermicity amounting to 77.8 kcal mol^{-1} according to the DFT-B3LYP calculations.[459] Self-consistent reaction field (SCRF) calculations (at the DFT-B3LYP level, using a spherical cavity and restricting the multipole expansion to the quadrupole moment) take into account the bulk dielectric properties of the surrounding water and reduce this value, but only to 54.6 kcal mol^{-1}. Thus, to get a realistic model, it is necessary to describe the nucleophile by a *chain* of water molecules (at least three) held by hydrogen bonds.[460] This chain can bridge the negative chloride ion and the point of attack of the olefin, **36** for the structure of the transition state of the nucleophilic attack (reproduced

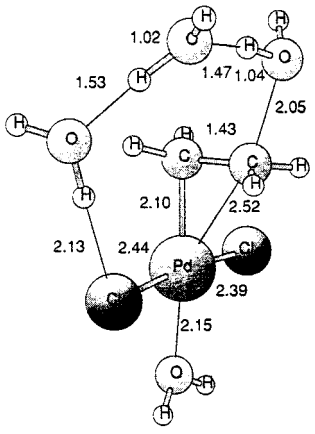

36

with permission from ref 460). Without inclusion of the bulk dielectric effects, this model yields an endothermic reaction, but on inclusion of these effects via SCRF calculations, a slight exothermicity is found, 4.5 kcal mol^{-1} with a large basis set including several polarization functions on both the ligands and the palladium.[460] This clearly shows the important role played by short-range *and* long-range effects. A small barrier (5.7 kcal mol^{-1}) is computed. This outside nucleophilic addition (which corresponds to a trans stereochemistry for the attack) is also found to be more exothermic than the cis attack (i.e., a cis migration from a hydroxide coordinated on palladium). All these features agree with the known experimental data on this process.

The mechanism of palladium-catalyzed cycloaddition reactions of methylenecyclopropane with olefins, as well as those of oxatrimethylenemethane (OTMM) and azatrimethylenemethane (ATMM) with olefins, have been investigated with HF and MP2 calculations.[461] The geometries were determined at the HF level and the energies recomputed at the MP2 level. The calculations have been carried out on the [Pd(η^2-methylenecyclopropane)(C_2H_4)(PH_3)], [Pd(η^3-OTMM)(C_2H_4)(PH_3)], and [Pd(η^3-ATMM)(C_2H_4)(PH_3)] model systems, assuming that the coupling is intramolecular. They show that the first step of the reaction has a transition state which involves the coupling of a π-allyl ligand (acting as a nucleophile) with the ethylene ligand. The energy barriers for this coupling are 26.4, 28.8, and 26.0 kcal mol^{-1}, respectively (MP2//HF values), thus underlining a similar behavior for the three systems. The preference for the [2 + 1] cycloaddition over the [3 + 2] cycloaddition observed in the products of the reaction for the heteroatom-substituted species is found to arise from the subsequent demetalation step: in the heteroatom case, this step involves a prototropic shift before the reductive elimination.[461]

4. Ligand Substitution Reactions

Ligand substitution reactions form an important class of reactions of square-planar Pd(II) and Pt(II) complexes.[462] There have been, in the past, several empirical or semiempirical studies of such processes which have been reviewed.[458,463] These studies gave some information about the σ and π electronic effects of the ligands and about the trans effect as well. Since then, few ab initio studies have been carried out to rationalize, on more quantitative grounds, the trans effect, the relative ease of the associative mechanism, and the dissociative mechanism and also to provide data for determination of analytical potential energy functions that can be used in further dynamic simulations.

Lin and Hall have determined, through a gradient geometry optimization, the geometry of the transition states for the associative pathway in substitution reactions on Pt and Rh complexes.[464] For platinum, the self-exchange of NH_3 in *trans*-[Pt(C_2H_4)Cl_2(NH_3)], *trans*-[Pt(CO)Cl_2(NH_3)], and *cis*-[Pt(H)Cl(NH_3)$_2$] was investigated. The calculations were carried out at the HF level with large-core pseudopotentials and a valence double-ζ basis set (a test calculation done at the GVB level showed that the HF level was a reasonable approximation). Since in these exchange reactions the entering and leaving groups were identical, the five-coordinate transition-state optimization could be done via a constrained energy minimization (this assumes that there is no intermediate). The corresponding geometries are shown in Figure 18 together with the corresponding SCF energy barriers. They point to a kinetic trans effect along the series C_2H_4 > CO > H > Cl in good agreement with the experimental order. Assuming the Pt−N distance as the reaction coordinate, a reaction path was computed and analyzed via a plot of the Lapla-

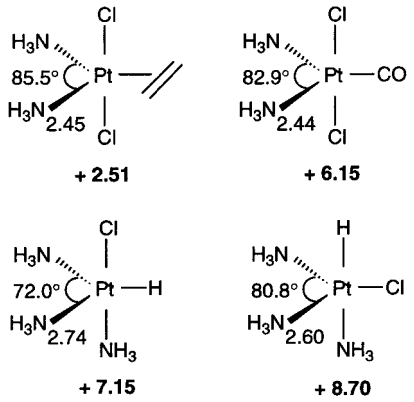

Figure 18. Geometries of the transition states for the *trans*-$Pt(C_2H_4)Cl_2(NH_3)$ + NH_3 substitution reaction, the *trans*-$Pt(CO)Cl_2(NH_3)$ + NH_3 substitution reaction, and the two possible courses of the *cis*-$Pt(H)Cl(NH_3)_2$ + NH_3 substitution reaction.

cian of the total electron density $-\nabla^2\rho$.[158] This analysis clearly shows that in the early stages of the reaction, the attack occurs at the apex of the square plane, the electron pair of the entering ligand using the empty p_z orbital. On further approach, the incoming ligand experiences electron−electron repulsion from the occupied d orbitals. To relieve part of this repulsion, it shifts away from the trans directing ligand and at the same time the leaving ligand is pushed down, this concomitant movement leading to the pseudo-trigonal-bipyramidal structure of the transition state. The trigonal-bipyramid-like (TBP) geometry of this transition state is characterized by a rather small angle (less than 90°) between the entering and leaving ligands in the equatorial plane and by correspondingly long metal−ligand bonds. This is traced to minimization of the repulsion between the d orbitals on the metal and the electron pairs on the entering and leaving ligands. This minimization is in turn related to both the σ and π properties of the trans directing ligand.

The more recent DFT study of Deeth and Elding of the water exchange on $[Pd(H_2O)_4]^{2+}$, $[Pt(H_2O)_4]^{2+}$, and *trans*-$[PdCl_2(H_2O)_2]$ also points to the bond stretching of the equatorial bonds in the TBP structure of the transition state for the associative mechanism.[465] The geometries were optimized at the LDA level, including spin-free relativistic corrections. For such systems that are essentially noncovalent, nonlocal corrections are found to somewhat deteriorate the results, the optimized geometries as well as the relative energies. On the other hand, solvation effects from the water molecules of the bulk need to be included in order to get meaningful results for the cationic systems. It turns out that the differential effects between the reactants and the transition state are well accounted for by the Born solvation model. Their contribution to the activation enthalpy for the water exchange at $[Pd(H_2O)_4]^{2+}$ is +17.8 kcal mol^{-1} for the associative mechanism and −15.8 kcal mol^{-1} for the dissociative exchange. Once these effects are included, the agreement between the computed activation energies and the experimental ones is very good. The dissociative and associative mechanism have been compared. In line with the known experimental data, the dissociative mechanism can be ruled out, the corresponding dissociation energy being much too high. Another interesting conclusion that emerges from this work is that the stretching of the equatorial bonds, as well as the release of solvent molecules in the transition state, counteracts the decrease in molar volume caused by the association of the entering water molecule into the inner coordination sphere, thus explaining the small volumes of activation observed experimentally.

A five-coordinate TBP-like geometry of the transition state has also been found by Morokuma and coworkers in their study of the water replacement reaction $[Pt(NH_3)_3(H_2O)]^{2+} + Cl^- \rightarrow [Pt(NH_3)_3Cl]^+ + H_2O$ taken as a model of the reaction $[Pt(dien)(H_2O)]^{2+} + Y^- \rightarrow [Pt(dien)Y]^+ + H_2O$ (dien = diethylenetriamine, $NH_2C_2H_4NHC_2H_4NH_2$).[466,467] Such exchange reactions between water and an incoming ligand Y are the second step of the solvation pathway of substitution reactions taking place in water, the first step consisting of the exchange between the leaving ligand X and water in $[Pt(dien)X]^+$.[462] The primary goal of this study was to determine an analytical potential energy function for the interaction between $[Pt(NH_3)_3(H_2O)]^{2+}$, Cl^-, and H_2O for further molecular simulation via Monte Carlo calculations. A potential function that assumes pairwise additivity cannot reproduce the ab initio potential energy, especially in the region of the transition state. The inclusion of repulsive three-body effects is crucial for a correct fitting of the ab initio potential energy function. This is best seen in Figure 19, which displays both energy profiles together with the corresponding geometries of intermediates and transition states for the reaction $[Pt(NH_3)_3(H_2O)]^{2+} + Cl^- \rightarrow [Pt(NH_3)_3Cl]^+ + H_2O$. Preliminary Monte Carlo calculations along the intrinsic reaction coordinate have also been performed. They show, as the reaction proceeds, an increase of the potential energy due to the reduction of the solvation ability of the system.[467]

We have seen in a previous subsection that for the CO coordination step of carbonylation reactions using either cationic or neutral Pd(II) complexes, the associative mechanism is the one that has been put forth by the theoretical studies.[412−414] Prior to their investigation of the CO insertion, Yates and coworkers had extended their methodological study of the reaction $Pd(PH_3) + CO \rightarrow PdCO + PH_3$ to the more realistic system $[Pd(HN{=}CHCOO)(CH_3)(PH_3)]$, **28**.[468] Thus, for each stationary point of the path of the reaction $[Pd(HN{=}CHCOO)(CH_3)(PH_3)] + CO \rightarrow [Pd(HN{=}CHCOO)(CH_3)(CO)] + PH_3$, a full geometry optimization has been done and different basis sets, pseudopotentials, and levels of theory, viz. HF, MP2, CCSD(T), and DFT with various functionals, have been tested. It has been concluded that quite reliable results can be obtained at the MP2 level with a small-core pseudopotential and a polarized double-ζ basis set. DFT methods have been found to yield correct geometries, except when using the B3LYP functional for the trigonal-bipyramid transition state. The optimized geometry in this case corresponds to the replacement of the chelate nitrogen rather than the phosphine, at variance with all other methods, which invariably gave a transition state corresponding to

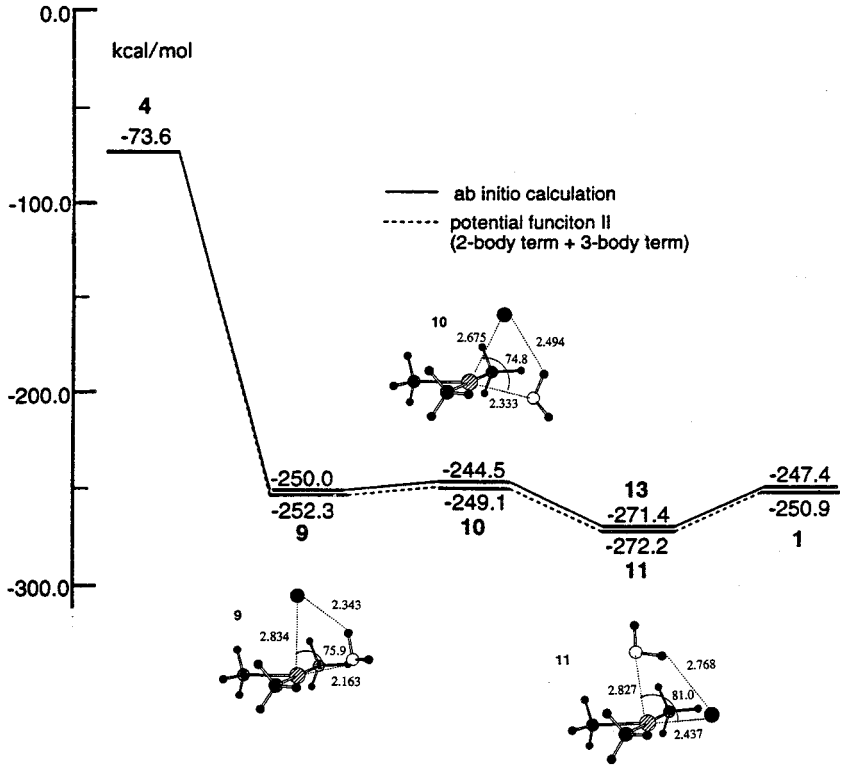

Figure 19. Potential energy profiles for the reaction $[Pt(NH_3)_3(H_2O)]^{2+} + Cl^- \rightarrow [Pt(NH_3)_3(Cl)]^+ + H_2O$ from the ab initio calculations and from an analytical potential function including the three-body terms, together with the optimized structures of the two five-coordinate intermediates and the transition state between them. (Reprinted with permission from ref 467.) Copyright 1995.

the replacement of the phosphine. Thus, some warning has to be given when this functional is used for optimizing transition structures that have one or several "isomers" close to each other.[468]

It should be mentioned that in some instances a dissociative mechanism can be preferred. Results from kinetic studies on the displacement of thioethers from the *cis*-$[PtPPh_2(Et_2S)_2]$ with pyridine or substituted pyridine have been interpreted as indicative of a dissociative mechanism. There the rate-determining step is the dissociation of thioether and the formation of a transient three-coordinate $[PtPPh_2(Et_2S)]$ intermediate.[469] Extended Hückel calculations and the corresponding molecular electrostatic potential calculations on the *cis*-$[PtCl_2(Me_2S)_2]$ and *cis*-$[PtMe_2(Me_2S)_2]$ have been used to rationalize these features.[469] It has been argued that when strong σ-donor ligands such as Me or Et are present, the Pt−S bond is lengthened and that the electron−electron repulsion from the d_{z^2} orbital is increased, these two factors disfavoring the association of the incoming ligand and favoring the dissociation of a thioether. Note also that either Me or Et make covalent bonds with the metal. One should stress that the ab initio calculations that favor the associative mechanism, so far, pertain to systems which do not have two strong covalently bound ligands. Systems such as the ones above might be worth investigating with ab initio methods.

5. Metal-Mediated Oxidation Reactions

The reaction of methane with the diatomic [PdO] has been investigated by Broclawik and co-workers as a first step toward a better understanding of the activation of methane on palladium and palladium oxide surfaces.[105] We have reviewed their DFT study of [PdO] alone. The same authors also considered its interaction with methane. The geometry optimizations, which were restricted to assumed approaches, were carried out at the LDA level, the relative energies being obtained with nonlocal corrections of the exchange and correlation functionals. Two molecular complexes have been obtained. In the first one, which corresponds to a collinear approach of CH_4 and [PdO], CH_4 is weakly bound (by 3.3 kcal mol^{-1}, NL-DFT value) in an η^2 fashion, but this does not lead to C−H bond cleavage. The second one is unbound with respect to the separated reactants but nevertheless corresponds to a very shallow minimum on the potential energy curve. It is lying 4.5 kcal mol^{-1} (NL-DFT value) above the collinear molecular complex and has one C−H bond bridging Pd−O. Further approaching CH_4 from Pd−O leads to cleavage of the C−H bond and the formation of a singlet, which is 32.8 kcal mol^{-1} below the separated reactants. Since the ground state of [PdO] is a triplet (vide supra), the system has to undergo a singlet−triplet crossing along the reaction path. An approximate transition state was located at a C−H bond stretch of 1.4 Å, with an activation energy of 21.2 kcal mol^{-1} above the separated reactants (or 24.5 kcal mol^{-1} above the collinear molecular complex). The authors have extended their study to the reaction with [RhO] and to the reaction with Pd_2 and $[Pd_2O]$.[393,470] We have already mentioned that the results obtained for Pd_2 were rather similar to those

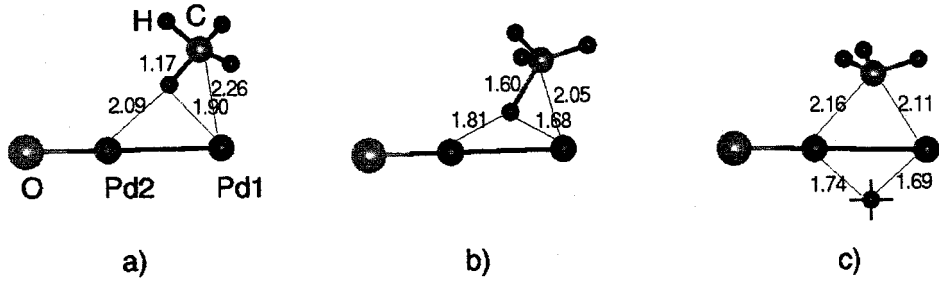

Figure 20. Optimized structures of the stationary points (precursor complex (a), transition state (b), and product (c)) for the constrained reaction path of the reaction $CH_4 + Pd_2O$. (Reprinted with permission from ref 393.) Copyright 1997.

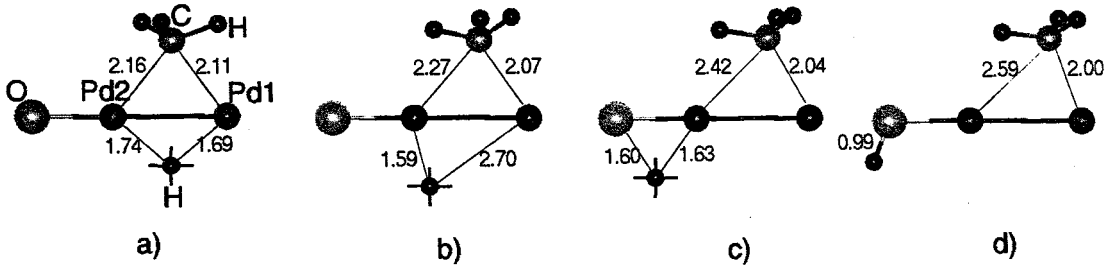

Figure 21. Optimized structures of the stationary points for the H migration in the $Pd_2O(H)(CH_3)$ system; starting structure (a), active intermediate (b), transition state (c), and product (d). (Reprinted with permission from ref 393).

that have been obtained later by Musaev et al.[237] via a full geometry optimization. For the activation of CH_4 on $[Pd_2O]$, the linearity of the $[Pd_2O]$ arrangement was maintained. Thus, as stated by the authors themselves, this investigation is not meant to represent the real surface of palladium oxide. It should merely help for understanding the mechanism of some possible elementary steps. It is therefore noteworthy that the reaction pathway obtained for $CH_4 + [Pd_2O]$, Figure 20, is quite similar to the one with Pd_2. In particular, an asymmetric transition state is found (see b of Figure 20) corresponding to an oxidative addition to the palladium atom and not to the Pd−O bond. The activation energy (with respect to the molecular precursor a) is 14.3 kcal mol^{-1} (NL-DFT value), to be compared to 5.2 kcal mol^{-1} for Pd_2 (vide supra). An interesting result of the study is the fate of product of the oxidative addition.[393] As seen in Figure 21, the hydrogen atom undergoes a shift from the bridging position between the two palladiums to the terminal position to the oxygen atom. Concomitantly, the bridging methyl shifts backward to the terminal palladium. The activation energy for this process is 27.1 kcal mol^{-1}. Broclawik et al. noticed that the methyl is now in a favorable position for the activation of the next C−H bond, such that the entire cycle may be repeated. They have not investigated this point further, however. In view of the results brought by Musaev et al.,[237] it would be quite interesting to have full geometry optimizations for such processes.

One may wonder why the oxidative addition of CH_4 on [PdO] could not also be a two-step process. Such a two-step process would involve first C−H oxidative addition on Pd, followed by the transfer to the oxygen atom. Indeed, in their study of the Pt^+-catalyzed oxidation of methane,[359] Schwarz, Siegbahn, and coworkers found that the two-step mechanism is more favorable than the one-step mechanism for the reaction $[PtO]^+ + CH_4$. Starting from an electrostatically bound $[OPt(CH_4)]^+$ system, the transition state for the one-step process was computed 8.8 kcal mol^{-1} (DFT-B3LYP value) *above* the transition state for the C−H bond oxidative addition on Pt and 5.0 kcal mol^{-1} *above* the transition state for the H migration from Pt to O. Note that at the PCI-80 level the C−H bond oxidative addition is downhill on the doublet surface and that the process involves a spin crossing since the ground state of $[OPt(CH_4)]^+$, as is the one of $[PtO]^+$, is a quartet. The results on $[PtO]^+$ may not be directly transferable to [PdO], however, since we have seen in the work of Musaev et al. on the oxidative addition on Pd_2 and Pt_2[237] that the C−H bond activation on a single metal atom seems to be specific to platinum.

Schwarz, Siegbahn et al. have also investigated for the Pt^+-catalyzed oxidation of methane[359] other pathways than the oxidative addition of CH_4 to $[PtO]^+$. Among these, another important pathway is the $[Pt(CH_2)]^+ + O_2 \rightarrow [PtO]^+ + CH_2O$ reaction. Many computational difficulties have been encountered due to large near-degeneracy effects arising from the combination of the doublet ground state of $[Pt(CH_2)]^+$ with the triplet ground state of O_2 to give a quartet ground state for $[PtO]^+$ and a singlet state for CH_2O, from sudden changes in the occupancy of the orbitals from one point of the potential energy surface to another. In fact, in many instances the wave function was not dominated by a single determinant, hence leading to unreliable MCPF and PCI-80 results. On the other hand and rather unexpectedly, the B3LYP energies gave results in qualitative agreement with the available experimental data. From the calculations it could be shown that the reaction $[Pt(CH_2)]^+ + O_2 \rightarrow [PtO]^+ + CH_2O$ proceeds through a four-membered metallacycle formed by the [2 + 2] addition of O_2 to $[Pt(CH_2)]^+$. For this reaction an estimate of the activation energy is 2.6 kcal mol^{-1} above the entrance channel. The corresponding product is a strongly bound electrostatic complex $[OPt(OCH_2)]^+$.

The relative feasibility of the various exit channels from this complex has also been assessed.[359]

Fantucci et al. reported a preliminary investigation of the mechanism of the epoxidation of olefins catalyzed by alkyl peroxo complexes of platinum(II).[471] The results are quite tentative, due to the fact no strict comparison of all possible steps could be made. Moreover, solvation effects are believed to be quite important since at some stage of the process a protonation reaction may be involved. The results led, however, to an interesting proposal for the mechanism that had not been considered experimentally before.[472] In this mechanism the Pt−OOH complex would first undergo a 1,2 shift of hydrogen over the O−O bond to generate a Pt−O(H)O isomer, with an oxywater-like structure. This isomer would then easily transfer its terminal hydrogen to the olefin. Support for this proposal comes from the lowering of the energy barrier for the 1,2 shift when going from the hydroperoxide HOOH or substituted hydroperoxides to the [$(PH_3)_2(CF_3)$Pt−OOH] and [$(PH_3)_2$(Cl)-Pt−OOH] complexes: in the former case, the barriers range between 52 and 65 kcal mol^{-1}, whereas they amount to 37.9 and 39.1 kcal mol^{-1} for the two platinum complexes.[471]

6. Studies of Catalytic Cycles

The understanding gained in the theoretical studies of the prototype reactions combined with the relatively good accuracy of the current methodologies has paved the way for studying full cycles in homogeneous catalysis (or a major part of these cycles). As far as palladium and platinum complexes are concerned, we have already mentioned the silastannation of acetylenes catalyzed by palladium complexes,[169] the hydrosilylation of ethylene catalyzed by Pt(0)bisphosphine complexes.[381] Sakaki has also performed a study of the disilylation of alkenes catalyzed by Pt(0)bisphosphine complexes.[473] The study of several steps of the oxidation of ethylene to acetaldehyde in water catalyzed by palladium chloride (Wacker process), including the influence of the water solvent, was first tackled by Siegbahn.[459,460] Very recently, van Santen and co-workers have analyzed, using DFT-B3LYP calculations, the same reaction catalyzed by palladium acetate dimers in acetic acid.[474] The thermochemistry of the oxidation of methane to methyl bisulfate, catalyzed by a bisamine Pt complex in the presence of sulfuric acid, has been assessed via DFT-B3LYP calculations, including solvation effects.[475] The results are in line with the mechanism proposed experimentally,[476] although as stated by the authors themselves, more work is needed especially with respect to the determination of the energy barriers of the various steps. Morokuma, Musaev, and co-workers have compared alkyne diboration and the alkene diboration reactions catalyzed by Pt(0)bisphosphine complexes.[384] They have also rationalized, on the basis of the propensity of [$Pd(PH_3)_2\{B(OH)_2\}_2$] intermediates to easily undergo the reductive elimination back to the reactants $Pd(PH_3)_2$ and [$(OH)_2$B−B$(OH)_2$], why Pd(0) complexes *do not* catalyze the same reaction.[385] They have extended the scope of their study of this class of reactions to the study of the alkyne thioboration, catalyzed either by Pd(0) or Pt(0) diphosphine complexes. They have, in particular, explained the inefficiency of Pt(0) complexes—in contrast to the alkyne diboration—as catalysts.[378] The mechanism of the Pd(0)-catalyzed C−C coupling reaction of an aryl with an olefin (the Heck reaction) in which the catalyst is a bisphosphine Pd(0) complex stabilized by the coordination of *N*-heterocyclic carbenes has been unravelled by Rösch and co-workers.[477] And last but not least, one should mention all the theoretical investigations of the polymerization of olefins[374,405,478−480] or of the copolymerization of carbon monoxide and olefins[400,418,481,482] that are both catalyzed by Pd complexes.

V. Conclusion and Perspectives

It should be clear from this review that the theoretical studies in palladium and platinum molecular chemistry have been done along two main directions. On the one hand, there has been an impressive amount of work devoted to small molecular systems involving one or very few metal atoms. For such systems, the performance of highly sophisticated methods with respect to accuracy and transferability could be tested. It has been shown that spin−orbit effects are of crucial importance to obtain reliable spectroscopic properties, especially for platinum systems. The necessity of using large and flexible basis sets contributes to the difficulty of such calculations. Yet there are, in some instances, still rather large discrepancies between theory and experiment for bond dissociation energies: representative examples include PdCO, PtCO, PdO, and $PdCH_2^+$. These issues have to be settled from both the theoretical and experimental sides. From a more chemical point of view, theoretical studies have been quite successful at analyzing and predicting trends, at delineating the factors that account for these trends. A coherent picture has emerged that relies on the extent of the sd hybridization in the metal atoms. The accuracy that is currently reached allows fruitful cooperative work between theory and experiment in gas-phase reactivity. In some cases, the theoretical studies have been of invaluable value for the understanding of such experiments. One should see more studies of that type in the near future.

Besides these studies on small molecular systems, the development of the computational machinery (on the software side as on the hardware side) has allowed one to tackle more and more accurately and reliably problems involving transition-metal complexes or molecular complexes. These comprise the rationalization of structural features (such as weak metal−metal interactions or metal−ligand interactions), the determination of reaction pathways in stoichiometric or catalytic processes, and the interplay between the structural and reactivity aspects in chemo-, regio-, or stereoselective reactions. It has been shown that in order to get results that are qualitatively correct, one needs basis sets which are at least of valence double-ζ quality and that include polarization functions (e.g., on the reacting atoms in reactivity studies). Relativistic effects have to be

taken into account, at least the spin-free ones. In standard treatments, this is generally done by using quasirelativistic pseudopotentials for Pd or Pt. Electron correlation effects also have to be accounted for, via either MP2 or DFT calculations. The most recent studies have taken advantage of the development of the DFT methods which have proven to be more and more reliable, especially for geometry optimizations (although some pathological cases still exist). There is also no doubt that the theoretical studies will rely more and more on integrated methods combining treatments of various kinds, e.g., quantum mechanics (with various methods for electron correlation including the DFT ones), molecular mechanics, molecular dynamics, Monte Carlo calculations, or Car−Parrinello-type methods. With such methods, one can now envision calculating very large systems, such as biological systems and dendrimers, or treating problems of enantioselective catalysis.

Another issue which will be important in the near future deals with the effects induced by the environment, e.g., the effects of the counterions, of the crystal, or of the solution. We have seen in this review some studies that have addressed this issue. Methodologies have to be assessed for treating solvation effects accurately. The continuum model, which is currently quite popular, has limitations, in particular when microsolvation effects are at work. Here too, integrated methods might be the panacea.

The way is therefore open to cope with problems of increasing complexity, a trend which is also observed in experimental studies. There is no doubt that one will see from the experimental side a call for theoretical studies of more modeling character.

VI. References

(1) Hartley, F. R. *The Chemistry of Platinum and Palladium*; Applied Science Publishers Ltd.: London, 1973.
(2) Jain, V. K.; Rao, G. S.; Jain, L. *Adv. Organomet. Chem.* **1987**, *27*, 113.
(3) Usón, R.; Fornies, J. *Adv. Organomet. Chem.* **1988**, *28*, 219.
(4) Buyers, P. K.; Canty, A. J.; Honeyman, R. T. *Adv. Organomet. Chem.* **1992**, *34*, 1992.
(5) Anderson, G. K. *Adv. Organomet. Chem.* **1993**, *35*, 1.
(6) Albeniz, A. C.; Espinet, P. In *Encyclopedia of Inorganic Chemistry*; King, R. B., Ed.; J. Wiley: New York, 1994; Vol. 6; p 3010.
(7) Suggs, J. W. In *Encyclopedia of Inorganic Chemistry*; King, R. B., Ed.; J. Wiley: New York, 1994; Vol. 6; p 3023.
(8) Tsuji, J. *Palladium Reagents and Catalysis: Innovations in Organic Synthesis*; Wiley: Chichester, 1995.
(9) *Comprehensive Organometallic Chemistry II*; Puddephatt, R. J., Ed.; Pergamon: Oxford, 1995; Vol. 9.
(10) *Comprehensive Organometallic Chemistry II*; Hegedus, L., Ed.; Pergamon: Oxford, 1995; Vol. 12.
(11) Negishi, E. I.; Copéret, C.; Ma, S.; Liou, M.-Y.; Liu, F. *Chem. Rev.* **1996**, *96*, 365.
(12) Rendina, L. M.; Puddephatt, R. J. *Chem. Rev.* **1997**, *97*, 1735.
(13) Veillard, A. *Chem. Rev.* **1991**, *91*, 743.
(14) Koga, N.; Morokuma, K. *Chem. Rev.* **1991**, *91*, 823.
(15) Moore, C. E. *Atomic Energy Levels As Derived From The Analyses of Optical Spectra*; U.S. Government Printing Office: Washington , DC, 1971.
(16) *Transition Metal Hydrides*; Dedieu, A., Ed.; VCH Publishers: New York, 1992.
(17) Grushin, V. V. *Chem. Rev.* **1996**, *96*, 2011.
(18) Balasubramanian, K.; Feng, P. Y.; Liao, M. Z. *J. Chem. Phys.* **1987**, *87*, 3981.
(19) Langhoff, S. R.; Petterson, L. G. M.; Bauschlicher, C. W. J. *J. Chem. Phys.* **1987**, *86*, 268.
(20) Siegbahn, P. E. M. *Theor. Chim. Acta* **1993**, *86*, 219.
(21) Balasubramanian, K. *J. Chem. Phys.* **1990**, *93*, 8061.
(22) LaJohn, L. A.; Christiansen, P. A.; Ross, R. B.; Atashroo, T.; Ermler, W. C. *J. Chem. Phys.* **1987**, *87*, 2812.
(23) Balasubramanian, K. *J. Phys. Chem.* **1989**, *93*, 6585.
(24) Lagerqvist, A.; Neuhaus, H.; Scullman, R. *Proc. Phys. Soc.* **1964**, *83*, 498.
(25) Malmberg, C.; Scullman, R.; Nylen, P. *Ark. Fys.* **1969**, *39*, 495.
(26) Tolbert, M. A.; Beauchamp, J. L. *J. Phys. Chem.* **1986**, *90*, 5015.
(27) Sjøvoll, M.; Fagerli, H.; Gropen, O.; Almlöf, J. *J. Chem. Phys.* **1997**, *107*, 5496.
(28) Jenderek, J.; Marian, C. M. *Theor. Chim. Acta* **1994**, *88*, 13.
(29) Fleig, T.; Marian, C. M. *J. Chem. Phys.* **1998**, *108*, 3517.
(30) Basch, H.; Topiol, S. *J. Chem. Phys.* **1979**, *71*, 802.
(31) Basch, H.; Cohen, D.; Topiol, S. *Isr. J. Chem.* **1980**, *19*, 233.
(32) Wang, S. W.; Pitzer, K. S. *J. Chem. Phys.* **1983**, *79*, 3851.
(33) Rohlfing, C. M.; Hay, P. J.; Martin, R. L. *J. Chem. Phys.* **1986**, *85*, 1447.
(34) Balasubramanian, K.; Feng, P. Y. *J. Chem. Phys.* **1990**, *92*, 541.
(35) Tobisch, S.; Rasch, G. *Chem. Phys. Lett.* **1990**, *166*, 311.
(36) Gropen, O.; Almlöf, J.; Wahlgren, U. *J. Chem. Phys.* **1992**, *96*, 8363.
(37) McCarthy, M. C.; Field, R. W.; Engelman, K., Jr.; Bernath, P. F. *J. Mol. Spectrosc.* **1993**, *158*, 208.
(38) Gustafsson, G.; Schullman, R. *Mol. Phys.* **1989**, *67*, 981.
(39) Dyall, K. G. *J. Chem. Phys.* **1993**, *98*, 9678.
(40) Visscher, L.; Saue, T.; Nieuwpoort, W. C.; Faegri, K.; Gropen, O. *J. Chem. Phys.* **1993**, *99*, 6704.
(41) Fleig, T.; Marian, C. M. *Chem. Phys. Lett.* **1994**, *222*, 267.
(42) *Relativistic Calculations on TM Complexes*; Marian, C. M., Ed.; Department of Chemical Physics and Material Science Centre, University of Groningen: Groningen, 1994.
(43) Sjøvoll, M.; Fagerli, H.; Gropen, O.; Almlöf, J.; Olsen, J.; Helgaker, T. U. *Int. J. Quantum Chem.* **1998**, *68*, 53.
(44) Heinemann, C.; Koch, W.; Schwarz, H. *Chem. Phys. Lett.* **1995**, *245*, 509.
(45) Stevens, W. J.; Krauss, M.; Basch, H.; Jasien, P. G. *Can. J. Chem.* **1992**, *70*, 612.
(46) Hess, B. A.; Marian, C. M.; Wahlgren, U.; Gropen, O. *Chem. Phys. Lett.* **1996**, *251*, 365.
(47) Marian, C. M.; Wahlgren, U. *Chem. Phys. Lett.* **1996**, *251*, 357.
(48) Zurita, S.; Rubio, J.; Illas, F.; Barthelat, J. C. *J. Chem. Phys.* **1996**, *104*, 8500.
(49) Balasubramanian, K. *J. Chem. Phys.* **1987**, *87*, 2800.
(50) Bagatur'yants, A. A.; Anikin, N. A.; Zhidomirov, G. M.; Kazanskii, V. B. *Russ. J. Phys. Chem.* **1981**, *55*, 1157.
(51) Blomberg, M.; Brandemark, U.; Pettersson, L.; Siegbahn, P. *Int. J. Quantum Chem.* **1983**, *23*, 855.
(52) Nakatsuji, H.; Hada, M. *Croat. Chim. Acta* **1984**, *57*, 1371.
(53) Jarque, C.; Novaro, O.; Ruiz, M. E.; Garcia-Prieto, J. *J. Am. Chem. Soc.* **1986**, *108*, 3507.
(54) Poulain, E.; Garcia-Prieto, J.; Ruiz, M. E.; Novaro, O. *Int. J. Quantum Chem.* **1986**, *29*, 1181.
(55) Low, J. J.; Goddard, W. A., III *Organometallics* **1986**, *5*, 609.
(56) Nakatsuji, H.; Hada, M.; Yonezawa, T. *J. Am. Chem. Soc.* **1987**, *109*, 1902.
(57) Balasubramanian, K. *J. Chem. Phys.* **1988**, *88*, 6955.
(58) Nakatsuji, H.; Matsuzaki, Y.; Yonezawa, T. *J. Chem. Phys.* **1988**, *88*, 5759.
(59) Gropen, O.; Sjøvoll, M.; Strømsnes, H.; Karlsen, E.; Swang, O.; Faegri, K., Jr. *Theor. Chim. Acta* **1994**, *87*, 373.
(60) Diez, R. P. *Chem. Phys. Lett.* **1998**, *287*, 542.
(61) Ziegler, T.; Li, J. *Can. J. Chem.* **1994**, *72*, 783.
(62) Heinemann, C.; Hertwig, R. H.; Wesendrup, R.; Koch, W.; Schwarz, H. *J. Am. Chem. Soc.* **1995**, *117*, 495.
(63) Zhang, H.; Balasubramanian, K. *J. Phys. Chem.* **1992**, *96*, 6981.
(64) Ozin, G. A.; Garcia-Prieto, J. *J. Am. Chem. Soc.* **1986**, *108*, 3099.
(65) Knight, L. B., Jr.; Cobranchi, S. T.; Herlong, J.; Kirk, T.; Balasubramanian, K.; Das, K. K. *J. Chem. Phys.* **1990**, *92*, 2721.
(66) Gusev, D. G.; Notheis, J. U.; Rambo, J. P.; Hauger, B. E.; Eisenstein, O.; Caulton, K. G. *J. Am. Chem. Soc.* **1994**, *116*, 7409.
(67) Siegbahn, P. E. M. *Theor. Chim. Acta* **1994**, *87*, 441.
(68) Hay, P. J.; Wadt, W. R. *J. Chem. Phys.* **1985**, *82*, 299.
(69) Siegbahn, P. E. M. *Theor. Chim. Acta* **1994**, *88*, 413.
(70) Reynolds, G. G.; Carter, E. A. *J. Phys. Chem.* **1994**, *98*, 8144.
(71) Macgregor, S. A.; Moock, K. H. *Inorg. Chem.* **1998**, *37*, 3284.
(72) Becke, A. D. *Phys. Rev. A* **1988**, *38*, 3098.
(73) Deeth, R. J.; Jenkins, H. D. B. *J. Phys. Chem. A* **1997**, *101*, 4793.
(74) Bray, M. R.; Deeth, R. J.; Paget, V. J.; Sheen, P. D. *Int. J. Quantum Chem.* **1996**, *61*, 85.
(75) Sakai, Y.; Oshibe, T.; Miyoshi, E. *Acta Crystallogr.* **1996**, *B52*, 251.
(76) Pacchioni, G.; Bagus, P. S. *Inorg. Chem.* **1992**, *31*, 4391.
(77) Fantucci, P.; Polezzo, S.; Sironi, M.; Bencini, A. *J. Chem. Soc., Dalton Trans.* **1995**, 4121.
(78) Frankcombe, K. E.; Cavell, K. J.; Yates, B. F.; Knott, R. B. *J. Phys. Chem.* **1995**, *99*, 14316.
(79) Matsubara, T.; Maseras, F.; Koga, N.; Morokuma, K. *J. Phys. Chem.* **1996**, *100*, 2573.
(80) Leoni, P.; Chiaradonna, G.; Pasquali, M.; Marchetti, F.; Fortunelli, A.; Germano, G. *Inorg. Chim. Acta* **1997**, *264*, 185.
(81) Blomberg, M. R. A.; Siegbahn, P. E. M.; Svensson, M. *Inorg. Chem.* **1993**, *32*, 4218.

(82) Siegbahn, P. E. M.; Blomberg, M. R. A.; Svensson, M. *J. Phys. Chem.* **1993**, *97*, 2564.
(83) Papai, I.; Goursot, A.; St-Amant, A.; Salahub, D. R. *Theor. Chim. Acta* **1992**, *84*, 237.
(84) Smith, G. W.; Carter, E. A. *J. Phys. Chem.* **1991**, *95*, 2327.
(85) Blomberg, M. R. A.; Lebrilla, C. B.; Siegbahn, P. E. M. *Chem. Phys. Lett.* **1988**, *150*, 522.
(86) Barnes, L. A.; Rosi, M.; Bauschlicher, C. W., Jr. *J. Chem. Phys.* **1990**, *93*, 609.
(87) Roszak, S.; Balasubramanian, K. *Chem. Phys. Lett.* **1993**, *212*, 150.
(88) Roszak, S.; Balasubramanian, K. *J. Phys. Chem.* **1993**, *97*, 11238.
(89) Grushow, A.; Ervin, K. M. *J. Chem. Phys.* **1997**, *106*, 9580.
(90) Chung, S.-C.; Krüger, S.; Pacchioni, G.; Rösch, N. *J. Chem. Phys.* **1995**, *102*, 3695.
(91) Li, J.; Schreckenbach, G.; Ziegler, T. *J. Am. Chem. Soc.* **1995**, *117*, 486.
(92) Snijders, J. G.; Baerends, E. J. *Mol. Phys.* **1978**, *36*, 1789.
(93) Snijders, J. G.; Baerends, E. J.; Ros, P. *Mol. Phys.* **1979**, *38*, 1909.
(94) Ziegler, T.; Tschinke, V.; Baerends, E. J.; Snijders, J. G.; Ravenek, W. *J. Phys. Chem.* **1989**, *93*, 3050.
(95) Jonas, V.; Thiel, W. *J. Chem. Phys.* **1995**, *102*, 8474.
(96) Ehlers, A. W.; Frenking, G. *Organometallics* **1995**, *14*, 423.
(97) Jonas, V.; Thiel, W. *Organometallics* **1998**, *17*, 353.
(98) Srdanov, V. I.; Harris, D. O. *J. Chem. Phys.* **1987**, *89*, 2658.
(99) Sassenberg, V.; Scullman, R. *Phys. Scr.* **1987**, *28*, 1983.
(100) Schwerdtfeger, P.; McFeaters, J. S.; Moore, J. J.; McPherson, D. M.; Cooney, R. P.; Bowmaker, G. A.; Dolg, M.; Andrae, D. *Langmuir* **1991**, *7*, 116.
(101) Bauschlicher, C. W.; Nelin, C. J.; Bagus, P. S. *J. Chem. Phys.* **1985**, *82*, 3265.
(102) Siegbahn, P. E. M. *Chem. Phys. Lett.* **1993**, *201*, 15.
(103) Siegbahn, P. E. M. *J. Phys. Chem.* **1993**, *97*, 9096.
(104) Huber, K. P.; Herzberg, G. *Molecular Spectra and Molecular Structure*; Van Nostrand Reinhold: New York, 1979.
(105) Broclawik, E.; Yamauchi, R.; Endou, A.; Kubo, M.; Miyamoto, A. *J. Chem. Phys.* **1996**, *104*, 4098.
(106) Kirchner, E. J. J.; Baerends, E. J.; Sloten, U. v.; Kleyn, A. W. *J. Chem. Phys.* **1992**, *97*, 3821.
(107) Carroll, J. J.; Haug, K. L.; Weisshaar, J. C.; Blomberg, M. R. A.; Siegbahn, P. E. M.; Svensson, M. *J. Phys. Chem.* **1995**, *99*, 13955.
(108) Ehlers, A. W.; Dapprich, S.; Vyboishchikov, S.; Frenking, G. *Organometallics* **1996**, *15*, 105.
(109) Carroll, J. J.; Weisshaar, J. C.; Siegbahn, P. E. M.; Wittborn, C. A. M.; Blomberg, M. R. A. *J. Phys. Chem.* **1995**, *99*, 14388.
(110) Bauschlicher, C. W.; Partridge, H.; Sheehy, J. A.; Langhoff, S. R.; Rosi, M. *J. Phys. Chem.* **1992**, *96*, 6969.
(111) Irikura, K. K.; Goddard, W. A., III *J. Am. Chem. Soc.* **1994**, *116*, 8733.
(112) Ohanessian, G.; Goddard, W. A., III *Acc. Chem. Res.* **1990**, *23*, 386.
(113) Siegbahn, P. E. M.; Blomberg, M. R. A.; Svensson, M. *Chem. Phys. Lett.* **1994**, *223*, 35.
(114) Eriksson, L. A.; Pettersson, L. G. M.; Siegbahn, P. E. M.; Wahlgren, U. *J. Chem. Phys.* **1995**, *102*, 872.
(115) Wesendrup, R.; Schröder, D.; Schwarz, H. *Angew. Chem., Int. Ed. Engl.* **1994**, *33*, 223.
(116) Perdew, J. P. *Phys. Rev. B* **1986**, *33*, 8822.
(117) Heinemann, C.; Schwarz, H.; Koch, W.; Dyall, K. G. *J. Chem. Phys.* **1995**, *104*, 4642.
(118) Ross, R. B.; Powers, J. M.; Atashroo, T.; Ermler, W. C.; LaJohn, L. A.; Christiansen, P. A. *J. Chem. Phys.* **1990**, *93*, 6654.
(119) Sirois, S.; Castro, M.; Salahub, D. R. *Int. J. Quantum Chem.* **1994**, *S28*, 645.
(120) Sakamoto, M.; Shimizu, I.; Yamamoto, A. *Organometallics* **1994**, *13*, 407.
(121) Sakaki, S.; Dedieu, A. *Inorg. Chem.* **1987**, *26*, 3278.
(122) Gauthron, I.; Mugnier, Y.; Hierso, K.; Harvey, P. D. *New J. Chem.* **1998**, *22*, 237.
(123) Flament, J. P.; Tadjeddine, M. *Chem. Phys. Lett.* **1995**, *238*, 193.
(124) Hay, P. J.; Wadt, W. R. *J. Chem. Phys.* **1985**, *82*, 270.
(125) Tadjeddine, A.; Peremans, A.; Rille, A. L.; Zheng, W. Q.; Tadjeddine, M.; Flament, J. P. *J. Chem. Soc., Faraday Trans.* **1996**, *92*, 3823.
(126) Decleva, P.; Ohno, M. *Chem. Phys.* **1992**, *164*, 73.
(127) Ohno, M.; Decleva, P.; Niessen, W. v. *J. Chem. Phys.* **1992**, *97*, 2767.
(128) Strout, D. L.; Miller, T. F., III; Hall, M. B. *J. Phys. Chem. A* **1998**, *102*, 6307.
(129) Siegbahn, P. E. M. *J. Am. Chem. Soc.* **1994**, *116*, 7722.
(130) Siegbahn, P. E. M. *J. Phys. Chem.* **1995**, *99*, 12723.
(131) Dewar, M. J. S. *Bull. Soc. Chim. (Fr.)* **1951**, *18*, C79.
(132) Chatt, J.; Ducanson, L. A. *J. Chem. Soc.* **1953**, 2939.
(133) Blomberg, M. R. A.; Siegbahn, P. E. M.; Svensson, M. *J. Phys. Chem.* **1992**, *96*, 9794.
(134) Ozin, G. A.; Power, W. G. *Inorg. Chem.* **1977**, *16*, 212.
(135) Garcia-Cuesta, I.; Sanchez de Meras, A.; Nebot-Gil, I. *Mol. Phys.* **1993**, *78*, 1449.
(136) Fahmi, A.; van Santen, R. A. *J. Phys. Chem.* **1996**, *100*, 5676.
(137) Minaev, B.; Ågren, H. *Int. J. Quantum Chem.* **1999**, *72*, 581.
(138) Roszak, S.; Balasubramanian, K. *Chem. Phys. Lett.* **1995**, *234*, 101.
(139) Bauschlicher, C. W.; Partridge, H.; Langhoff, S. R. *J. Phys. Chem.* **1992**, *96*, 3273.
(140) Cheng, P. T.; Cook, C. D.; Nyburg, S. C.; Wan, K. Y. *Inorg. Chem.* **1971**, *10*, 2210.
(141) Cheng, P. T.; Nyburg, S. C. *Can. J. Chem.* **1972**, *50*, 912.
(142) Love, R. A.; Koetzle, T. F.; Williams, G. J. B.; Andrews, L. C.; Bau, R. *Inorg. Chem.* **1975**, *14*, 2653.
(143) Morokuma, K.; Borden, W. T. *J. Am. Chem. Soc.* **1991**, *113*, 1912.
(144) Li, J.; Schreckenbach, G.; Ziegler, T. *Inorg. Chem.* **1995**, *34*, 3245.
(145) Sakaki, S.; Ieki, M. *Inorg. Chem.* **1991**, *30*, 4218.
(146) Koga, N.; Morokuma, K. *Chem. Phys. Lett.* **1993**, *202*, 330.
(147) Bo, C.; Costas, M.; Poblet, J. M. *J. Phys. Chem.* **1995**, *99*, 5914.
(148) Frenking, G.; Antes, I.; Böhme, M.; Dapprich, S.; Ehlers, A. W.; Jonas, V.; Neuhaus, A.; Otto, M.; Stegmann, R.; Veldkamp, A.; Vyboishchikov, S. F. In *Reviews in Computational Chemistry*; Lipkowitz, K. B., Boyd, D. B., Eds.; VCH Publishers: New York, 1996; Vol. 8, p 63.
(149) Mortimer, C. T. *Rev. Inorg. Chem.* **1984**, *6*, 233.
(150) Fagan, P. J.; Calabrese, J. C. *Acc. Chem. Res.* **1992**, *25*, 134.
(151) Fagan, P. J.; Calabrese, J. C.; Malone, B. *Science* **1991**, *252*, 1160.
(152) Lichtenberger, D. L.; Wright, L. L.; Gruhn, N. E.; Rempe, M. E. *Synth. Met.* **1993**, *59*, 353.
(153) Koga, N.; Morokuma, K. *Chem. Phys. Lett.* **1991**, *196*, 191.
(154) Lichtenberger, D. L.; Wright, L. L.; Gruhn, N. E.; Rempe, M. E. *J. Organomet. Chem.* **1994**, *478*, 213.
(155) Lopez, J. A.; Mealli, C. *J. Organomet. Chem.* **1994**, *478*, 161.
(156) Fagan, P. J.; Calabrese, J. C.; Malone, B. *J. Am. Chem. Soc.* **1991**, *113*, 9408.
(157) Bader, R. F. W. *Atoms in Molecules: A Quantum Theory*; Clarendon Press: Oxford, U.K., 1990.
(158) Bader, R. F. W. *Chem. Rev.* **1991**, *91*, 893.
(159) Dolg, M.; Pyykkö, P.; Runeberg, N. *Inorg. Chem.* **1996**, *35*, 7450.
(160) Sugimoto, M.; Horiuchi, F.; Sakaki, S. *Chem. Phys. Lett.* **1997**, *274*, 543.
(161) Strömberg, S.; Svensson, M.; Zetterberg, K. *Organometallics* **1997**, *16*, 3165.
(162) Siegbahn, P. E. M.; Strömberg, S.; Zetterberg, K. *Organometallics* **1996**, *15*, 5542.
(163) Cundari, T. R.; Gordon, M. S. *J. Mol. Structure (THEOCHEM)* **1994**, *313*, 47.
(164) Rizopoulos, A. L.; Sigalas, M. P. *New J. Chem.* **1994**, *18*, 197.
(165) Russo, N.; Toscano, M.; Rizopoulos, A. L.; Sigalas, M. P. *Inorg. Chim. Acta* **1998**, *273*, 72.
(166) de Vaal, P.; Dedieu, A. *J. Organomet. Chem.* **1994**, *478*, 121.
(167) Pfeffer, M. *Recl. Trav. Chim. Pays-Bas* **1990**, *109*, 567.
(168) Ryabov, A. D.; van Eldik, R.; Borgne, G. L.; Pfeffer, M. *Organometallics* **1993**, *12*, 1386.
(169) Hada, M.; Tanaka, Y.; Ito, M.; Murakami, M.; Amii, H.; Ito, Y.; Nakatsuji, H. *J. Am. Chem. Soc.* **1994**, *116*, 8754.
(170) Siegbahn, P. E. M. *Theor. Chim. Acta* **1994**, *87*, 277.
(171) Sugimoto, M.; Yamasaki, I.; Mizoe, N.; Anzai, M.; Sakaki, S. *Theor. Chem. Acc.* **1999**, *102*, 377.
(172) Steinborn, D.; Tschoerner, M.; Zweidorf, A. V.; Sieler, J.; Bögel, H. *Inorg. Chim. Acta* **1995**, *234*, 47.
(173) Engel, P. F.; Pfeffer, M.; Dedieu, A. *Organometallics* **1995**, *14*, 3423.
(174) Nakai, H.; Fukada, S.; Nakatsuji, H. *J. Phys. Chem. A* **1997**, *101*, 973.
(175) Farrar, D. H.; Payne, N. C. *J. Organomet. Chem.* **1981**, *220*, 251.
(176) Glanville, J. O.; Stewart, J. M.; Grim, S. O. *J. Organomet. Chem.* **1967**, *7*, 9.
(177) Fantucci, P.; Pizzotti, M.; Porta, F. *Inorg. Chem.* **1991**, *30*, 2277.
(178) Fantucci, P.; Lolli, S. *J. Mol. Catal.* **1993**, *82*, 131.
(179) Fantucci, P.; Lolli, S.; Pizzotti, M. *Inorg. Chem.* **1994**, *33*, 2779.
(180) Yoshida, T.; Tatsumi, K.; Matsumoto, M.; Nakatsu, K.; Nakamura, A.; Fueno, T.; Otsuka, S. *Nouv. J. Chim.* **1979**, *3*, 761.
(181) Nakamura, S.; Morokuma, K. *Organometallics* **1988**, *7*, 1904.
(182) Hofmann, P.; Perez-Moya, L. A.; Steigelmann, O.; Riede, J. *Organometallics* **1992**, *11*, 1167.
(183) Hofmann, P. Private communication.
(184) Rohmer, M.-M.; Grand, A.; Bénard, M. *J. Am. Chem. Soc.* **1990**, *112*, 2875.
(185) Dickman, M. H.; Doedens, R. J. *Inorg. Chem.* **1982**, *21*, 682.
(186) Yang, D. S.; Bancroft, M.; Puddephatt, R. J.; Tse, J. S. *Inorg. Chem.* **1990**, *29*, 2496.
(187) Geoffroy, M.; Bernardinelli, G.; Castan, P.; Chermette, H.; Deguenon, D.; Nour, S.; Weber, J.; Wermeille, M. *Inorg. Chem.* **1992**, *31*, 5056.
(188) Ahlrichs, R.; Ballauf, M.; Eichkorn, K.; Hanemann, O.; Kettenbach, G.; Klüfers, P. *Chem. Eur. J.* **1998**, *4*, 835.
(189) Lamoen, D.; Parrinello, M. *Chem. Phys. Lett.* **1996**, *248*, 309.
(190) Fleischer, E. B.; Miller, C. K.; Webb, L. E. *J. Am. Chem. Soc.* **1964**, *86*, 2342.

(191) Shi, J.-C.; Wen, T.-B.; Zheng, Y.; Zhong, S.-J.; Wu, D.-X.; Liu, Q.-T.; Kang, B.-S.; Wu, B.-M.; Mak, T. C. W. *Polyhedron* **1996**, *16*, 369.
(192) Palmer, M.; Carter, K.; Harris, S. *Organometallics* **1997**, *16*, 2448.
(193) DePriest, J.; Zheng, G. Y.; Woods, C.; Rillema, D. P.; Mirikova, N. A.; Zandler, M. E. *Inorg. Chim. Acta* **1997**, *264*, 287.
(194) Desmarais, N.; Adamo, C.; Panunzi, B.; Barone, V.; Giovannitti, B. *Inorg. Chim. Acta* **1995**, *238*, 159.
(195) Schlecht, S.; Faza, N.; Massa, W.; Dapprich, S.; Frenking, G.; Dehnicke, K. *Z. Anorg. Allg. Chem.* **1998**, *624*, 1011.
(196) Wehman-Ooyevaar, I. C. M.; Grove, D. M.; Kooijman, H.; van der Sluis, P.; Spek, A. L.; van Koten, G. *J. Am. Chem. Soc.* **1992**, *114*, 9916.
(197) Wehman-Ooyevaar, I. C. M.; Grove, D. M.; de Vaal, P.; Dedieu, A.; van Koten, G. *Inorg. Chem.* **1992**, *31*, 5484.
(198) Milet, A.; Dedieu, A. *Theor. Chim. Acta* **1995**, *92*, 361.
(199) Canty, A. J.; Dedieu, A.; Jin, H.; Milet, A.; Richmond, M. K. *Organometallics* **1996**, *15*, 2845.
(200) Milet, A.; Dedieu, A.; Canty, A. J. *Organometallics* **1997**, *16*, 5331.
(201) O'Reilly, A. A.; White, P. S.; Templeton, J. L. *J. Am. Chem. Soc.* **1996**, *118*, 5684.
(202) Visentin, T.; Kochanski, E.; Dedieu, A. *J. Mol. Struct. (THEOCHEM)* **1998**, *431*, 255.
(203) Visentin, T.; Dedieu, A.; Kochanski, E.; Padel, L. *J. Mol. Struct. (THEOCHEM)* **1999**, *459*, 201.
(204) Junicke, H.; Schenzel, K.; Heinemann, F. W.; Pelz, K.; Bögel, H.; Steinborn, D. *Z. Anorg. Allg. Chem.* **1997**, *623*, 603.
(205) Kaim, W.; Klein, A.; Hazenzahl, S.; Stoll, H.; Zalis, S.; Fiedler, J. *Organometallics* **1998**, *17*, 237.
(206) Swang, O.; Blom, R.; Ryan, O. B.; Faegri, K., Jr. *J. Phys. Chem.* **1996**, *100*, 17334.
(207) Åkesson, R.; Pettersson, L. G. M.; Sandström, M.; Wahlgren, U. *J. Am. Chem. Soc.* **1994**, *116*, 8691.
(208) Siegbahn, P. E. M.; Crabtree, R. H. *Mol. Phys.* **1996**, *89*, 279.
(209) Groning, O.; Elding, L. I. *Inorg. Chem.* **1989**, *28*, 3866.
(210) Aullon, G.; Alvarez, S. *Inorg. Chem.* **1996**, *35*, 3137.
(211) Ziegler, T.; Nagle, J. K.; Snijders, J. G.; Baerends, E. J. *J. Am. Chem. Soc.* **1989**, *111*, 5631.
(212) Nagle, J. K.; Balch, A. L.; Olmstead, M. M. *J. Am. Chem. Soc.* **1988**, *110*, 319.
(213) Liao, M.-S.; Zhang, Q.-E. *Inorg. Chem.* **1997**, *36*, 396.
(214) Liao, M.-S.; Zhang, Q.-E.; Schwarz, W. H. E. *Z. Anorg. Allg. Chem.* **1998**, *624*, 1419.
(215) Yakovlev, A. L.; Neyman, K. M.; Zhidomirov, G. M.; Rösch, N. *J. Phys. Chem.* **1996**, *100*, 3482.
(216) Kozelka, J.; Savinelli, R.; Berthier, G.; Flament, J.-P.; Lavery, R. *J. Comput. Chem.* **1993**, *14*, 45.
(217) Yao, S.; Plastaras, J. P.; Marzilli, L. G. *Inorg. Chem.* **1994**, *33*, 6061.
(218) Cundari, T. R.; Fu, W.; Moody, E. W.; Slavin, L. L.; Snyder, L. A.; Sommerer, S. O.; Klinkman, T. R. *J. Phys. Chem.* **1996**, *100*, 18057.
(219) Chval, Z.; Sip, M. *J. Phys. Chem. B* **1998**, *102*, 1659.
(220) Nikolov, G. S.; Trendafilova, N.; Schöneberger, H.; Gust, R.; Kritzenberger, J.; Yersin, H. *Inorg. Chim. Acta* **1994**, *217*, 159.
(221) Carloni, P.; Andreoni, W.; Hütter, J.; Curioni, A.; Giannozzi, P.; Parrinello, M. *Chem. Phys. Lett.* **1995**, *234*, 50.
(222) Carloni, P.; Andreoni, W. *J. Phys. Chem.* **1996**, *100*, 17797.
(223) Tornaghi, E.; Andreoni, W.; Carloni, P.; Hütter, J.; Parrinello, M. *Chem. Phys. Lett.* **1995**, *246*, 469.
(224) Balasubramanian, K. *J. Chem. Phys.* **1988**, *89*, 6310.
(225) Blomberg, M. R. A.; Siegbahn, P. E. M. *Chem. Phys. Lett.* **1991**, *179*, 524.
(226) Lin, S.-S.; Strauss, B.; Kant, A. *J. Chem. Phys.* **1969**, *51*, 2282.
(227) Blomberg, M. R. A.; Siegbahn, P. E. M.; Svensson, M. *J. Phys. Chem.* **1992**, *96*, 5783.
(228) Goursot, A.; Papai, I.; Salahub, D. R. *J. Am. Chem. Soc.* **1992**, *114*, 7452.
(229) Perdew, J. P.; Yue, W. *Phys. Rev. B* **1986**, *33*, 8800.
(230) Nakao, T.; Dixon, D. A.; Chen, H. *J. Phys. Chem.* **1993**, *97*, 12665.
(231) Seminario, J. M.; Concha, M. C.; Politzer, P. *Int. J. Quantum Chem.* **1993**, *S27*, 263.
(232) Seminario, J. M.; Zacarias, A. G.; Castro, M. *Int. J. Quantum Chem.* **1997**, *61*, 515.
(233) Valerio, G.; Toulhoat, H. *J. Phys. Chem.* **1996**, *100*, 10827.
(234) Estiú, G. L.; Zerner, M. C. *J. Phys. Chem.* **1994**, *98*, 4793.
(235) Lee, C.; Wang, W.; Parr, R. G. *Phys. Rev. B* **1988**, *37*, 785.
(236) Becke, A. D. *J. Chem. Phys.* **1993**, *98*, 5648.
(237) Cui, Q.; Musaeev, D. G.; Morokuma, K. *J. Chem. Phys.* **1998**, *108*, 8418.
(238) Balasubramanian, K. *J. Chem. Phys.* **1987**, *87*, 6573.
(239) Müller, U.; Sattler, K.; Xhie, J.; Venkkateswaran, N.; Raima, G. *J. Vac. Sci. Technol. B* **1991**, *9*, 829.
(240) Miedema, A. R.; Gingerich, K. A. *J. Phys. B* **1979**, *12*, 2081.
(241) Gupta, S. A.; Nappi, B. M.; Gingerich, K. A. *Inorg. Chem.* **1981**, *20*, 966.
(242) Wang, H.; Carter, E. A. *J. Phys. Chem.* **1992**, *96*, 1197.
(243) Balasubramanian, K. *J. Chem. Phys.* **1989**, *91*, 307.
(244) Ervin, K. M.; Ho, J.; Lineberger, W. C. *J. Chem. Phys.* **1988**, *89*, 4515.
(245) Cui, Q.; Musaeev, D. G.; Morokuma, K. *J. Phys. Chem. A* **1998**, *102*, 6373.
(246) Rubio, J.; Zurita, S.; Barthelat, J. C.; Illas, F. *Chem. Phys. Lett.* **1994**, *217*, 283.
(247) Dai, D.; Balasubramanian, K. *J. Chem. Phys.* **1995**, *103*, 648.
(248) Wang, H.; Carter, E. A. *J. Am. Chem. Soc.* **1993**, *115*, 2357.
(249) Engel, N. *Acta Metall.* **1967**, *15*, 557.
(250) Brewer, L. *Acta Metall.* **1967**, *15*, 553.
(251) Brewer, L. *Science* **1968**, *161*, 115.
(252) Dai, D.; Balasubramanian, K. *J. Phys. Chem.* **1992**, *96*, 3279.
(253) Dai, D.; Balasubramanian, K. *J. Chem. Phys.* **1994**, *100*, 1994.
(254) Payne, N. C.; Ramachandran, R.; Schoettel, G.; Vittal, J. J.; Puddephatt, R. J. *Inorg. Chem.* **1991**, *30*, 4048.
(255) Valerio, G.; Toulhouat, H. *J. Phys. Chem. A* **1997**, *101*, 1969.
(256) Dai, D.; Roszak, S.; Balasubramanian, K. *J. Chem. Phys.* **1996**, *104*, 1471.
(257) Roszak, S.; Balasubramanian, K. *J. Chem. Phys.* **1995**, *103*, 1043.
(258) Pyykkö, P. *Chem. Rev.* **1997**, *97*, 597.
(259) Sakaki, S.; Ogawa, M.; Musahi, Y. *J. Phys. Chem.* **1995**, *99*, 17314.
(260) Yoshida, T.; Yamagata, T.; Tulip, T. H.; Ibers, J. A.; Otsuka, S. *J. Am. Chem. Soc.* **1978**, *100*, 2063.
(261) Dedieu, A.; Hoffmann, R. *J. Am. Chem. Soc.* **1978**, *100*, 2074.
(262) Hubig, S. M.; Drouin, M.; Michel, A.; Harvey, P. D. *Inorg. Chem.* **1992**, *31*, 5375.
(263) Harvey, P. D.; Murtaza, Z. *Inorg. Chem.* **1993**, *32*, 4721.
(264) Couture, C.; Farrar, D. H.; Fisher, D. S.; Gukathasan, R. R. *Organometallics* **1987**, *6*, 532.
(265) Yamamoto, Y.; Takahashi, K.; Yamazaki, H. *Chem. Lett.* **1985**, 201.
(266) Müller, T. E.; Ingold, F.; Menzer, S.; Mingos, D. M. P.; Williams, D. J. *J. Organomet. Chem.* **1997**, *528*, 163.
(267) Tanase, T.; Nomura, T.; Fukushima, T.; Yamamoto, Y.; Kobayashi, K. *Inorg. Chem.* **1993**, *32*, 4578.
(268) Liu, H.; Tan, A. L.; Mok, K. F.; Hor, T. S. A. *J. Chem. Soc., Dalton Trans.* **1996**, 4023.
(269) Provencher, R.; Harvey, P. D. *Inorg. Chem.* **1996**, *35*, 2113.
(270) Modinos, A.; Woodward, P. *J. Chem. Soc., Dalton Trans.* **1974**, 1516.
(271) Budzelaar, P. H. M.; van Leeuwen, P. W. V. M.; Robeek, C. F.; Orpen, A. G. *Organometallics* **1992**, *11*, 23.
(272) Bender, R.; Braunstein, P.; Dedieu, A.; Dusausoy, Y. *Angew. Chem., Int. Ed. Engl.* **1989**, *28*, 923.
(273) Kurosawa, H.; Hirako, K.; Natsume, S.; Ogoshi, S.; Kanehisa, N.; Kai, Y.; Sakaki, S.; Takeuchi, K. *Organometallics* **1996**, *15*, 2089.
(274) Sakaki, S.; Takeuchi, K.; Sugimoto, M.; Kurosawa, H. *Organometallics* **1997**, *16*, 2995.
(275) Sieler, J.; Helms, M.; Gaube, W.; Svensson, A.; Lindquist, O. *J. Organomet. Chem.* **1987**, *320*, 129.
(276) Leoni, P.; Pasquali, M.; Fadini, L.; Albinati, A.; Hofmann, P.; Metz, M. *J. Am. Chem. Soc.* **1997**, *119*, 8625.
(277) Leoni, P.; Pasquali, M.; Pieri, G.; Albinati, A.; Pregosin, P. S.; Rüegger, H. *Organometallics* **1995**, *14*, 3143.
(278) Usón, R.; Fornies, J.; Sanz, J. F.; Usón, M. A.; Usón, I.; Herrero, S. *Inorg. Chem.* **1997**, *36*, 1912.
(279) Cordogan, J. A.; Gomez-Lara, J.; Cabrera, A.; Rosas, N. *J. Mol. Struct. (THEOCHEM)* **1997**, *392*, 223.
(280) Murahashi, T.; Otani, T.; Mochizuki, E.; Kai, Y.; Kurosawa, H.; Sakaki, S. *J. Am. Chem. Soc.* **1998**, *120*, 4536.
(281) Mann, K. R.; Gordon, J. G., II; Gray, H. B. *J. Am. Chem. Soc.* **1975**, *97*, 3553.
(282) Krogmann, K. *Angew. Chem., Int. Ed. Engl.* **1969**, *8*, 35.
(283) Connick, W. B.; Marsh, R. E.; Schaefer, W. P.; Gray, H. B. *Inorg. Chem.* **1997**, *36*, 913.
(284) Mealli, C.; Pichierri, F.; Randaccio, L.; Zangrando, E.; Krumm, M.; Holtenrich, D.; Lippert, B. *Inorg. Chem.* **1995**, *34*, 3418.
(285) Aullón, G.; Alvarez, S. *Chem. Eur. J.* **1997**, *3*, 655.
(286) Novoa, J. J.; Aullón, G.; Alemany, P.; Alvarez, S. *J. Am. Chem. Soc.* **1995**, *117*, 7169.
(287) Aullón, G.; Alemany, P.; Alvarez, S. *Inorg. Chem.* **1996**, *35*, 5061.
(288) Navarro, J. A. R.; Romero, M. A.; Salas, J. M.; Quiros, M.; Bahraoui, J. E.; Molina, J. *Inorg. Chem.* **1996**, *35*, 7829.
(289) Rosa, A.; Ricciardi, G.; Baerends, E. J. *Inorg. Chem.* **1998**, *37*, 1368.
(290) Yip, H.-K.; Lin, H.-M.; Cheung, K.-K.; Che, C.-M.; Wang, Y. *Inorg. Chem.* **1994**, *33*, 1644.
(291) Aullón, G.; Alemany, P.; Alvarez, S. *J. Organomet. Chem.* **1994**, *478*, 75.
(292) Capdevila, M.; Clegg, W.; Gonzales-Duarte, P.; Jarid, A.; Lledós, A. *Inorg. Chem.* **1996**, *35*, 490.
(293) Bencini, A.; Vaira, M. d.; Morassi, R.; Stoppioni, P.; Mele, F. *Polyhedron* **1995**, *15*, 2079.
(294) Aullón, G.; Ujaque, G.; Lledós, A.; Alvarez, S.; Alemany, P. *Inorg. Chem.* **1998**, *37*, 804.

(295) Aullón, G.; Ujaque, G.; Lledós, A.; Alvarez, S. *Chem. Eur. J.* **1999**, *5*, 1391.
(296) Masdeu, A. M.; Ruiz, A.; Castillón, S.; Claver, C.; Hitchcock, P. B.; Chaloner, P. A.; Bo, C.; Poblet, J. M.; Sarasa, P. *J. Chem. Soc., Dalton Trans.* **1993**, 2689.
(297) Kumar, C.; Chattopadhyay, S.; Sinha, C.; Chakravorty, A. *Inorg. Chem.* **1994**, *33*, 6140.
(298) Bella, S. D.; Lanza, G.; Fragalà, I.; Marks, T. J.; Ratner, M. A. *Inorg. Chem.* **1995**, *34*, 1983.
(299) Klein, A.; Kaim, W.; Hornung, F. M.; Fiedler, J.; Zalis, S. *Inorg. Chim. Acta* **1997**, *264*, 269.
(300) Arena, C. G.; Ciani, G.; Drommi, D.; Faraone, F.; Proserpio, D. M.; Rotondo, E. *J. Organomet. Chem.* **1994**, *484*, 71.
(301) Pichierri, F.; Chiarparin, E.; Zangrando, E.; Randaccio, L.; Holthenrich, D.; Lippert, B. *Inorg. Chim. Acta* **1997**, *264*, 109.
(302) Leoni, P.; Pasquali, M.; Fortunelli, A.; Germano, G.; Albinati, A. *J. Am. Chem. Soc.* **1998**, *120*, 9564.
(303) Appleton, T. G.; Byriel, K. A.; Garett, J. M.; Hall, J. R.; Kennard, C. H. L.; Mathieson, M. T.; Stranger, R. *Inorg. Chem.* **1995**, *34*, 5646 and references therein.
(304) Stranger, R.; Medley, G. A.; McGrady, J. E.; Garrett, J. M.; Appleton, T. G. *Inorg. Chem.* **1996**, *35*, 2268.
(305) Cotton, F. A.; Gu, J.; Murillo, C. A.; Timmons, D. J. *J. Am. Chem. Soc.* **1998**, *120*, 13280.
(306) Duran, N.; Gonzalez-Duarte, P.; Lledós, A.; Parella, T.; Sola, J.; Ujaque, G.; Clegg, W.; Fraser, K. A. *Inorg. Chim. Acta* **1997**, *265*, 89.
(307) Manojlovic-Muir, L.; Muir, K. W.; Lloyd, B. R.; Puddephatt, R. J. *J. Chem. Soc., Chem. Commun.* **1983**, 1336.
(308) Ferguson, G.; Lloyd, B. R.; Puddephatt, R. J. *Organometallics* **1986**, *5*, 344.
(309) Puddephatt, R. J.; Manojlovic-Muir, L.; Muir, K. W. *Polyhedron* **1990**, *9*, 2767.
(310) Ramachandran, R.; Yang, D.-S.; Payne, N. C.; Puddephatt, R. J. *Inorg. Chem.* **1992**, *31*, 4236.
(311) Bradford, A. M.; Kristof, E.; Rashidi, M.; Yang, D.-S.; Payne, N. C.; Puddephatt, R. J. *Inorg. Chem.* **1994**, *33*, 2355.
(312) Xiao, J.; Hao, L.; Puddephatt, R. J.; Manojlovic-Muir, L.; Muir, K. W. *J. Am. Chem. Soc.* **1995**, *117*, 6316.
(313) Harvey, P. D.; Provencher, P. *Inorg. Chem.* **1993**, *32*, 61.
(314) Harvey, P. D.; Hubig, S. M.; Ziegler, T. *Inorg. Chem.* **1994**, *33*, 3700.
(315) Harvey, P. D.; Hierso, K.; Braunstein, P.; Morise, X. *Inorg. Chim. Acta* **1996**, *250*, 337.
(316) Harvey, P. D.; Provencher, R.; Gagnon, J.; Zhang, T.; Fortin, D.; Hierso, K.; Drouin, M.; Socol, S. M. *Can. J. Chem.* **1996**, *74*, 2268.
(317) Gauthron, I.; Mugnier, Y.; Hierso, K.; Harvey, P. D. *Can. J. Chem.* **1997**, *75*, 1182.
(318) Imhof, D.; Venanzi, L. M. *Chem. Soc. Rev.* **1994**, 185.
(319) Bengtsson-Kloo, L.; Iapalucci, C. M.; Longoni, G.; Ulvenlund, S. *Inorg. Chem.* **1998**, *37*, 4335.
(320) Grönbeck, H.; Andreoni, W. *Chem. Phys. Lett.* **1997**, *269*, 385.
(321) Mingos, D. M. P.; Slee, T. *J. Organomet. Chem.* **1990**, *394*, 679 and references therein.
(322) Spivak, G. J.; Puddephatt, R. J. *Inorg. Chim. Acta* **1997**, *264*, 1.
(323) Hao, L.; Manjlovic-Muir, L.; Muir, K. W.; Puddephatt, R. J.; Spivak, G. J.; Vittal, J. J.; Yufit, D. *Inorg. Chim. Acta* **1997**, *265*, 65.
(324) Yamamoto, Y.; Yamazaki, H. *Inorg. Chim. Acta* **1994**, *217*, 121.
(325) Tanase, T.; Yamamoto, Y.; Puddephatt, R. J. *Organometallics* **1996**, *15*, 1502.
(326) Tanase, T.; Ukaji, H.; Kudo, Y.; Ohno, M.; Kobayashi, K.; Yamamoto, Y. *Organometallics* **1994**, *13*, 1374.
(327) Tanase, T.; Ukaji, H.; Takahata, H.; Toda, H.; Igoshi, T.; Yamamoto, Y. *Organometallics* **1998**, *17*, 196.
(328) Zhang, T.; Drouin, M.; Harvey, P. D. *Inorg. Chem.* **1999**, *38*, 1305.
(329) Olmstead, M. L.; Ginwalla, A. S.; Noll, B. C.; Tinti, D. S.; Balch, A. L. *J. Am. Chem. Soc.* **1996**, *118*, 7737.
(330) *Theoretical Aspects of Homogeneous Catalysis, Applications of Ab Initio Molecular Orbital Theory*; Leeuwen, P. W. N. M. v., Morokuma, K., Lenthe, J. H. v., Eds.; Kluwer Academic Publishers: Dordrecht, 1995.
(331) Musaev, D. G.; Morokuma, K. In *Advances in Chemical Physics*; Prigogine, I., Rice, S. A., Eds.; J. Wiley: New York, 1996; Vol. XCV, p 61.
(332) *Transition State Modeling for Catalysis*; Truhlar, D. G., Morokuma, K., Eds.; ACS Symposium Series 721; American Chemical Society: Washington, DC, 1999.
(333) Kitaura, K.; Obara, S.; Morokuma, K. *J. Am. Chem. Soc.* **1981**, *103*, 2891.
(334) Noell, J. O.; Hay, P. J. *J. Am. Chem. Soc.* **1982**, *104*, 4578.
(335) Obara, S.; Kitaura, K.; Morokuma, K. *J. Am. Chem. Soc.* **1984**, *106*, 7482.
(336) Low, J. J.; Goddard, W. A., III *J. Am. Chem. Soc.* **1984**, *106*, 6928.
(337) Low, J. J.; Goddard, W. A., III *J. Am. Chem. Soc.* **1984**, *106*, 8321.
(338) Low, J. J.; Goddard, W. A., III *J. Am. Chem. Soc.* **1986**, *108*, 6115.
(339) Hay, P. J. In *Transition Metal Hydrides*; Dedieu, A., Ed.; VCH Publishers Inc.: New York, 1992; p 127.
(340) Hay, P. J. *New J. Chem.* **1991**, *15*, 735.
(341) Packett, D. L.; Trogler, W. C. *Inorg. Chem.* **1988**, *27*, 1768.
(342) Crabtree, R. H.; Hamilton, D. G. *Adv. Organomet. Chem.* **1988**, *28*, 299.
(343) Crabtree, R. H. *Chem. Rev.* **1995**, *95*, 987.
(344) Arndtsen, B. A.; Bergman, R. G.; Mobley, T. A.; Peterson, T. H. *Acc. Chem. Res.* **1995**, *28*, 154.
(345) Shilov, A. E.; Shul'pin, G. B. *Chem. Rev.* **1997**, *97*, 2879.
(346) Blomberg, M. R. A.; Siegbahn, P. E. M.; Nagashima, U.; Wennerberg, J. *J. Am. Chem. Soc.* **1991**, *113*, 424.
(347) Blomberg, M. R. A.; Siegbahn, P. E. M.; Svensson, M. *J. Am. Chem. Soc.* **1992**, *114*, 6095.
(348) Siegbahn, P. E. M.; Blomberg, M. R. A.; Svensson, M. *J. Am. Chem. Soc.* **1993**, *115*, 1952.
(349) Siegbahn, P. E. M.; Svensson, M. *Chem. Phys. Lett.* **1993**, *216*, 147.
(350) Sakaki, S.; Ogawa, M.; Kinoshita, M. *J. Chem. Phys.* **1995**, *99*, 9933.
(351) Siegbahn, P. E. M.; Blomberg, M. R. A. *J. Am. Chem. Soc.* **1992**, *114*, 10548.
(352) Siegbahn, P. E. M.; Blomberg, M. R. A.; Svensson, M. *J. Am. Chem. Soc.* **1993**, *115*, 4191.
(353) Wittborn, A. M. C.; Costas, M.; Blomberg, M. R. A.; Siegbahn, P. E. M. *J. Chem. Phys.* **1997**, *107*, 4318.
(354) Hada, M.; Nakatsuji, N.; Nakai, H.; Gyobu, S.; Miki, S. *J. Mol. Struct. (THEOCHEM)* **1993**, *281*, 207.
(355) Swang, O.; Faegri, K.; Gropen, O. *J. Phys. Chem.* **1994**, *98*, 3006.
(356) Blomberg, M. R. A.; Siegbahn, P. E. M.; Svensson, M. *J. Phys. Chem.* **1994**, *98*, 2062.
(357) Irikura, K. K.; Beauchamp, J. L. *J. Phys. Chem.* **1991**, *95*, 8344.
(358) Heinemann, C.; Wesendrup, R.; Schwarz, H. *Chem. Phys. Lett.* **1995**, *239*, 75.
(359) Pavlov, M.; Blomberg, M. R. A.; Siegbahn, P. E. M.; Wesendrup, R.; Heinemann, C.; Schwarz, H. *J. Phys. Chem. A* **1997**, *101*, 1567.
(360) Sakaki, S.; Ieki, M. *J. Am. Chem. Soc.* **1993**, *115*, 2373.
(361) Sakaki, S.; Biswas, B.; Sugimoto, M. *J. Chem. Soc., Dalton Trans.* **1997**, 803.
(362) Su, M.-D.; Chu, S.-Y. *Inorg. Chem.* **1997**, *37*, 33400.
(363) Pross, A.; Shaik, S. *Acc. Chem. Res.* **1983**, *16*, 363.
(364) Sakaki, S.; Biswas, B.; Sugimoto, M. *Organometallics* **1998**, *17*, 1278.
(365) Yamamoto, Y.; Al-Masum, M.; Asao, N. *J. Am. Chem. Soc.* **1994**, *116*, 6019.
(366) Hill, G. S.; Puddephatt, R. J. *Organometallics* **1998**, *17*, 1478.
(367) Milet, A.; Dedieu, A.; Kapteijn, G.; van Koten, G. *Inorg. Chem.* **1997**, *36*, 3223.
(368) Koga, N.; Morokuma, K. *J. Phys. Chem.* **1990**, *94*, 5454.
(369) Margl, P.; Ziegler, T.; Blöchl, P. E. *J. Am. Chem. Soc.* **1995**, *117*, 12625.
(370) Calhorda, M. J.; Brown, J. M.; Cooley, N. A. *Organometallics* **1991**, *10*, 1431.
(371) Milet, A.; Dedieu, A.; Canty, A. J. *Organometallics* **1997**, *16*, 5331.
(372) Su, M.-D.; Chu, S.-Y. *Chem. Phys. Lett.* **1998**, *282*, 25.
(373) Dedieu, A.; Hutschka, F.; Milet, A. In *Transition State Modeling for Catalysis*; Truhlar, D. G., Morokuma, K., Eds.; ACS Symposium Series 721; American Chemical Society: Washington, DC, 1999; p 100.
(374) Musaev, D. G.; Svensson, M.; Morokuma, K.; Strömberg, S.; Zetterberg, K.; Siegbahn, P. E. M. *Organometallics* **1997**, *16*, 1933.
(375) Shilov, A. E. In *Activation and Functionalization of Alkanes*; Hill, C. L., Ed.; J. Wiley: New York, 1984.
(376) Siegbahn, P. E. M.; Crabtree, R. H. *J. Am. Chem. Soc.* **1996**, *118*, 4442.
(377) Crabtree, R. H.; Siegbahn, P. E. M.; Eisenstein, O.; Rheingold, A. L.; Koetzle, T. F. *Acc. Chem. Res.* **1996**, *29*, 348.
(378) Cui, Q.; Musaev, D. G.; Morokuma, K. *Organometallics* **1998**, *17*, 1383.
(379) Sakaki, S.; Ieki, M. *J. Am. Chem. Soc.* **1991**, *113*, 5063.
(380) Sakaki, S.; Ogawa, M.; Musahi, Y.; Arai, T. *Inorg. Chem.* **1994**, *33*, 1660.
(381) Sakaki, S.; Mizoe, N.; Sugimoto, M. *Organometallics* **1998**, *17*, 2510.
(382) Sakaki, S.; Ujino, Y.; Sugimoto, M. *Bull. Chem. Soc. Jpn.* **1996**, *69*, 3047.
(383) Sakaki, S.; Kikuno, T. *Inorg. Chem.* **1997**, *36*, 226.
(384) Cui, Q.; Musaev, D. G.; Morokuma, K. *Organometallics* **1997**, *16*, 1355.
(385) Cui, Q.; Musaev, D. G.; Morokuma, K. *Organometallics* **1998**, *17*, 742.
(386) Balasubramanian, K. *J. Chem. Phys.* **1991**, *94*, 1253.
(387) Poulain, E.; Bertin, V.; Castillo, S.; Cruz, A. *J. Mol. Catal. A* **1997**, *116*, 385.

(388) Mitchell, P. C. H.; Wolohan, P.; Thompsett, D.; Cooper, S. J. *J. Mol. Catal. A* **1997**, *119*, 223.
(389) Castillo, S.; Cruz, A.; Bertin, V.; Poulain, E.; Arellano, J. S.; Del Angel, G. *Int. J. Quantum Chem.* **1997**, *62*, 29.
(390) Miller, W. H. *J. Phys. Chem.* **1983**, *87*, 3811.
(391) Mamaev, V. M.; Gloriozov, I. P.; Simonyan, V. V.; Zernova, E. V.; Prisyajnyuk, A. V.; Ustynyuk, Y. A. *Mendeleev Commun.* **1997**, 246.
(392) Fayet, P.; Kaldor, A.; Cox, D. M. *J. Chem. Phys.* **1990**, *92*, 254.
(393) Broclawik, E.; Yamauchi, R.; Endou, A.; Kubo, M.; Miyamoto, A. *Int. J. Quantum Chem.* **1997**, *61*, 673.
(394) Mamaev, V. M.; Gloriozov, I. P.; Simonyan, V. V.; Prisyajnyuk, A. V.; Ustynyuk, Y. A. *Mendeleev Commun.* **1996**, 146.
(395) Dai, D.; Liao, D. W.; Balasubramanian, K. *J. Chem. Phys.* **1995**, *102*, 7530.
(396) Johnson, L. K.; Killian, C. M.; Brookhart, M. *J. Am. Chem. Soc.* **1995**, *117*, 6414.
(397) Killian, C. M.; Tempel, D. T.; Johnson, L. K.; Brookhart, M. *J. Am. Chem. Soc.* **1996**, *118*, 11664.
(398) Drent, E.; Budzelaar, P. H. M. *Chem. Rev.* **1996**, *96*, 663.
(399) Johnson, L. K.; Mecking, S.; Brookhart, M. *J. Am. Chem. Soc.* **1996**, *118*, 267.
(400) Nozaki, K.; Sato, N.; Tonomura, Y.; Yasutomi, M.; Tayaka, H.; Hiyama, T.; Matsubara, T.; Koga, N. *J. Am. Chem. Soc.* **1997**, *119*, 12795.
(401) Siegbahn, P. E. M. *Chem. Phys. Lett.* **1993**, *205*, 290.
(402) Siegbahn, P. E. M. *J. Am. Chem. Soc.* **1993**, *115*, 5803.
(403) Siegbahn, P. E. M. *J. Organomet. Chem.* **1994**, *478*, 83.
(404) Rix, F. C.; Brookhart, M. *J. Am. Chem. Soc.* **1995**, *117*, 1137.
(405) Strömberg, S.; Zetterberg, K.; Siegbahn, P. E. M. *J. Chem. Soc., Dalton Trans.* **1997**, 4147.
(406) Sakaki, S.; Ogawa, M.; Musashi, Y.; Arai, T. *J. Am. Chem. Soc.* **1994**, *116*, 7258.
(407) Rocha, W. R.; de Almeida, W. B. *Organometallics* **1998**, *17*, 1961.
(408) Coussens, B. B.; Buda, F.; Oevering, H.; Meier, R. J. *Organometallics* **1998**, *17*, 795.
(409) Creve, S.; Oevering, H.; Coussens, B. B. *Organometallics* **1999**, *18*, 1967.
(410) Green, M. L. H.; Sella, A.; Wong, L.-L. *Organometallics* **1992**, *11*, 2650.
(411) Bercaw, J. E.; Burger, B. J.; Green, M. L. H.; Santarsiero, B. D.; Sella, A.; Trimmer, M. S.; Wong, L.-L. *J. Chem. Soc., Chem. Commun.* **1989**.
(412) Markies, B. A.; Wijkens, P.; Dedieu, A.; Boersma, J.; Spek, A. L.; van Koten, G. *Organometallics* **1995**, *14*, 5628.
(413) Frankcombe, K.; Cavell, K.; Knott, R.; Yates, B. *J. Chem. Soc., Chem. Commun.* **1996**, 781.
(414) Frankcombe, K. E.; Cavell, K. J.; Yates, B. F.; Knott, R. B. *Organometallics* **1997**, *16*, 3199.
(415) Groen, J. H.; Zwart, A. d.; Vlaar, M. J. M.; Ernsting, J. M.; van Leeuwen, P. W. N. W.; Vrieze, K.; Kooijman, H.; Smeets, W. J. J.; Spek, A. L.; Budzelaar, P. H. M.; Xiang, Q.; Thummel, R. P. *Eur. J. Inorg. Chem.* **1998**, 1129.
(416) Blomberg, M. R. A.; Karlsson, C. A. M.; Siegbahn, P. E. M. *J. Phys. Chem.* **1993**, *97*, 9341.
(417) Koga, N.; Morokuma, K. *New J. Chem* **1991**, *15*, 749.
(418) Svensson, M.; Matsubara, T.; Morokuma, K. *Organometallics* **1996**, *15*, 5568.
(419) Green, M. J.; Britovsek, G. J. P.; Cavell, K. L.; Gerhards, F.; Yates, B. F.; Frankcombe, K.; Skelton, B. W.; White, A. H. *J. Chem. Soc., Dalton Trans.* **1998**, 1137.
(420) Rocha, W. R.; de Almeida, W. B. *Int. J. Quantum Chem.* **1997**, *65*, 643.
(421) Trost, B. M. *Acc. Chem. Res.* **1980**, *13*, 385.
(422) Tsuji, J. *Tetrahedron* **1986**, *42*, 4361.
(423) Consiglio, G.; Waymouth, R. W. *Chem. Rev.* **1989**, *89*, 257.
(424) Pfalz, A. *Acc. Chem. Res.* **1993**, *26*, 339.
(425) Trost, B. M. *Acc. Chem. Res.* **1996**, *29*, 355.
(426) Trost, B. M.; Vranken, D. L. *Chem. Rev.* **1996**, *96*, 395.
(427) Bäckvall, J.-E. *Acc. Chem. Res.* **1983**, *16*, 335.
(428) Bäckvall, J.-E. *Pure Appl. Chem.* **1992**, *64*, 229.
(429) *Comprehensive Organometallic Chemistry*; Pergamon Press: Oxford, 1982; Vol. 6.
(430) Norrby, P. O.; Åkermark, B.; Haeffner, F.; Hansson, S.; Blomberg, M. *J. Am. Chem. Soc.* **1993**, *115*, 4859.
(431) Sjögren, M.; Hansson, S.; Norrby, P.-O.; Åkermark, B.; Cucciolito, M. E.; Vitagliano, A. *Organometallics* **1992**, *11*, 3954.
(432) Peña-Cabrera, E.; Norrby, P.-O.; Sjögren, M.; Vitagliano, A.; Felice, V. D.; Oslob, J.; Ishii, S.; O'Neill, D.; Åkermark, B.; Helquist, P. *J. Am. Chem. Soc.* **1996**, *118*, 4299.
(433) Sakaki, S.; Nishikawa, M.; Ohyoshi, A. *J. Am. Chem. Soc.* **1980**, *102*, 4062.
(434) Curtis, M. D.; Eisenstein, O. *Organometallics* **1984**, *3*, 887.
(435) Nakatsuji, K.; Yamaguchi, M.; Murata, I.; Tatsumi, K.; Nakamura, A. *Organometallics* **1984**, *3*, 1257.
(436) Bigot, B.; Delbecq, F. *New J. Chem.* **1990**, *14*, 659.
(437) Szabó, K. J. *Organometallics* **1996**, *15*, 1128.
(438) Sakaki, S.; Satoh, H.; Shono, H.; Ujino, Y. *Organometallics* **1996**, *15*, 1713.
(439) Carfagna, C.; Galarini, R.; Linn, K.; Lopez, J. A.; Mealli, C.; Musco, A. *Organometallics* **1993**, *12*, 3019.
(440) Goddard, R.; Krüger, C.; Mark, F.; Stanfield, R.; Zhang, X. *Organometallics* **1985**, *4*, 285.
(441) Szabó, K. J. *J. Am. Chem. Soc.* **1996**, *118*, 7818.
(442) Szabó, K. J. *Chem. Eur. J.* **1997**, *3*, 592.
(443) Castagno, A. M.; Aranyos, A.; Szabó, K. J.; Bäckvall, J.-E. *Angew. Chem., Int. Ed. Engl.* **1995**, *34*, 2551.
(444) Aranyos, A.; Szabó, K. J.; Castano, A. M.; Bäckvall, J.-E. *Organometallics* **1997**, *16*, 1058.
(445) Ward, T. R. *Organometallics* **1996**, *15*, 2836.
(446) Szabó, K. J.; Hupe, E.; Larsson, A. L. E. *Organometallics* **1997**, *16*, 3779.
(447) Blöchl, P. E.; Togni, A. *Organometallics* **1996**, *15*, 4125.
(448) Margl, P.; Schwarz, K.; Blöchl, P. E. *J. Chem. Phys.* **1994**, *100*, 8194.
(449) Blöchl, P. E. *Phys. Rev. B* **1994**, *50*, 17953.
(450) Togni, A.; Burckhardt, U.; Gramlich, V.; Pregosin, P. S.; Salzmann, R. *J. Am. Chem. Soc.* **1996**, *118*, 1031.
(451) Hagelin, H.; Åkermark, B.; Norrby, P.-O. *Chem. Eur. J.* **1999**, *5*, 902.
(452) Cossi, M.; Barone, V.; Cammi, R.; Tomasi, J. *Chem. Phys. Lett.* **1996**, *255*, 327.
(453) Cramer, C. J.; Truhlar, D. G. *Science* **1992**, *256*, 213.
(454) Szabó, K. J. *Organometallics* **1998**, *17*, 1677.
(455) Hegedus, L. S. *Tetrahedron* **1986**, *40*, 2415.
(456) Smidt, J.; Hafner, W.; Jira, R.; Sieber, R.; Rüttinger, R.; Kojer, H. *Angew. Chem.* **1959**, *71*, 176.
(457) Smidt, J.; Hafner, W.; Jira, R.; Sieber, R.; Sedlmeier, J.; Sable, A. *Angew. Chem.* **1962**, *74*, 93.
(458) Dedieu, A. In *Theoretical Aspects of Homogeneous Catalysis, Applications of Ab Initio Molecular Orbital Theory*; van Leeuwen, P. W. N. M., Morokuma, K., van Lenthe, J. H., Eds.; Kluwer Academic Publishers: Dordrecht, 1995; p 167.
(459) Siegbahn, P. E. M. *J. Am. Chem. Soc.* **1995**, *117*, 5409.
(460) Siegbahn, P. E. M. *J. Phys. Chem.* **1996**, *100*, 14672.
(461) Oishi, Y.; Sakamoto, E.; Fujimoto, H. *Inorg. Chem.* **1996**, *35*, 231.
(462) Cross, R. J. *Adv. Inorg. Chem.* **1989**, *34*, 219.
(463) Dedieu, A. In *Topics in Physical Organometallic Chemistry*; Freund Publishing House: London, 1985; Vol. 1, p 1.
(464) Lin, Z.; Hall, M. B. *Inorg. Chem.* **1991**, *30*, 646.
(465) Deeth, R. J.; Elding, L. I. *Inorg. Chem.* **1996**, *35*, 5019.
(466) Muguruma, C.; Koga, N.; Kitaura, K.; Morokuma, K. *Chem. Phys. Lett.* **1994**, *224*, 139.
(467) Muguruma, C.; Koga, N.; Kitaura, K.; Morokuma, K. *J. Chem. Phys.* **1995**, *103*, 9274.
(468) Frankcombe, K. E.; Cavell, K. J.; Yates, B. F. *J. Phys. Chem.* **1996**, *100*, 18363.
(469) Romeo, R.; Grassi, A.; Scolaro, L. M. *Inorg. Chem.* **1992**, *31*, 4383.
(470) Broclawik, E.; Haber, J.; Endou, A.; Stirling, A.; Yamauchi, R.; Kubo, M.; Miyamoto, A. *J. Mol. Catal. A* **1997**, *119*, 35.
(471) Fantucci, P.; Lolli, S.; Pizzotti, M.; Ugo, R. *Inorg. Chem. Acta* **1998**, *270*, 479.
(472) Zanardo, A.; Pinna, F.; Michelin, R. A.; Strukul, G. *Inorg. Chem.* **1988**, *27*, 1966.
(473) Sakaki, S.; Ogawa, M.; Musahi, Y. *J. Organomet. Chem.* **1997**, *535*, 25.
(474) Kragten, D. D.; van Santen, R. A.; Lerou, J. J. *J. Phys. Chem. A* **1999**, *103*, 80.
(475) Mylvaganam, K.; Backsay, G. B.; Hush, N. S. *J. Am. Chem. Soc.* **1999**, *121*, 4633.
(476) Periana, R. A.; Taube, D. J.; Gamble, S.; Taube, H.; Satoh, T.; Fuji, H. *Science* **1998**, *280*, 560.
(477) Albert, K.; Gisdakis, P.; Rösch, N. *Organometallics* **1998**, *17*, 1608−1616.
(478) Musaev, D. G.; Froese, R. D. J.; Morokuma, K. *New J. Chem.* **1997**, *21*, 1269.
(479) Froese, R. D. J.; Musaev, D. G.; Morokuma, K. *J. Am. Chem. Soc.* **1998**, *120*, 1581.
(480) Musaev, D. G.; Froese, R. D. J.; Morokuma, K. *Organometallics* **1998**, *17*, 1850.
(481) Margl, P.; Ziegler, T. *J. Am. Chem. Soc.* **1996**, *118*, 7337.
(482) Margl, P.; Ziegler, T. *Organometallics* **1996**, *15*, 5519.

CR980407A